UNIVERSIDAD AUTÓNOMA DE NUEVO LEÓN

FACULTAD DE INGENIERÍA MECÁNICA Y ELÉCTRICA

TESIS

SYNTHESIS OF CARBON NANOTUBES ON SURFACE OF RECOVERED CARBON FIBERS BY CHEMICAL VAPOR DEPOSITION, AS A SIZING PROCESS TO OBTAIN A HYBRID MATERIAL

SAIDA MAYELA GARCÍA MONTES

EN OPCIÓN AL GRADO DE DOCTOR EN INGENIERÍA DE MATERIALES

DICIEMBRE, 2017

UNIVERSIDAD AUTÓNOMA DE NUEVO LEÓN

FACULTAD DE INGENIERÍA MECÁNICA Y ELÉCTRICA

SUBDIRECCIÓN DE ESTUDIOS DE POSGRADO

TESIS

SYNTHESIS OF CARBON NANOTUBES ON SURFACE OF RECOVERED CARBON FIBERS BY CHEMICAL VAPOR DEPOSITION, AS A SIZING PROCESS TO OBTAIN A HYBRID MATERIAL

SAIDA MAYELA GARCÍA MONTES

EN OPCIÓN AL GRADO DE DOCTOR EN INGENIERÍA DE MATERIALES

SAN NICOLÁS DE LOS GARZA NUEVO LEÓN, MÉXICO **DICIEMBRE, 2017**

Abstract

Carbon fibers recovered from composite materials in structural components reaching end-of-life can be treated with the synthesis of carbon nanotubes (CNTs) directly grown on the carbon fibers (CFs) surface to produce reinforcements which can be used in new high-performance composite materials. The development of high performance materials with improved properties by anchorage and growth of Carbon Nanotubes on Carbon Fibers surface is increasing the interest of industry and related technology departments. CNTs attached to CFs surface are interesting candidates for novel composite materials with exceptional mechanical, thermal and electrical properties. Synthesis of carbon nanotubes using catalytic Chemical Vapor Deposition (CVD) method is an increasing area of academic research which is also attracting industrial attention due to the relatively low synthesis temperatures ranging from 500°C to 1100°C which can be easily scaled-up for industrialization. In this research, the CVD method was used and studied for the synthesis and growth of CNTs on CFs influenced by the concentration of Nickel (Ni) nanoparticles as a catalyst. The CNTs were synthesized by decomposing Ethanol and Isopropanol as a carbon source, which at the same time worked as a solvent, in an Argon (Ar) atmosphere. Moreover, $Ni(NO_3)_2$ * $6H_2O$ was used as precursor of Ni nanoparticles. Ni concentration experimentally controlled between 0 – 5.96 wt %. The CFs were recovered from an epoxy-carbon fiber composite reaching end-of-life by a thermal recycling process of pyrolysis at a temperature of 480°C for 30 min. Before the CNTs synthesis, the CFs were analyzed by Scanning Electron Microscopy (SEM) and Energy Dispersive Spectroscopy (EDS) to identify elements present on CF surface. The EDS results showed that the original sizing on CFs

surface was removed. All samples were characterized by different techniques such as Scanning Electron Microscopy (SEM) for morphology, Raman Spectroscopy for structural characterization and Pseudo-Mechanical testing to evaluate the CNTs anchorage to the CF surface.

Published Material

TITLE	Carbon Fiber Recovery using Water and Benzyl Alcohol in Subcritical and Supercritical Conditions for Chemical Recycling of Thermoset Composite Materials
AUTHORS	Rodolfo Morales Ibarra, Mitsuru Sasaki, Motonobu Goto, Armando T. Quitain, Saida Mayela García Montes & Juan A. Aguilar-Garib
JOURNAL	Journal of Material Cycles and Waste Management
PUBLISHER	Springer
ACCEPTED	March 26th 2014
PUBLISHED	April 20th 2014
RELATED SOCIETIES	Official Journal of the Japan Society of Material Cycles and Waste Management (JSMCWM) and the Korea Society of Waste Management (KSWM)
ISSN	1438-4957
DOI	10.1007/s10163-014-0252-z.

Table of Contents

1. Introduction

1.1. Justification

Carbon nanotubes (CNTs) are a recently discovered form of carbon with a graphitic lattice and a long, tubular structure. CNTs have been the subject of much interest in recent years, due to their attractive mechanical properties (~1000 GPa Young's modulus), tunable electronic behavior (conducting or semi-conducting depending on tube chirality), and unique dimensions (1–100 nm diameter, up to several cm length). As a result of these properties, nanotubes have potential applications in many fields, including composite reinforcement, sizing agent, transistors and logic circuits, field emission sources, and hydrogen storage. CNTs can be grown by a variety of means, the most common of which are: arc discharge, laser ablation, and chemical vapor deposition (CVD) [1, 14].

The increasing use of composite materials in industry has triggered the research and development of different recycling methods for end-of-life components. The recovery of CF from composite materials is highly desirable for the economic, environmental, and development purposes. Recycling composite materials is a developing industry which is driven by the economical and environmental benefits but that it is also supported by regulations and incentives to benefit its users by lowering the costs of materials, the development of necessary technology and to avoid losing the intrinsically developed value of the material itself. The technologies for recycling thermoset composite materials have a level of readiness prepared for industrial escalation; however, these methods have to be adjusted for industrial purposes of carbon fiber recovery, in accordance with other factors

such as costs, type of reactors, environmental issues, and properties of recovered fibers which suffer degradation throughout the recycling processes.

Degradation of carbon fibers and even the loss of the original sizing create an opportunity to develop novel revalorization ways of the degraded carbon fibers in order to be considered for reuse in new components [2].

The potential of CF sizing with CNTs represent great opportunity for its application in the different industries. CNTs have been the focus of much research with reports of exceeding mechanical properties due to their size and covalently bonded carbon atoms [3]. The most straightforward way to synthesize CNTs onto fibers is coating fiber with CNTs, which requires sized fibers [4]. There are two common strategies to bring CNTs in polymer composites: via dispersing CNTs into matrix to form three phase composites with fibers; and attaching directly CNTs on fibers surface. Research demonstrates that homogeneous and stable dispersion of CNTs in polymer matrix is a factor for forming high performance composites [3, 4].

In this Research, CNTs were synthesized directly on the carbon fibers surface to produce a "nanocarbon" sizing as reinforcements which can be potentially used in new high performance composite materials. We studied the influence of carbon source, the variation of Ni concentration and reaction temperature on synthesis of CNTs on CF by CVD method.

1.2. General Objective

Synthesize carbon nanotubes on surface of recovered carbon fibers by Chemical Vapor Deposition using an alcohol as carbon source and Ni nanoparticles as catalyst.

1.3. Specific Objectives

- Recovering Carbon Fiber from an epoxy-carbon fiber composite reaching end-of-life by a thermal recycling process of pyrolysis.

- Synthesizing Carbon Nanotubes on Carbon Fiber recovered by CVD process using Ethanol as Carbon Source.

- Synthesizing Carbon Nanotubes on Carbon Fiber recovered by CVD process using Isopropanol as Carbon Source.

- Study the influence of the variation of Ni concentration of Synthesis of Carbon Nanotubes on Carbon Fiber Recovered by CVD process.

- Synthesizing Carbon Nanotubes on Carbon Fiber decreasing the Reaction Temperatures from 800 to 600°C.

1.4. Hypothesis

Is possible Synthesize Carbon nanotubes on surface of recovered carbon fibers by CVD process using Alcohol as carbon source under argon atmosphere.

2. Literature Review - Carbon Nanotubes

The carbon atoms in a carbon nanotube (CNT) are bonded trigonally in a curved sheet (graphite layer) that forms a hollow cylinder in nanoscale, similar to that in other fullerenes. The length of CNTs may range from less than a micron to several millimeters or even centimeters. Their unique nanostructures result in many extraordinary properties such as high tensile strength, high electrical and thermal conductivities, high ductility, high thermal and chemical stability, making them suitable for various applications.

2.1. Structures of Carbon Nanotubes

CNTs are typically categorized as single-walled CNT (SWCNT), Double-walled CNT (DWCNT) and multi-walled CNT (MWCNT) with respect to the number of graphene layers (Figure 2.1). CNTs are often found in bundles, ropes, or fibers. These three-dimensional structures form through the van der Waals interaction between the tube surfaces, which also influence the properties of the bundles [5]. The nature of the atomic bonding in a CNT is described by applied quantum chemistry, or specifically, orbital hybridization. The chemical bonds in CNTs are all sp^2 bonds, similar to those of graphene, which are stronger than sp and sp^3 bonds.

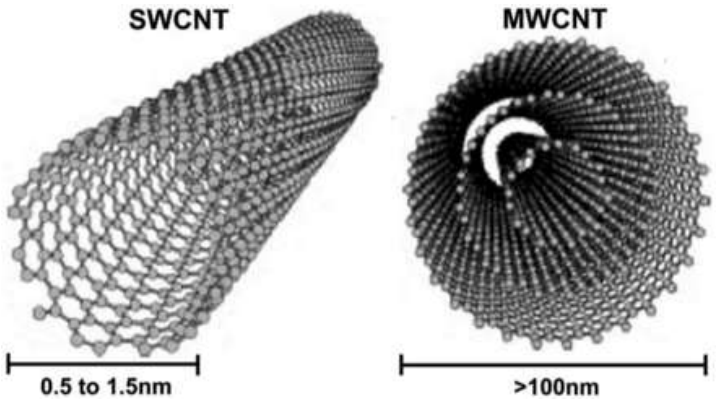

Figure 2.1 Representation of single-walled carbon nanotubes (SWCNTs) and multi-walled carbon nanotubes (MWCNTs).

Figure 2.1 shows a schematic representation of single-walled carbon nanotubes (SWCNTs) and multi-walled carbon nanotubes (MWCNTs). SWCNT is formed by only one rolled-up graphene sheet, while MWCNT is composed of more than one rolled-up concentric graphene sheet. SWCNT have diameters ranging from 0.5 to 1.5 nm and lengths ranging from 100 nm up to several micrometers, whereas MWCNT have larger diameters (more than 100 nm) and lengths ranging from 0.1 to 50 μm. Figure 2.2 shows CNTs bundles. The orientation of tubes in a bundle can be compared to the staking of graphene layers. For nanotubes bundles, however, we have to additionally consider the chirality of the tubes. The structural influence on the bundle properties is especially interesting for bundles of tubes that consist of only one chirality (monochiral bundles), as these have uniform properties needed, e.g., for electronics devices.

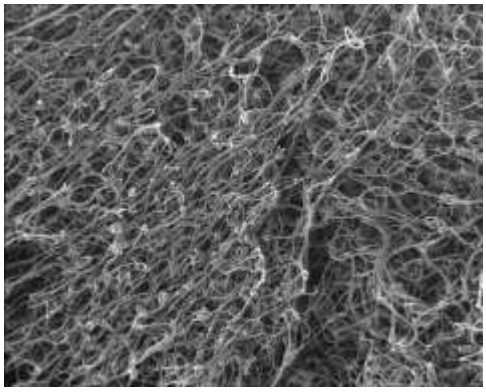

Figure 2.2 Example of Carbon Nanotubes bundles

CNTs and related nanostructures have been one of the most scientifically studied material systems in the recent years ever since their well-known experimental discovery. A large variety of potential applications have been envisioned, some of which have already been realized while others are still under study.

The most intriguing properties of CNTs lie in their unique quasi one-dimensional nanoscale structures that are intrinsically anisotropic: properties in the longitudinal direction are drastically different from those in the azimuthal directions.

2.1.1. Single-Walled Carbon Nanotubes

SWCNT consists of one layer of graphene sheet. Figure 2.1 shows the atomic structure of an SWCNT. SWCNTs can be synthesized by CVD, arc discharge, and thermo catalytical disproportionation of carbon monoxide. Now massive amount of SWCNTs is produced

mainly by CVD methods. Most SWCNTs have a diameter close to 1 nm, with length extendable up to millimeter or even centimeter scales.

The structure of an SWCNT can be conceptualized by wrapping a graphene layer into a seam less cylinder. Figure 2.3 shows how an SWCNT is rolled up from a graphene layer. The way the layer is wrapped is represented by a pair of indices *(n,m)* called the chiral vector $\mathbf{C}_h = n\mathbf{a}_1 + m\mathbf{a}_2$, where $\mathbf{a}_1$ and $\mathbf{a}_2$ are defined in Figure 2.3. The integers *n* and *m* denote the number of unit vectors along two directions in the honeycomb crystal lattice of a graphitic layer. If $n = m$, the SWCNTs are called *arm-chair* (Fig. 2.3a). If $m = 0$, they are called *zig-zag* (Fig. 2.3b), and the rest are called *chiral* (Fig. 2.3c).

SWCNTs have unique electrical properties. For a given *(n,m)* SWCNT, if $n = m$, the CNT is metallic with low energy properties of a Tomonaga-Luttinger liquid, and the rest of the SWCNTs can be either metallic or semiconducting depending on their chirality (or equivalently speaking, their diameter), as theoretically predicted and experimentally confirmed. The unique physical properties of SWCNTs are reviewed in various books and literatures.

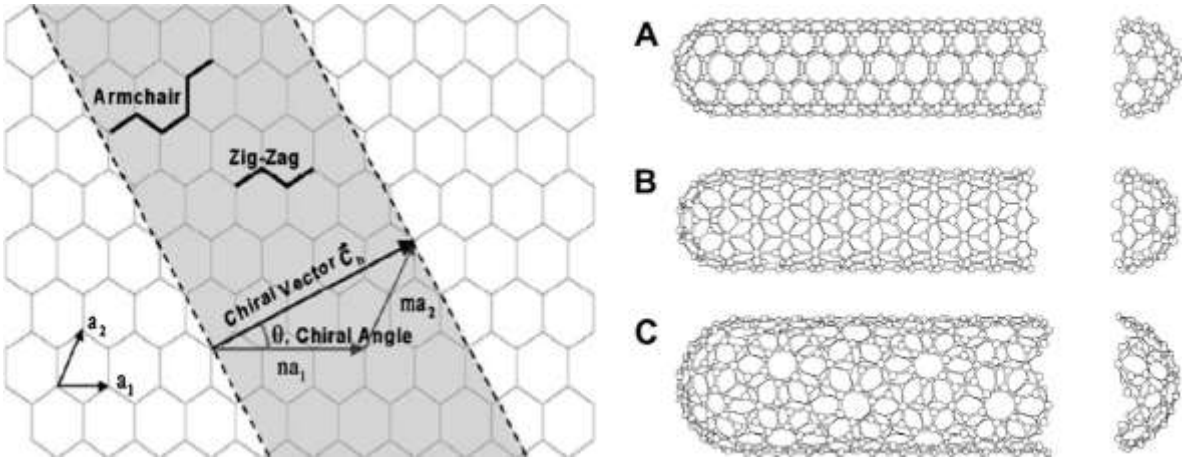

Figure 2.3 Schematic diagram showing how a hexagonal sheet of graphene is rolled to form a CNT with different chiralities (A: armchair; B: zigzag; C: chiral).

2.1.2. Double-Walled Carbon Nanotubes

DWCNTs were observed during arc-discharge synthesis and during the disproportionation of carbon monoxide. The presence of DWCNTs was related to the nature of the catalyst. Now DWCNTs can be synthesized by CVD methods and produced at gram scales.

DWCNTs are interesting members of the CNT family because their morphology and most physical properties are similar to those of SWCNTs, while their electrical and chemical properties are significantly improved for many application considerations. DWCNTs are especially important when functionalization is required to add new properties to the CNTs. In the case of SWCNTs, covalent functionalization will break some C=C bonds, leaving holes in the CNT structures and thus modifying both their mechanical and electrical properties. In the case of DWCNTs, only the outer walls are modified and therefore many properties are well preserved.

2.1.3. Multi-Walled Carbon Nanotubes

The MWCNT structure (Figure 2.1) can be conceptualized by wrapping several graphene layers into a concentric seamless cylinder. There are two models, namely the Russian Doll model and the Parchment model, which can be used to describe the structures of MWCNTs. In the Russian Doll model, graphene sheets are arranged in the form of concentric cylinders, for example, a $(0, 8)$ SWCNT within a wider $(0, 10)$ SWCNT. The inter-layer distance in an MWCNT is slightly above that in graphene, which is approximately 3.3Å, suggesting a different layer-stacking mechanism. In the Parchment model proposed in 1960 to explain the cylindrical structure of carbon fibers, a single continuous graphitic layer scrolls or rolls up to form concentric tubes [6].

2.2. Properties of Carbon Nanotubes

2.2.1. Optical Properties

Defect-free nanotubes, especially SWCNTs, offer direct band gap and well-defined band and subband structure, which is ideal for optical and optoelectronic applications. Optical spectra have been established for individual SWCNTs and ropes using resonant Raman, fluorescence, and ultraviolet to the near infrared (UV-VIS-NIR) spectroscopies. In addition, electrically induced optical emission and photoconductivity have been studied for individual SWCNTs.

Optical and optoelectronic properties can be understood from the band structure or DOS of a SWCNT. The one-dimensional DOS of a SWCNT can be derived from that for graphite with the expression as follows:

$$\rho(\varepsilon) = \frac{4}{l}\frac{2}{\sqrt{3\gamma a}}\sum_{m=-\infty}^{\infty} g(\varepsilon, \varepsilon_m)$$

2.2.2. Chemical Properties

Small radius, large specific surfaces and σ-π rehybridization make CNTs very attractive in chemical and biological applications because of their strong sensitivity to chemical or environmental interactions. The chemical properties of interest include opening, wetting, filling, adsorption, charge transfer, doping, intercalation, etc. Applications include chemical and biological separation, purification, sensing and detection, energy storage, and electronics. Intercalation of the alkali metals with nanotubes is used for enhanced metallic conductivity or halogens with nanotubes for charge- or energy-storage applications. Experimental observation and theoretical calculations show that these intercalating agents mainly enter intertube spaces or defects on nanotubes for enhanced electrochemical capability for charge transfer and storage. CNT electrodes basically inherit from graphite electrodes several advantages such as broad window of reduction and oxidation, chemical inertness or corrosion resistance, and biological compatibility. However, their nanoscale dimension provides unique electrochemical properties in greatly improved sensitivity and speed in chemical and biological sensor applications.

2.2.3. Thermal Properties

Graphite and diamond show extraordinary heat capacity and thermal conductivity. It can be expected that nanotubes have similar thermal properties at room and elevated temperatures but unusual behavior at low temperatures because of the effects of phonon quantization. Both theory and experiment show that intertube coupling in SWCNT bundles and MWCNTs is weak in temperature region of >100 K. The specific heat of MWNTs has not been examined theoretically in detail. Experimental results on MWCNTs show a temperature-dependent specific heat, which is consistent with weak interlayer coupling, although different measurements show slightly different temperature dependencies.

When T >100 K, an SWCNT, SWCNT bundle, and MWCNT all follow or are close to specific heat relation of graphite, about 700 mJ/gK. However, at lower temperatures, CNTs show quantum confinement effects. For example, the heat capacity (mJ/gK) is 0.3 for a (10,10) SWCNT, ~0 for SWCNT bundle and graphite, and 2 to 10 for a MWCNT or bundle.

The thermal conductivity of both SWCNTs and MWCNTs should reflect the on-tube phonon structure, regardless of intertube coupling. Measurements of the thermal conductivity of bulk samples show graphite-like behavior for MWCNTs but quite different behavior for SWCNTs, specifically a linear temperature dependence at low T, which is consistent with one-dimensional phonons. Thermal conductivity is one dimensional for nanotubes like electrical conductivity. Theoretical calculations and experimental measurements showed that the thermal conductivity for a SWCNT ropes and MWCNTs at

room temperature could vary between 1800 and 6000 W/mK whereas more than 3000 W/mK is firmly confirmed from the measurement of a single MWCNT.

2.2.4. Mechanical Properties

σ bonding is the strongest in nature, and thus a nanotube that is structured with all σ bonding is regarded as the ultimate fiber with the strength in its tube axis. Both experimental measurements and theoretical calculations agree that a nanotube is as stiff as or stiffer than diamond with the highest Young's modulus and tensile strength. Most theoretical calculations are carried out for perfect structures and give very consistent results. Table 2.1 summarizes calculated Young's modulus (tube axis elastic constant) and tensile strength for (10,10) SWCNT and bundle and MWCNT with comparison with other materials. The calculation is in agreement with experiments on average. Experimental results show broad discrepancy, especially for MWCNTs, because MWCNTs contain different amount of defects from different growth approaches.

Table 2.1 Mechanical Properties of Nanotubes

	Young's modulus (GPa)	Tensile Strength (GPa)	Density (g/cm^3)
MWNT	1200	~150	2.6
SWNT	1054	75	1.3
SWNT bundle	563	~150	1.3
Graphite (in-plane)	350	2.5	2.6
Steel	208	0.4	7.8

Source: J. Lu and J. Han, Int. J. High Speed Electron. Sys. 9, 101 (1998).

In general, various types of defect-free nanotubes are stronger than graphite. This is mainly because the axial component of σ bonding is greatly increased when a graphene sheet is rolled over to form a seamless cylinderical structure or a SWCNT. Young's modulus is independent of tube chirality, but dependent on tube diameter. The highest value is from tube diameter between 1 and 2 nm, about 1 TPa. Large tube is approaching graphite and smaller one is less mechanically stable. When different diameters of SWCNTs consist in a coaxial MWCNT, the Young's modulus will take the highest value of a SWCNT plus contributions from coaxial intertube coupling or van der Waals force. Thus, the Young's modulus for MWCNT is higher than a SWCNT, typically 1.1 to 1.3 TPa, as determined both experimentally and theoretically. On the other hand, when many SWCNTs are held together in a bundle or a rope, the weak van der Waal force induces a strong shearing among the packed SWCNTs. This does not increase but decreases the Young's modulus. It is shown experimentally that the Young's modulus decreases from 1 TPa to 100 GPa when the diameter of a SWCNT bundle increases from 3 nm (about 7 (10,10) SWCNTs) to 20 nm.

2.2.5. Electronic Properties

Electronic properties of nanotubes have received the greatest attention in nanotube research and applications. Extremely small size and the highly symmetric structure allow for remarkable quantum effects and electronic, magnetic, and lattice properties of the nanotubes. Earlier theoretical calculations and later experimental measurements have

confirmed many extraordinary electronic properties, for example, the quantum wire feature of a SWCNT, SWCNT bundle, and MWCNT and the metallic and semiconducting characteristics of a SWCNT.

In the simplest model, the electronic properties of a nanotube derived from the dispersion relation of a graphene sheet with the wave vectors (k_x, k_y)

$$E(k_x, k_y) = \pm\gamma\left\{1 + 4\cos\left(\frac{\sqrt{3}k_x a}{2}\right)\cos\left(\frac{k_y a}{2}\right) + 4\cos^2\left(\frac{k_y a}{2}\right)\right\}^{1/2}$$

where γ is the nearest neighbor-hopping parameter and a is lattice constant. γ = 2.5 – 3.2 eV from different sources and a = 0.246 nm.

When the graphene is rolled over to form a nanotube, a periodic boundary condition is imposed along the tube circumference or the C direction. This condition quantizes the two-dimensional wave vector k = (k_x, k_y) along this direction. The k satisfying $k \cdot C = 2\pi q$ is allowed where q is an integer. This leads to the following condition at which metallic conductance occurs:

$$(n - m) = 3q$$

This suggests that one third of the tubes are metallic and two thirds are semiconducting. The band gap for a semiconducting tube is give by:

$$E_g = 2d_{cc}\gamma/D \text{ [7]}$$

2.3. Characterization Techniques

Raman spectroscopy, Thermogravimetric Analysis (TGA), Scanning Electron Microscopy (SEM), Transmission Electron Microscopy (TEM), and X-ray Diffraction (XRD) are used to characterize the CNTs.

Raman spectroscopy provides some information of CNTs such as the presence of SWCNTs and the degree of graphitization of sample. Raman spectroscopy is a quick and non-destructive technique to analyze carbon sample. RBM are the peaks found at low wave number, <350 cm^{-1}. These modes created by the symmetrical expansion and contraction of the tubes around the tubes axis by the carbon atoms moving radially, and they are unique to CNTs. The presence of SWCNTs in the sample is confirmed by the appearance of RBM peaks. However, RBM peaks are not appeared in the Raman spectra of MWCNTs due to the very low intensity of RBM peaks. The low intensity is because of the peaks are broadened by the interactions between the carbon layers. The most intense peak in the spectra of CNTs is the G band that can be found around 1590 cm^{-1}. The G band is a feature of all sp^2 bonded carbon materials. While the G band is associated with high order in sp^2 bonded carbon materials, the D band is related with disorder. The D band is different from the RBM and the G band because it is a defect-mediated mode. The D band appears around 1350 cm^{-1} and is similar with the Raman band found in the spectrum of diamond. Therefore the D band has been attributed to sp^3 bonding defects in the nanotubes. A common way to measure the quality of a CNT samples is the ratio of the intensity of the D band to the G band, I_D/I_G. Pure, defect free SWCNTs have low I_D/I_G ratio. In other words, carbon atoms are sp^2 bonded with few defects. Large quantities of

impurities or defects in the nanotubes in the sample were indicated by a high I_D/I_G ratio. A typical Raman spectrum is shown as below Figure 2.4.

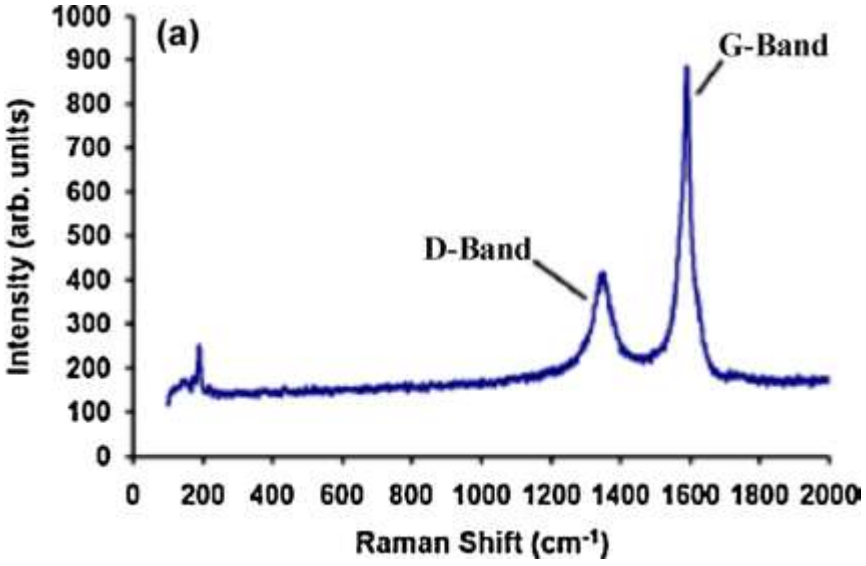

Figure 2.4.- Raman spectrum for SWCNTs samples

TGA is an analytical technique used to determine thermal stability of a material and its fraction of volatile components by monitoring the change in weight that occurs as a specimen is heated. The measurement is normally conducted in air or in an inert atmosphere, such as Helium or Argon, and the weight is recorded as a function of increasing temperature. Sometimes, the measurement is performed in a lean oxygen atmosphere ((1 to 5) % O_2 in N_2 or He) to slow down oxidation. In the case of CNTs, the weight change in an air atmosphere is typically a superposition of the weight loss due to oxidation of carbon into gaseous carbon dioxide and the weight gain due to oxidation of residual metal catalyst into solid oxides. TGA can be used to determine the percentage yield of the carbon deposit (Figure 2.5). The carbon content of the catalyst was calculated

as 100 x (m1 - m2)/m1, where m1 and m2 are the weights of the sample before and after the carbon oxidation, respectively.

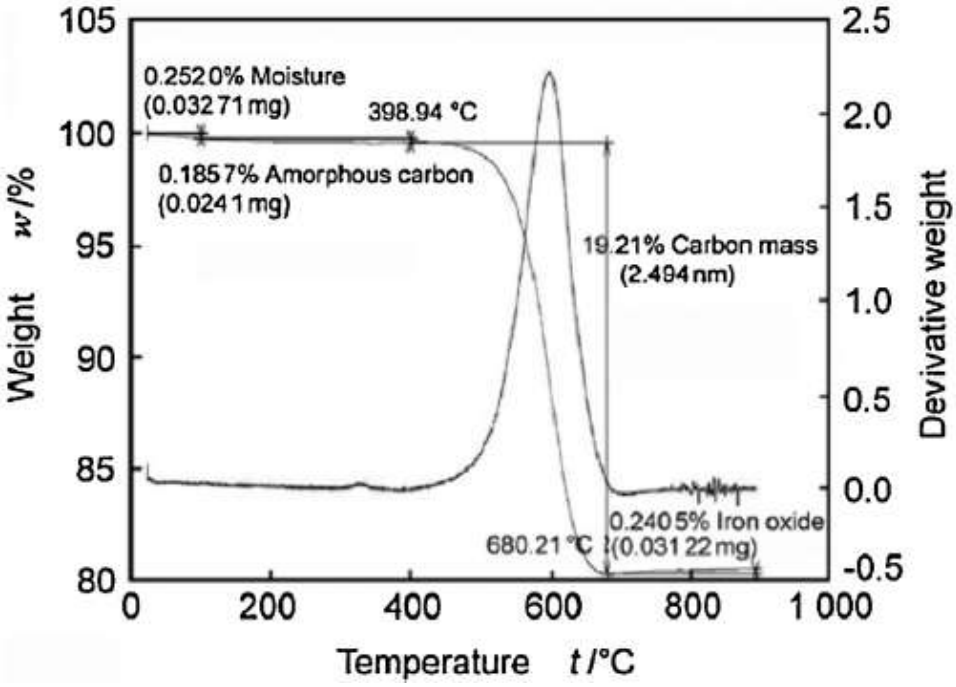

Figure 2.5.- Thermal Analysis of carbon samples

SEM is a characterization tool to examine the topography, morphology, composition and crystallographic information of materials. Electron beam is used to scan samples in a SEM. When the electron beam is moved across the surface of the sample, the charge will be accumulated on it that would affect the imaging if the sample is not conducting.

In TEM, a beam of electrons is transmitted through the sample and an image is formed onto a phosphor screen so that the image can be seen which is different with SEM. As the electron pass through the sample, internal structure of CNTs can be observed to differentiate between SWCNT and MWCNT. The diameter of CNTs can be measured from

the TEM images. Energy dispersive X-ray (EDX) spectra can be also collected to provide information about the element exists in the samples.

When X-rays interact with a crystalline substance (phase), a diffraction pattern is created. The XRD pattern of a pure substance can be described as a fingerprint of the substance because the same substance always gives the same pattern. In a mixture of substances, each gives its pattern independently of the others. The graphite peak could be observed at 26.18 due to the formation of CNTs. As can be seen in Figure 2.6, the intensity of graphite peak becomes stronger with the increase of reaction temperature. It is because the amount and quality of CNTs were increased at higher reaction temperatures. Therefore, this method is ideally suited for characterization and identification of polycrystalline phases.

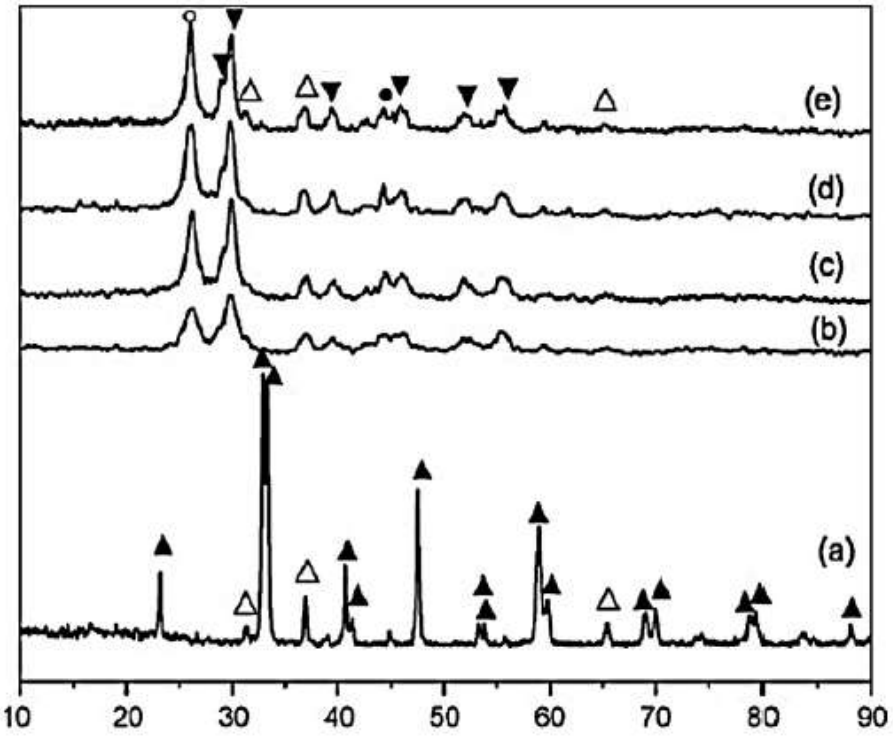

Figure 2.6.- XRD patterns of CNTs at different temperatures in presence of Co-La-O catalyst [8]

2.4. Synthesis Methods of Carbon Nanotubes

There have been a considerable efforts at synthesis and purification of MWCNT for the measurements of its physical properties. The time is, however, gradually maturing toward its industrial application. As to SWCNT, it could not be efficiently obtained at first and, furthermore, both of its purification and physical properties measurement were difficult. In 1996, it became that SWCNT could be efficiently synthesized and, since then, it has become widely studied mainly from the scientific viewpoints. In what follows, the synthesis and purification of MWCNT and SWCNT are to be summarized itemisingly. Ever since, the discovery of CNTs, several ways of preparing them has been explored. The CNTs have been synthesized by various methods e.g. electric arc discharge, laser evaporation and chemical vapor deposition. These methods are very useful and are of widespread importance.

2.4.1. Electric Arc Discharge

This method creates CNTs through arc-vaporization of two carbon rods placed end to end, separated by approximately 1mm, in an enclosure that is usually filled with inert gas at low pressure (Figure 2.7). A direct current of 50 to 100A, driven by a potential difference of approximately 20 V, creates a high temperature arc discharge between the two electrodes. The arc provides high temperatures which are needed to vaporize carbon atoms into a plasma (>3000°C).

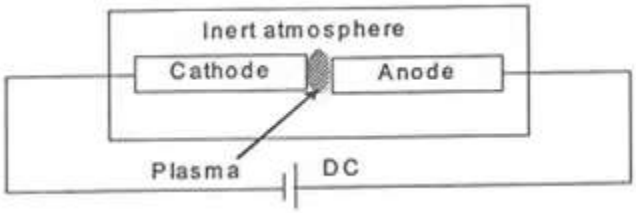

Figure 2.7.- Schematic of Arc Discharge Method

The discharge vaporizes the surface of one of the carbon electrodes, and forms a small rod-shaped deposit on the other electrode. The arc-discharge method is the one by which CNTs were first produced and recognized.

The yield of CNTs depends on the stability of the plasma formed between the electrodes, the current density, inert gas pressure and cooling of electrodes and chamber. Among the various inert gases, helium (He) gives the best results, probably due to its high ionization potential.

2.4.2. Laser Ablation

The laser furnace (Figure 2.8), which consists of a furnace, a quartz tube with a window, a target carbon composite doped with catalytic metals, a water-cooled trap, and flow systems for the buffer gas to maintain constant pressures and flow rates. A laser beam (typically a YAG or CO_2 laser) is introduced through the window and focused onto the target located in the center of the furnace. The target is vaporized in high-temperature Ar buffer gas and forms SWCNTs. The Ar flow rate and pressure are typically 1 $cm \cdot s^{-1}$ and 500 torr, respectively. The SWCNTs produced are conveyed by the buffer gas

to the trap, where they are collected. The vaporization surface is kept as fresh as possible by changing the focus point or moving the target.

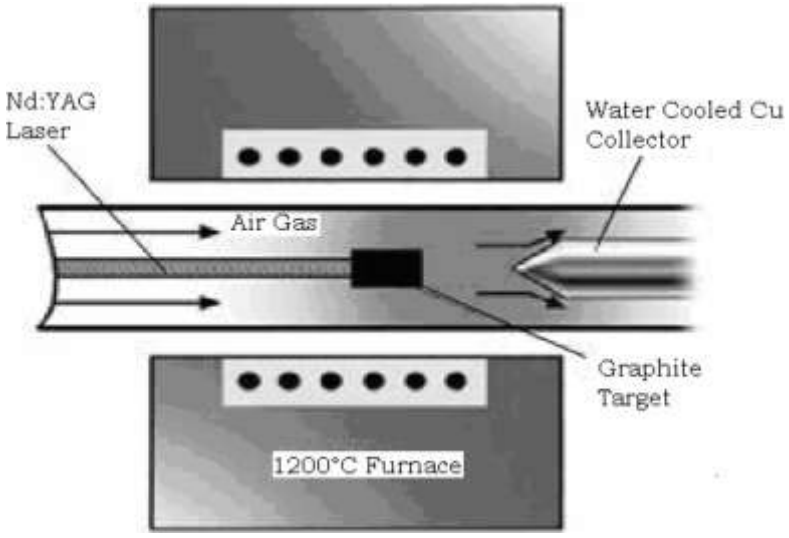

Figure 2.8.- Schematic drawing of a laser ablation apparatus

The method has several advantages, such as high-quality SWCNT production, diameter control, investigation of growth dynamics, and the production of new materials. High-quality SWCNTs with minimal defects and contaminants, such as amorphous carbon and catalytic metals, have been produced using the laser-furnace method together with purification processes. High crystallinity has been known to originate in high-power laser vaporization, homogeneous annealing conditions, and target materials without hydrogen. SWCNT diameter can be controlled by changing the furnace temperature, catalytic metals, and flow rate. However, the laser technique is not economically advantageous because the process involves high purity graphite rods, high power lasers and low yield of CNTs.

2.4.3. Chemical Vapor Deposition

The chemical vapor deposition (CVD) is another popular method for producing CNTs in which a hydrocarbon vapor is thermally decomposed in the presence of a metal catalyst. The method is also known as thermal or catalytic CVD to distinguish it from the many other kinds of CVD used for various purposes. Compared with high temperature arc-discharge and laser methods, CVD is a simple and economic technique for synthesizing CNTs at relatively low temperature and ambient pressure, at the cost of crystallinity. It is versatile in that it harnesses a variety of hydrocarbons in any state (solid, liquid, or gas), enables the use of various substrates, and allows CNT growth in a variety of forms, such as powder, thin or thick films, aligned or entangled, straight or coiled, or even a desired architecture of nanotubes at predefined sites on a patterned substrate. It also offers better control over growth parameters.

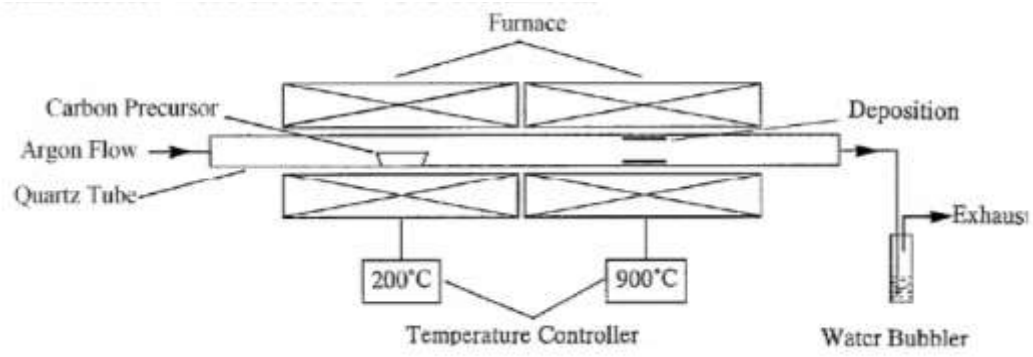

Figure 2.9.- Schematic diagram of a CVD setup

Figure 2.9 shows a schematic diagram of the setup used for CNT growth by CVD in its simplest form. The process involves passing a hydrocarbon vapor (typically for 15-60

minutes) through a tube furnace in which a catalyst material is present at sufficiently high temperature (600-1200°C) to decompose the hydrocarbon. CNTs grow over the catalyst and are collected upon cooling the system to room temperature. In the case of a liquid hydrocarbon (benzene, alcohol, etc.), the liquid is heated in a flask and an inert gas purged through it to carry the vapor into the reaction furnace. The vaporization of a solid hydrocarbon (camphor, naphthalene, etc.) can be conveniently achieved in another furnace at low temperature before the main, high temperature reaction furnace. The catalyst material may also be solid, liquid, or gas and can be placed inside the furnace or fed in from outside. Pyrolysis of the catalyst vapor at a suitable temperature liberates metal nanoparticles in situ (the process is known as the floating catalyst method). Alternatively, catalyst-plated substrates can be placed in the hot zone of the furnace to catalyze CNT growth. Catalytically decomposed carbon species of the hydrocarbon are assumed to dissolve in the metal nanoparticles and, after reaching super saturation, precipitate out in the form of a fullerene dome extending into a carbon cylinder (like the inverted test tube shown in Figure 2.10) with no dangling bonds and, hence, minimum energy. When the substrate-catalyst interaction is strong, a CNT grows up with the catalyst particle rooted at its base (known as the "base growth model"). When the substrate-catalyst interaction is weak, the catalyst particle is lifted up by the growing CNT and continues to promote CNT growth at its tip (the "tip growth model"). Formation of SWNTs or MWNTs is governed by the size of the catalyst particle. Broadly speaking, when the particle size is a few nanometers, SWCNTs form, whereas particles a few tens of nanometers wide favor MWCNT formation.

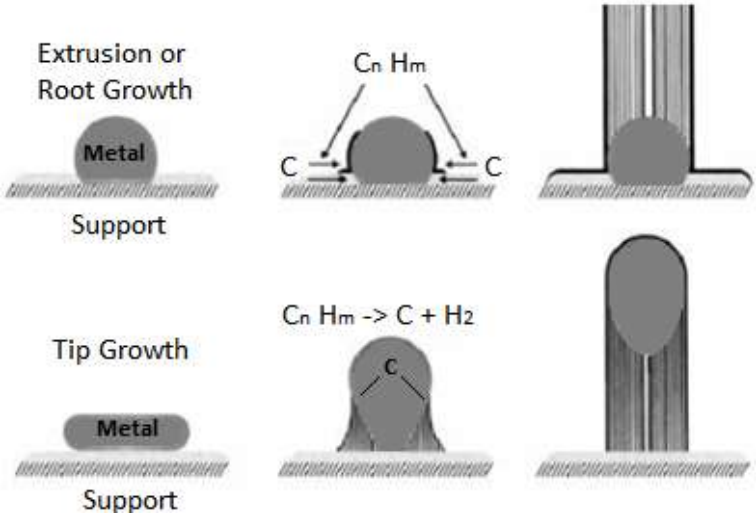

Figure 2.10.- Probable models for CNT growth

The three main parameters for CNT growth in CVD are the hydrocarbon, catalyst, and growth temperature. General experience is that low-temperature CVD (600-900°C) yields MWCNTs, whereas a higher temperature (900-1200°C) reaction favors SWCNT growth, indicating that SWCNTs have a higher energy of formation (presumably owing to their small diameters, which results in high curvature and high strain energy). This could explain why MWCNTs are easier to grow from most hydrocarbons than SWCNTs, which can only be grown from selected hydrocarbons (e.g. CO, CH_4, etc., that have a reasonable stability in the temperature range of 900-1200°C). Common efficient precursors of MWCNTs (e.g. acetylene, benzene, etc.) are unstable at higher temperatures and lead to the deposition of large amounts of carbonaceous compounds other than CNTs.

The growth of CNTs is catalyzed by transition metals. The metals such as Fe, Co, Ni are most commonly used for CNT growth, since the phase diagram of carbon and these metals suggests finite solubility of carbon in these transition metals at high temperatures. On

saturation the carbon precipitates out. This leads to the formation of CNTs under the growth mechanism outlined above. It is remarkable that transition metals have proven to be efficient catalysts not only in CVD but also in arc-discharge and laser methods. This indicates that these apparently different methods might have a common growth mechanism for CNTs, which is not yet clear. The catalyst particle size has been found to dictate the tube diameter. Hence, metal nanoparticles of controlled size can be used to grow CNTs of controlled diameter. Therefore, catalyst materials such as solid organometallocenes (ferrocene, cobaltocene, nickelocene) which liberate nanometal particles in-situ are used to catalyze CNT growth. Thin films of catalyst coated onto various substrates have also proved successful in achieving uniform CNT deposits. In addition, the material, morphology, and textural properties of the substrate greatly affect the yield and quality of the resulting CNTs. Substrates such as silica, quartz, alumina and zeolite are mostly used. The key to obtaining high yields of pure CNTs is achieving hydrocarbon decomposition on catalyst sites alone and avoiding spontaneous pyrolysis. CNTs have been successfully synthesized using organometallic compounds (nickel phthalocyanine and ferrocene) as carbon-cum-catalyst precursors, though the as-grown CNTs were mostly metal encapsulated. [9]

3. Literature Review - Treatment and Sizing of Carbon Fiber, Recovery/Recycling and Revalorization of Carbon Fibers by Synthesis of Carbon Nanotubes on Carbon Fiber

3.1. Introduction

Carbon fibers (CFs) have received much attention lately for their many potential applications in different matrix materials owing to their properties, processability, and recyclability. However, raw CFs need to be treated and/or sized as part of the manufacturing process. Designing a suitable surface-treatment method is a requisite to ensure that the high strength of the CFs is maintained during handling and composite manufacture. The surface treatment or sizing method is also equally important to ensure the formation of CF-matrix interface.

3.1.1. Oxidation of Carbon Fibers Treatment

The effects of oxidation on the CFs have been thoroughly investigated because of its importance in the fields of nuclear, medical, and materials science. Basically, the effect of the oxidation on CFs manifests as the displacement of carbon atoms from their graphitic structures. A number of oxidizing agents and gases have been used to surface treat the CFs, such as HNO_3, H_2SO_4, H_2O_2, NaOCl, $KMnO_4$, RuO_4, $NaClO_3$, $Na_2Cr_2O_7$, $NaIO_4$, air, CO_2, and H_2O.

3.1.2. Plasma Treatment

Plasma is a partially or fully ionized gas containing electrons, ions, and neutral atoms or molecules; also called the fourth state of matter. Gas plasma can be produced by introducing the desired gas into a vacuum chamber, typically 0.1–10 Torr, and subsequently exciting the gas using radiofrequency energy. The free radicals and electrons created in the plasma collide with the exposed surface of the material, rupturing covalent bonds and creating free radicals. Plasma composed of inorganic gases such as argon, helium, hydrogen, nitrogen, and oxygen leads to the implantation of atoms, radical generation, and etching reactions while plasma composed of organic gases such as hydrocarbons and alkylsilanes leads to polymerforming reactions. Gases as O_2, air, Ar/O_2, F_2, CF_3CH_2F, NH_3, CO_2, Ar, He.

3.1.3. Other surface modification methods

Radiation. Methods used for the oxidation of such nonpolar CF surfaces. Each of the methods mentioned above might cause a loss of fiber strength if the treatment is excessively extended. Similarly, gamma ray or neutron radiation changes the microstructure of the carbon materials and causes losses in the mechanical properties at high radiation doses. It is known that the radiation affects the crystal lattice by either the displacement of atoms within the lattice or electronic excitation. The electrons stripped from the atoms are believed to cause dimensional (topographical) change in the CFs and

create active sites on the fiber surfaces, which may bind with the functional groups of the bulk polymers.

Fluorination. Recently, several studies pertaining to the fluorination of CFs have been published. The degree of fluorination depends on the nature of the fibers and fluorination method used. A large amount of the intercalated fluorine could be obtained using either well-graphitized structure or more extensive fluorine treatment at higher temperature and pressure. The reaction of fluorine and graphite at low temperature is kinetically hindered by the formation of covalent C–F bonds on the outer surface, which prevents further migration of fluorine into the interplanar space, and thus further fluorination. The fluorination of the CFs, in particular the formation of graphite intercalation compounds or covalent and insulating graphite fluorides, (CF)n or (C_2F)n, strongly influences the physical properties such as layer structure and tensile and interfacial strength.

Polymer Coating. Wei et al. reported the grafting of polyesters onto the surfaces of the vapor grown carbon nanofibers (VGCF) by the anionic ring-opening alternating copolymerization of epoxides with cyclic acid anhydrides initiated by COOK groups introduced onto the VGCF surface. In addition, the electrical properties of the conductive composites prepared from the polyester-grafted VGCF were investigated. They investigated the stability of the dispersion of poly(SO-alt-PAn)-grafted HDVGCF in THF. The untreated HDVGCF precipitated within 1 d as mentioned above. On the contrary, poly(SO-alt-PAn)-grafted HDVGCF yielded a stable dispersion in a solvent, such as THF, suitable for grafted polyesters. The precipitation of poly (SO-alt-PAn)-grafted HDVGCF was scarcely observed even after 4 weeks. The grafted polyester chains were mainly grafted onto the

edges of VGCF because of the presence of the carboxyl groups on the edges. However, it seemed that the grafting of the polyester onto the wall of the VGCF had also proceeded. Both polyester chains on the edges and wall of VGCF played an important role in the destruction the entanglement.

Grafting with Inorganic Materials. Recently, the surfaces of the CFs have been modified with inorganic materials such as silica, metals, and carbon nanomaterials. Deng et al. prepared the two-dimensional ultrathin mesoporous $NiCo_2O_4$ nanosheets on the CF paper (CFP) through a facile solvothermal method combined with post-thermal treatment. The well-interconnected ultrathin $NiCo_2O_4$ nanosheets directly grown on the carbon nanofibers would allow for easy diffusion of the electrolyte, shorten the transport path of ions and electrons, and accommodate the strain during cycling. The Ni–Co precursor nanosheets were uniformly grown on the carbon nanofibers, forming a large-scale conformal coating.

Du et al. prepared a novel and sensitive CF electrode (CFE) modified with graphene flowers and used to simultaneously determine ascorbic acid (AA), dopamine (DA), and uric acid (UA). They found that the layered petal graphene flowers homogeneously bloomed on the surface of the CFE. Moreover, sharp and obvious oxidation peaks were found at the resultant electrode, in contrast with the CFE and glassy carbon electrode (GCE), for the oxidation of AA, DA, and UA.

Shazed et al. prepared the growing carbon nanotubes (CNTs) on the surface of the high-performance CFs. The growth of the CNT on CF was conducted via floating catalyst

chemical vapor deposition (CVD). CNT was vigorously grown on the surface of the CF at 800 and 700 °C. The high density of CNT was desirable owing to the purpose of the production of high-performance fiber-reinforced composites. However, the coatings were found to be more uniform with minimal clumping and agglomeration at 700 °C. It was deduced that under the given experimental conditions, higher temperature led to a higher degree of catalyst agglomeration, which affected the homogeneous growth of the CNT. Furthermore, a lower synthesis temperature was desirable to minimize the heating energy and protect the CF from being damaged by unnecessarily high heat levels. The growth of CNTs was of the multiwalled type. After 30 min of reaction time, it could be seen that a coating with an apparent thickness of 3 μm had been established. [10]

3.1.4. Sizing

The commercially available CFs are normally coated by a sizing layer on the surface, which usually is either a solution or emulsion consisting of polymeric components. The presence of sizing in the CFs/sizing and sizing/matrix interfaces plays an important role in controlling certain properties of the composites. Conventional sizing such as film formers, emulsifiers, antistatic, and coupling agents is generally designed to protect the fiber surface and promote the adhesion between the fiber and matrix. The sizing could alter the handling of the CFs, which includes protection, alignment, and wettability of fibers. The typical sizing materials include epoxy, polyester, nylon, urethane, and others.

The application of sizing is normally termed either size or finish and could beachieved by:

- deposition from solution of a polymer
- deposition of a polymer onto fiber surface by electrodeposition
- deposition of a polymer onto fiber surface by electropolymerization
- plasma polymerization

Recently, sizing agents containing CNTs were used to size the glass fibers or fabrics in order to improve the mechanical or electrical properties of glass fiber composites. Liu et al. disclosed a sizing approach to fabricate the CNT/CF-hybrid fiber in detail by employing a sizing agent containing MWCNTs. MWCNTs were chemically modified with an amine monomer and mixed with thermoplastic polymer sizing agent. After the modification, the MWCNTs were uniformly dispersed in the sizing agent. Unsized CF tow was sized using the sizing agents containing MWCNT, while the CNT/CF-hybrid fiber was fabricated. The MWCNT–COOH was reacted with phthalazinone-containing diamine (DHPZDA) in dimethyl formamide (DMF) at 130 °C followed by the addition of dicyclohexylcarbodiimide over 6 h under uninterrupted stirring to introduce the amine monomer on the surfaces of the MWCNTs (marked as MWCNT–DHPZDA). It was found that the CNTs were attached to the fiber surface along the outer edges of the grooves and a hierarchical structure was observed in all the images. It was also observed that there were wide and deep grooves along the axial direction of the CFs before and after sizing. This indicated that the PPEK

absorption did not fill the grooves on the fiber surface because of the nano-sized thickness of the sizing agent layer [10].

3.2. Recovery/Recycling and Revalorization of Carbon Fibers

Recovery of carbon fibers by recycling thermoset composites is highly desirable from both economic and environmental perspectives; reducing waste disposal of scrap from production parts and end-of-life products. Revalorization of recovered/recycled carbon fibers from end-of-life thermoset composites is being developed by synthesis of CNTs directly on surface carbon fibers to produce reinforcements which can be used in new high-performance composite materials with exceptional mechanical, thermal and electrical properties.

The composites industry has increased globally; in 2000, the European consumption of thermoset composites reached 106 tons per year; in 2005, plastics production in Japan was over 6.1 million tons and more than 210 million tons worldwide, and in 2008, the global demand of carbon fibers reached 20,000 tons per year. The advantages of composite materials are many, including monolithic construction of components, lower density, high resistance and relatively good behavior in fatigue compared to metals in structural applications such as aerospace and automotive. Consequently, manufacturers are increasing the percentage of composite materials used in aircraft and automobiles, such that, the latest designs of commercial aircraft are being constructed with more than 50% in weight of composites, namely, carbon fiber and epoxy resin systems. The

mechanical properties of recovered carbon fibers, specifically tensile strength, is one of the most important outputs from a reuse standpoint, the revalorization is then the best approach for processing of recovered/recycled carbon fibers in order to develop new reinforcements for new high-performance materials.

Fiber reinforced composites have been widely used in aerospace applications because of their high performance and their ability to vary fiber architecture to meet final performance requirements. Performance of composite materials depends not only on properties of fiber and matrices, but also on the interface between them. Good interfacial adhesion provides composites with structural integrity and efficient load transfer from fiber to matrix. Carbon fiber-reinforced composites, in particular, have enabled remarkable improvements in structural performance due to their desirable and tailorable mechanical properties. However, ultimate performance of carbon fiber composites can be limited by resin dominated properties such as interlaminar shear strength or by longitudinal fiber compression.

The aim of recycling processes is to reduce environmental impact by reusing materials in a more sustainable way. In general, it makes sense to try to recover as much economic value from a material in a recycling operation since the value of a material represents to a large extent the input of resources needed to produce the material or the scarcity of the material. Recycling processes in which a more valuable recyclate is produced are therefore likely to reduce environmental impact the most and they are also more likely to be cost effective. Recycling polymer composites based on thermoset matrices is much more difficult as the polymer cannot be remolded. Recycling processes have therefore been

developed to separate and recover valuable materials from thermoset composites that have the potential to be reused.

A number or recycling technologies have been proposed and developed for thermoset composite materials and these are summarized in Figure 3.1. Mainly, there are three categories of process: those that involve mechanical comminution techniques to reduce the size of the scrap to produce recyclates; and those that use thermal and/or chemical processes to break the scrap down into materials and energy.

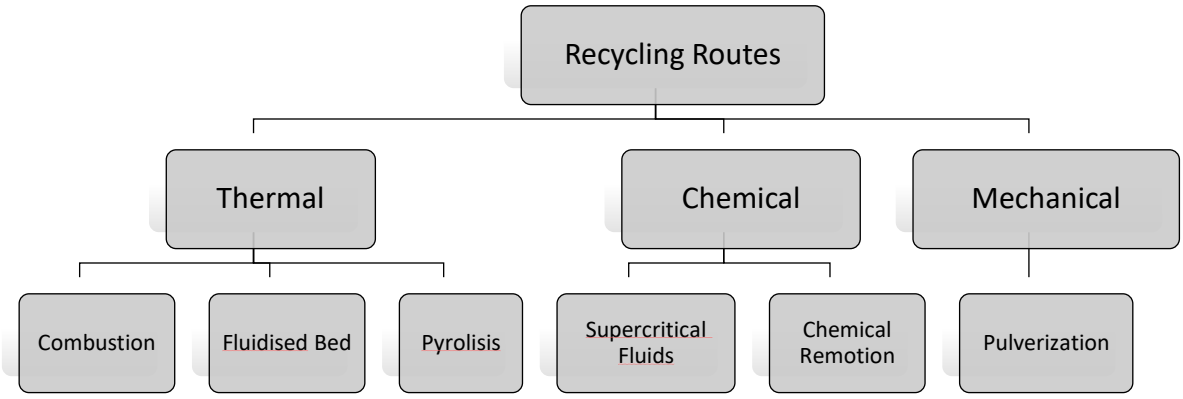

Figure 3.1. - Potential recycling processes for thermoset composite materials.

Mechanical techniques can recycle all of the composite material, but the recyclate does not usually provide the same function as the original material and so there is a reduction in value. The simplest thermal process is combustion with energy recovery. Whilst this is a robust process capable of dealing with a wide range of different materials, only the energy value in the scrap composite is recovered. Pyrolysis and other chemical processes have the advantage of being able to recover material from the polymer separated from the

inorganic components of the composites, such as carbon fibers. In some pyrolysis processes the fibers recovered are contaminated with char and in general the processes are less tolerant of mixed and contaminated materials. In a thermoset composite the most valuable constituent within the material is usually the reinforcement fiber, particularly in the case of carbon fiber composites, where the value of the carbon fiber is typically an order of magnitude greater than that of the polymer. In the fluidized bed thermal process the aim is to recover high grade fiber from carbon fiber reinforced thermoset composites. This is done by removing the polymer from the fiber by an oxidative thermal process to yield clean fibers. The process also has the advantage of being tolerant to mixed and contaminated materials and so it is particularly suitable for recycling waste composites from end-of-life products. [2]

Incorporating highly conductive and high strength elements between fibers, tows, and lamellae; it could also be possible to create robust networks which controllably bridge resin rich areas to significantly improve mechanical, thermal and electrical properties. Both chemical and physical methods have been explored for increasing the adhesion between the fiber and matrix, including surface treatments, fiber wiskerization and roughening. However, these methods can also introduce mechanical defects onto the fiber and create bulky or impenetrable additional phases around the fiber. By directly growing nanomaterials with a high aspect ratio and desirable thermal, electrical and mechanical properties onto the reinforcing fiber, it is anticipated that hybrid fibers with highly tailored surface area and properties can be created with either improve ultimate properties or new functionality within a structural composites. Many studies have sought

to improve the properties of high performance composites through addition of nanomaterials into the resin, CNTs are thought to be promising candidates for selective reinforcement of matrix-rich interlaminar regions due to their nanoscale diameter, high aspect ratios and desirable mechanical, electrical, and thermal properties. These same attributes are also useful for the modification of interfacial properties. When properly designed, CNTs have the potential to work with carbon fiber to make multifunctional, lightweight structural composites with superior strength.

Growth of CNTs at the surface of carbon fibers to create hierarchical carbon structures is a promising approach for improving mechanical, electrical, and thermal properties of a structural composite. [17]

CNTs have been the subject of much interest in recent years, due to their attractive mechanical properties (1000 GPa Young's modulus), tunable electronic behavior (conducting or semi-conducting depending on tube chirality), and unique dimensions (1–100 nm diameter, up to several cm length). As a result of these properties, nanotubes have potential applications in many fields, including composite reinforcement [1].

Their use in polymeric matrices can be double, either aiming at the synthesis of a material with specific functional or structural requirements. Based on their exceptional tensile strength and modulus, CNTs are deemed to improve the tensile properties of the composite material and increase the fracture energy once a crack is initiated [17].

Exceedingly high mechanical properties of the CNTs have attracted attention for the development of super strong light weight structures. In order to effectively translate the

extreme mechanical properties and low densities of CNTs into strong composite structures, a sufficient volume fraction of CNTs should be dispersed into the matrix, possibly aligned parallel to the load direction [17].

Applications for the reuse of the recovered carbon fibers are being investigated while revalorization is an interesting prospect for technological-commercial scale operations.

3.3. Synthesis of Carbon Nanotubes on Carbon Fibers by Chemical Vapor Deposition

Several variations of the chemical vapor deposition method have been used to synthesize CNTs on carbon fibers, these experimental variations, proposed mechanisms, results of the experimental developments and characterization of the resulting materials are of special interest for this research. Different CVD methods have been employed to investigate the effect of growth condition. These procedures vary in both growth temperature (800 °C, 750 °C and 700 °C) and the flow rate of the carbon source/catalyst (xylene/ferrocene) mixture (10 sccm, 5 sccm and 5 sccm, respectively). These procedures have been previously shown to yield high density, long, and uniformly covered CNT arrays with different orientation on quartz substrates. In each case, a small bundle of less than 100 carbon fibers are spread across a ceramic tray and placed into a quartz tube. The tube is purged with argon, raised to the specified temperature and injected with the reactive gas mixture for 5, 10, 15 and 30 min. The schematics of this method is shown in Figure 3.2.

Before the sample was removed, the tube and sample was cooled under flowing argon to room temperature. [17]

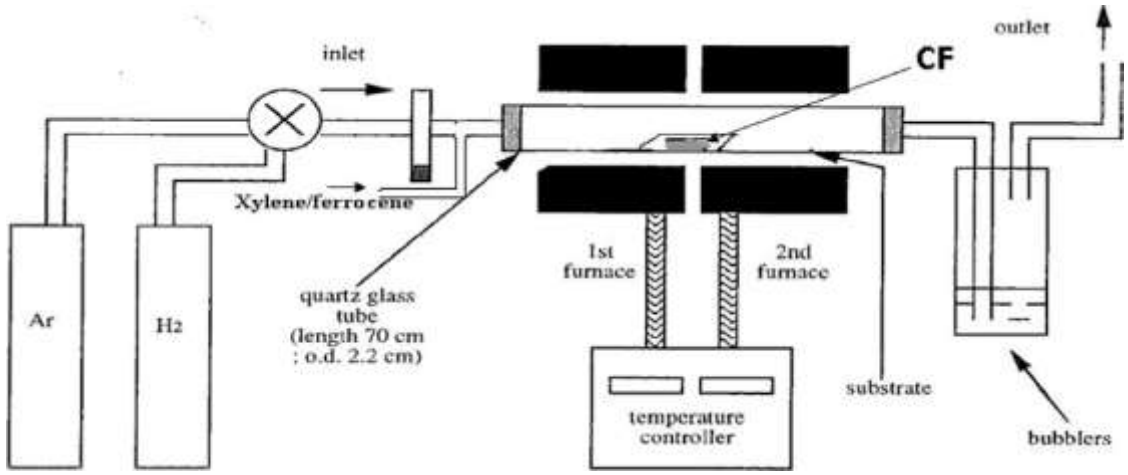

Figure 3.2.- Schematic illustration of the procedure for the growth of CNTs on the carbon fibers. A vapor mixture made from a 0.01 g/ml mixture of ferrocene in xylene is carried with flowing argon and hydrogen to the heated quartz chamber with outside tube temperature of 700–800 °C. CNT's grow upon a carbon fiber substrate within the quartz tube for a given length of time.

The growth of CNTs using vapor phase CVD, modeled after the spray pyrolysis method has also been employed. Three mixtures have been used: one of 3 wt.% ferrocene ($(C_5H_5)_2Fe$) dissolved in benzene, one at 8 wt.% ferrocene in benzene, and one of 5 wt.% $NiCl_2$ dissolved in equal quantities methanol and benzene. These reactant mixtures were stored in a syringe and dispensed through a 27 gauge needle into an argon jet ranging between 6 • 104 sccm and 9 • 104 sccm, which sprayed the reactant solution into a 27 mm inner diameter tube furnace held at 850 °C. In some cases, a slower, 200–400 sccm argon flow has been used, and the reactant solutions have been allowed to slowly evaporate into the argon, rather than being sprayed into the chamber. Reactants were dispensed at rates between 0.1 ml/min and 1.0 ml/min, with the rate controlled by

pressurizing the open end of the syringe; the equipment used is shown in Figure 3.3. Growth began in the vapor phase and continued on quartz substrates, and would last between 10 min to nearly 5 h, with 5–25 ml reactant solution consumed. [1]

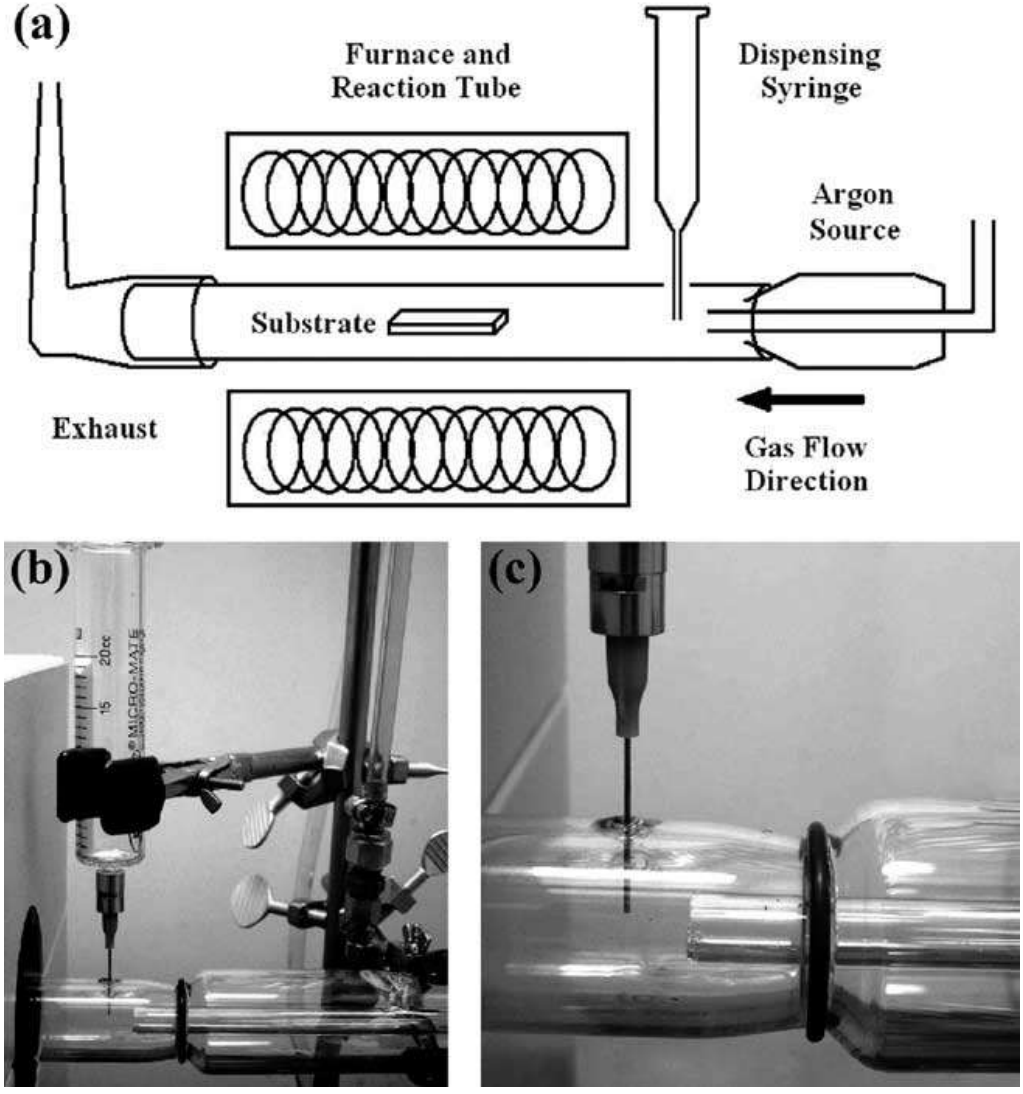

Figure 3.3.- (a) Schematic of complete furnace and reactant introduction assembly used for spray pyrolysis (b) and (c) close up view of syringe and needle position and argon jetting apparatus.

With these methods a novel composite material, made of a carbon fiber core, both PAN and Pitch-based, coated with a 3-dimensional distribution of CNT has also been

recently obtained. The CNT synthesis catalyzed by Ni clusters previously deposited on the fiber surface using electro-deposition technique (ELD) and the CNT growth process performed with the hot filament chemical vapor deposition (HFCVD) technique [17].

CNTs have been grown on the carbon substrates kept inside the quartz reactor by thermal decomposition of hydrocarbons, e.g. toluene in presence of iron catalyst obtained by the decomposition of the organometallic like ferrocene. In an experimental setup, a single zone furnace instead of conventional two zone furnace was used. The furnace provided a constant temperature zone of 18 cm in the centre. The carbon substrates were kept in the quartz reactor placed inside the furnace muffle as shown in Figure. 3.4. The reaction zone was maintained at 750 °C. Once the temperature is reached, the solution containing a mixture of ferrocene and toluene in particular proportion (0.077 g ferrocene in 1 ml toluene) is injected in the reactor at a point where the temperature is 200 °C. Argon is also fed along with the charge as a carrier gas and its flow rate adjusted so that the maximum amount of precursor is consumed inside the desired zone. A blank CVD run was carried out to assess the quality of the CNTs produced inside the reactor. Once the uniform growth of the tubes was ensured, experiments were performed with different carbon substrates of known weight placed in the constant temperature zone of the reactor. All the experiments were run under identical conditions [17].

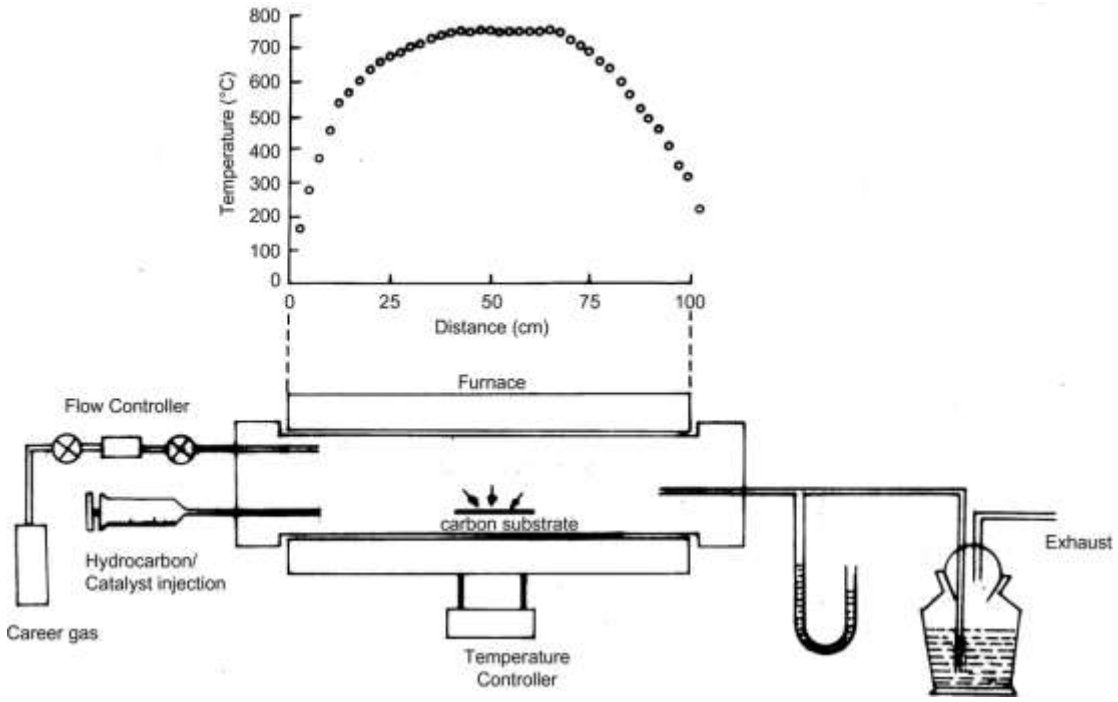

Figure 3.4.- Schematic diagram of the CVD reactor along with the temperature profile.

3.4. Proposed Mechanisms of Synthesis of Carbon Nanotubes on Carbon Fibers

In order to fully optimize the production of CNTs, the growth mechanisms involved in their formation must be completely understood, and a number of theories have been proposed to describe this growth. One mechanism to describe the formation of CNTs, in the presence of a metal catalyst is based on the processes involved in carbon fiber formation; carbon diffuses into nanometer-scale catalytic particles. When the solubility limit within the metal is reached, this carbon precipitates out with a graphitic structure. Depending on the size of the catalyst particle, graphite, carbon filaments, or CNTs can form (in order of decreasing particle size and increasing particle curvature). As more

carbon is deposited on the catalyst, it will either diffuse into or over the surface of the particle and become incorporated into the graphitic lattice, increasing the tube's length. During the formation of carbon fibers or nanotubes, the original catalyst particles will either remain fixed to the substrate (called root growth) or detach from the surface and remain encapsulated within the opposite end (called tip growth). A mechanism explaining the vapor phase growth of CNTs with continuous catalyst availability describes that nanotubes nucleate and grow by a tip growth mechanism. Metal catalyst particles initially rise with the tube tips as they grow, although friction between the particles and the tube walls eventually causes the particles to become fixed in place. Growth would slowly occur on the open tube tip until another catalyst particle deposited, restarting the process. In vapor phase growth, which occurs in the spray pyrolysis samples, as the metal catalyst and carbon source enter the furnace chamber, both compounds are broken down to form free metal and carbon atoms. The metal atoms can aggregate into small, nano-sized particles, which serve as the basis for nanotube growth. The diffusion of carbon into these clusters begins to occur soon after the formation of the particles themselves. Carbon saturation is quickly reached, and the precipitation of graphite starts, as described in the root growth model. These nanotube ‘‘embryos’’ then reach and affix to the surface of the substrate. Once a number of these embryos have attached to this surface, additional growth will cause adjacent nanotubes to come into contact, impinging and supporting each other. As the tubes lengthen, this impingement will cause the tube growth to be directed perpendicular to the substrate surface, forming the densely packed, well-aligned mats observed experimentally; this process is illustrated schematically in Figure 3.5. The loss of

alignment occasionally observed at substrate edges (where exposed tubes are not completely surrounded by adjacent tubes), further suggests that interactions and ‘‘crowding’’ between tubes is the cause of the good nanotube alignment observed.

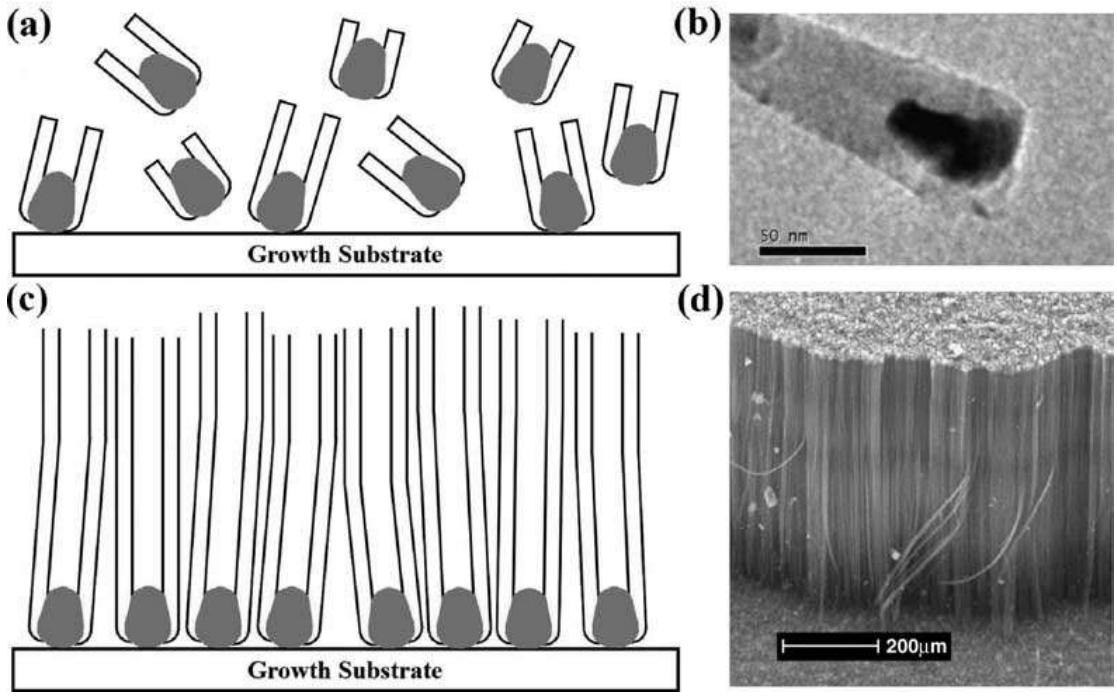

Figure 3.5.- Initial CNT growth mechanism (a) CNT ‘‘embryos’’ form in the vapor and deposit on substrate, (b) TEM image of nanotube end showing catalyst particle shape (50 nm scale bar), (c) continued growth, high surface density causes alignment, (d) SEM image of densely packed, well-aligned CNT sample (200 lm scale bar).

As the tube grows past an encased particle, it remains open, as described by the root growth theory. Additional metal atoms could travel down this open channel, and combine with the catalyst cluster. By this method, the encapsulated metal particle could increase in volume beyond its initial size. Constraining forces from the walls of the encapsulating nanotube would confine the catalyst particle to a fixed diameter, so any additional growth would have to be in the axial direction, resulting in a particle with a high aspect ratio; this

process is shown in Figure 3.6. The diameter restriction provided by the inner nanotube walls also explains why the widths of all the particles observed in the middle of nanotubes matched the inner diameter of those CNTs. The eventual length to which a particular particle could grow would be determined by the availability of additional catalyst material and the growth rate of the CNT itself. Fast nanotube growth relative to catalyst particle elongation would decrease the likelihood of metal atoms reaching the catalyst particle (having to travel an increasing distance down the tube), and in these cases the formation of new trapped particles would be preferred.

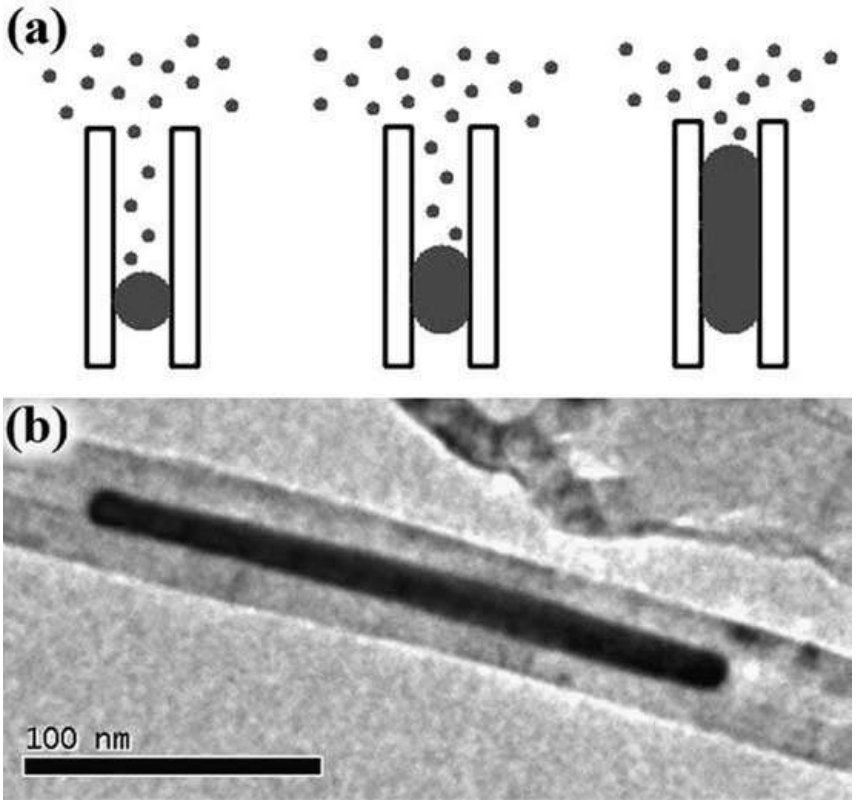

Figure 3.6.- Method of formation of high aspect ratio metal catalyst particles (a) accumulation of metal catalyst atoms in open tube end, and the elongation of the trapped particle, (b) experimentally observed high aspect ratio catalyst particle encapsulated within nanotube walls.

In addition to free catalyst atoms in the vapor, nanotube ‘‘embryos’’ will continue to form and exist in the vapor. If a nanotube ‘‘embryo’’ deposits on an exposed open end, a slightly different process would occur, as illustrated in Figure 3.7. If an ‘‘embryo’’ of smaller diameter reached the open tube end, it would be encased in the original tube, and both the existing and the new, smaller diameter tube would continue to grow, forming a multiwalled tube with a thicker wall than before, as shown in Figure 3.7a. If an embryo of similar or greater size were to deposit on the exposed end, it would join with the existing tube in order to minimize the strain energy of the graphitic sheets surrounding the particle. However, the new, larger diameter tube would effectively terminate the growth of the original diameter tube, and continued growth would be as a larger diameter tube, as in Figure 3.7b. If a smaller nanotube embryo became attached at a slightly different angle to the original tube, the forces from the original tube walls would dominate and cause the tube to continue growth in the original direction. A larger tube could also cause the direction of nanotube growth to change, as illustrated in Figure 3.7c. Additionally, because the growth end of the nanotube remains open even after a new particle in encapsulated, not only can the aspect ratio of the new particle be increased, but the process can be repeated, leading to multiple particles encased inside a single tube; this was observed repeatedly in the CNTs produced by vapor phase growth and never observed in tubes grown using thermal CVD. [1]

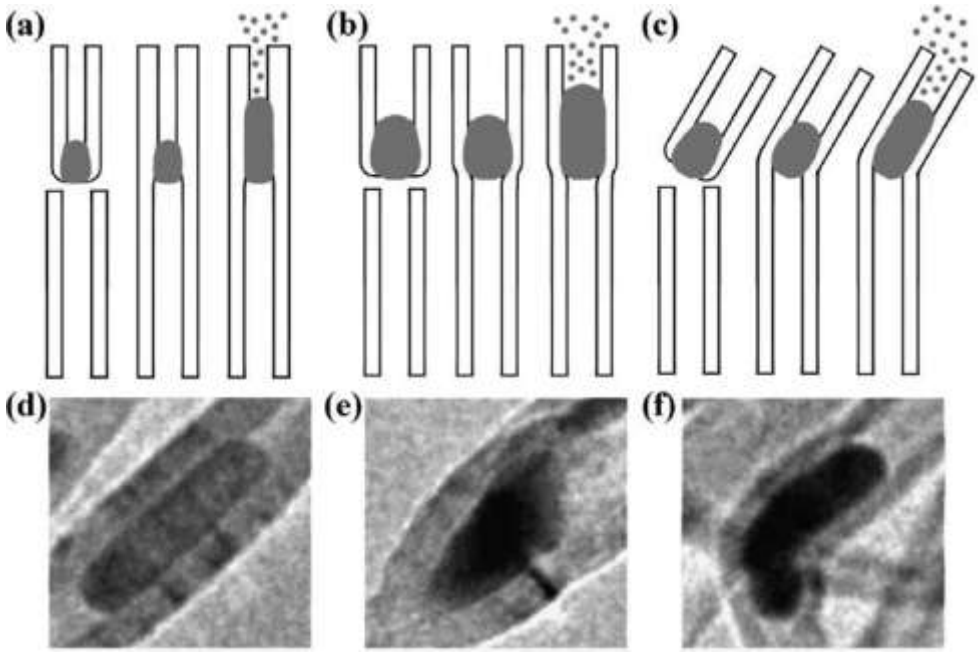

Figure 3.7 (a)–(c).- Schematic diagrams of metal catalyst particle encapsulation within an existing CNT, (a) incorporation of a smaller CNT embryo in an existing tube end, (b) incorporation of a larger CNT embryo, (c) change in growth direction caused by CNT embryo incorporation, (d)–(f) TEM micrographs of experimentally observed examples of (a)–(c), respectively.

3.5. Previous Experimental Results of Synthesis of Carbon Nanotubes on Carbon Fibers

3.5.1. Synthesis of Carbon Nanotubes on Carbon Fibers

CNTs are being produced by CVD method. Figures 3.8 and 3.9, respectively, show the SEM and the TEM micrographs of the CNTs produced inside the reactor during the blank run. It is seen from the Figures that the CNTs are multiwalled with outer diameter in the range of 10–60 nm and their lengths ranging in several microns. As seen from Figure 3.9 the catalyst particles are encapsulated inside the nanotube cavity [17].

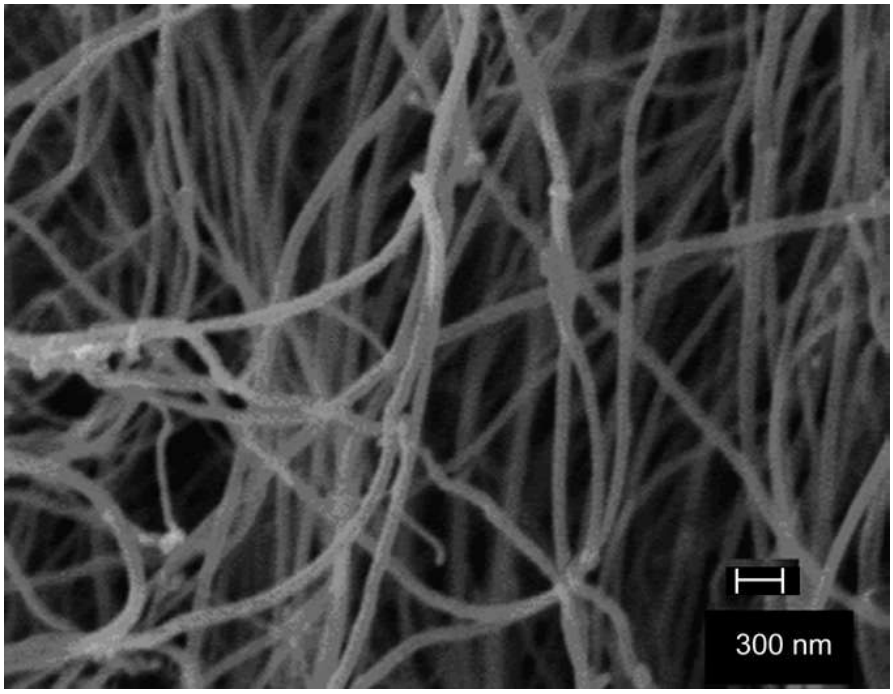

Figure 3.8.- SEM micrograph of the CNTs produced by CVD.

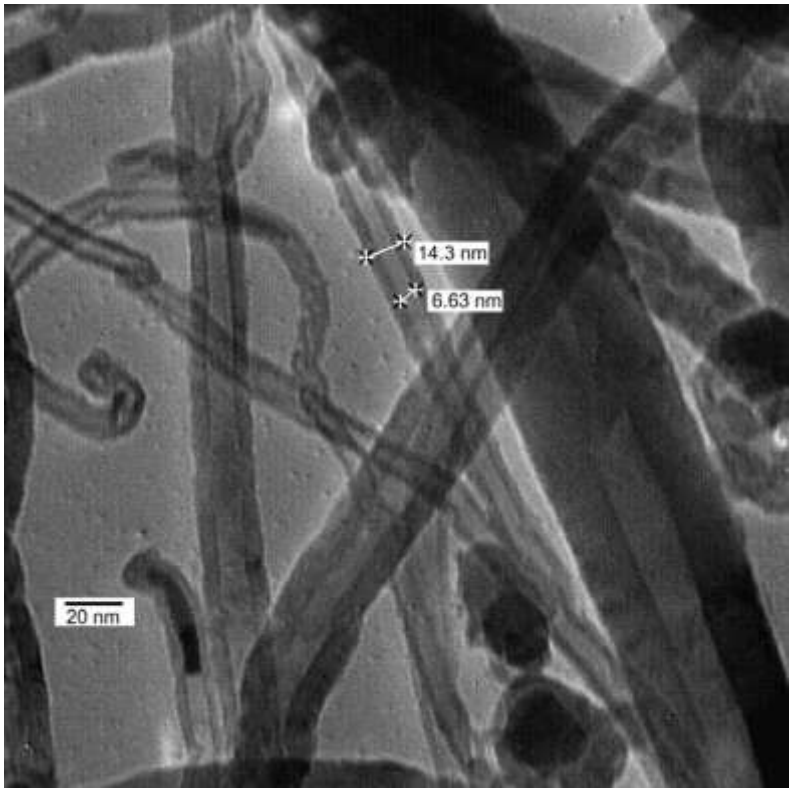

Figure 3.9.- TEM micrograph of the CNTs produced by CVD.

SEM micrographs of CNTs grown on the bunch of carbon fiber tows are shown in Figure 3.10 a and b. It should be mentioned here that all these micrographs are taken on the samples which have been ultrasonically treated to remove any loose material sticking to the substrate. The micrograph shows a uniform anchoring of CNTs on the individual carbon filament suggesting carbon fiber surface equally attractive growth surface like silica or quartz. It was observed that though the amount of CNTs deposited on the substrate increased with deposition time, but the growth rate was found to be non-linear and tends to taper off with time. This is quite evident from the samples taken out after different time intervals. The sample shown in the Figure 3.10a contains 9.1% by weight of CNTs grown after 90 min where as it was 8.82 g after 60 min of deposition time. The trend was found to be similar for the other two substrates as discussed in the following text. The micrograph in Figure 3.10b suggests that the initial growth of CNTs is on the available carbon fiber surface. Once the complete carbon surface is saturated, further growth of CNTs is in the form of ropes surrounding the carbon fiber bundles itself. These CNTs form bridges between the adjacent carbon filaments. Composites formed by using these carbon fiber tows are named UD hybrid composites.

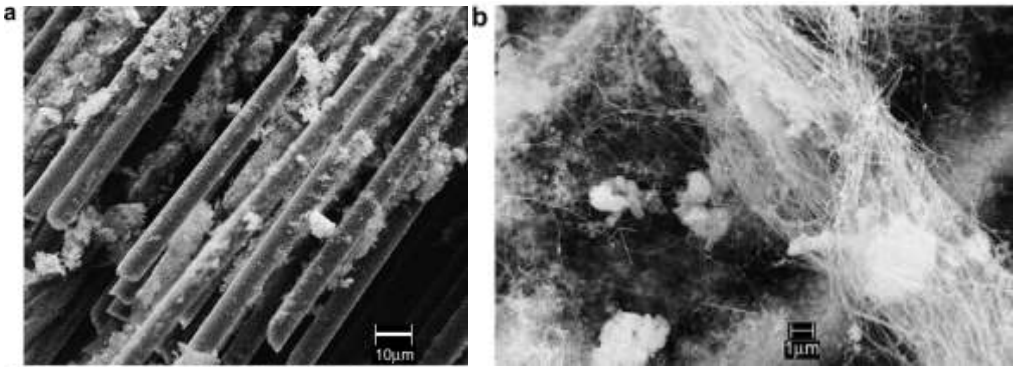

Figure 3.10. (a and b) SEM micrographs of CNTs grown on carbon fiber tows after ultrasonication

Figure 3.11 shows a very uniform growth of CNTs on the carbon cloth substrate. The amount of nanotubes deposited is around 8% after 90 min. The magnified view in the inset shows quite dense and entangled CNTs between individual carbon filaments and also inside the voids between the cross-over points of these tows. Composites formed by such hybrid preforms are named 2D hybrid composites.

Figure 3.11.- SEM micrograph of CNTs grown on carbon fiber cloth after ultrasonication

The carbon fiber felt offers a 3D carbon fiber network. It was found that in such type of network about 18.4% by weight of CNTs could be introduced in 90 min of deposition time which is almost double than what could be achieved with previous two substrates. The large weight gain in case of felt is due to the growth of tubes inside the fine porosity

developed by the carbon fiber network as a result of large exposed surface area. Figure 3.12a shows that the individual filament of carbon felt is coated with CNTs very uniformly as in the case of UD and 2D networks. Figure 3.12b shows that the CNTs are strongly anchored on the carbon fiber surface by forming bridges/scaffolding between the filaments.

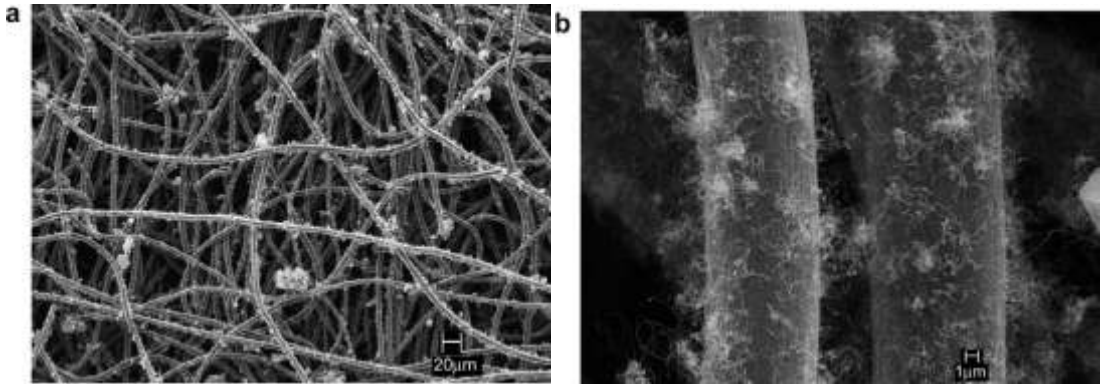

Figure 3.12.- (a and b) SEM micrograph of CNTs grown on carbon fiber felt after ultrasonication.

The growth of CNTs on the carbon fiber surface by CVD processing has been varied by changing three parameters: (1) growth temperature, (2) flow rate of the carbon source/catalyst mixture, and (3) growth time. These parameters not only affect CNTs morphology, density and coverage, but also can significantly impact mechanical properties of CNT/CF assemblies. The investigation of these factors was performed using CVD procedures which vary in temperature (700 °C, 750 °C and 800 °C) and feed rate of the hydrocarbon/catalyst vapors (5 sccm and 10 sccm) as a function of CNT growth time on unsized (T650-35) and sized (T650-UC-309) carbon fiber surfaces. The morphology of CNTs/CF and the CNT density were characterized by SEM.

According to the CNT growth mechanism, the CNT density and morphology on the carbon fiber surface could be influenced by either the feed rate or temperature. Figure 3.13 shows SEM images of CNTs/CF ‘‘as-grown” samples that were grown for 30 min at different temperature and flow rates. From these images, we can see that morphology and density (coverage) of CNTs are different with various temperature and xylene/ferrocene mixture flow rate. At a temperature of 700 °C, the density of CNTs on the carbon fiber surface is very low. Some researchers have attributed this to the low solubility of carbon in iron catalyst at temperature lower than the carbon–iron eutectic temperature of 723 °C. The insufficient thermal activation of ferrocene decomposition by the iron catalyst needed for the nucleation and/or of growths processes on the carbon fiber surface may also play a role. As the growth temperature increased from 700 to 750 °C, the density of CNTs on carbon fiber surface increased substantially. With the further increase in growth temperature from 750 to 800 °C and the feed rate from 5 to 10 sccm, the morphology of CNTs changed from being predominantly aligned and uniform in length to predominantly non-aligned and variable in length. The increase in array disorder with increased temperature and flow rate is likely due to the activation of competing nucleation and growth mechanism. At a moderate temperature of 750 °C and a lower feed rate of 5 sccm, the kinetics appear to favor stable growth of CNT to produce aligned CNTs with uniform lengths.

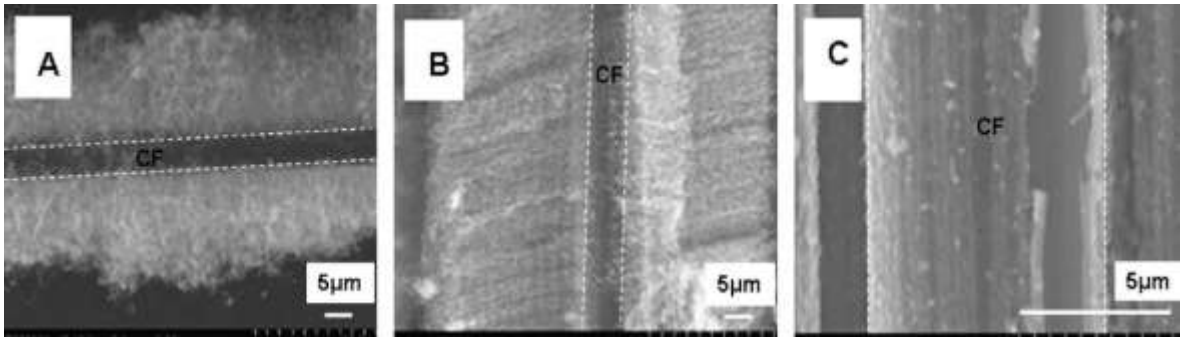

Figure 3.13.- The effect of CVD temperature, xylene: ferrocene flow rate, and time (temp/rate/time) on CNT morphology procedure A: 800 °C/10 sccm/30 min, procedure B: 750 °C/5 sccm/30 min; and procedure C: 700 °C/5 sccm/30 min

In addition to dictating CNT morphology with processing condition, growth time is another important variable that can be used to both understand the growth process and tailor the interfacial properties of the resulting assembly. In this study, the CNT morphologies on sized and unsized T650 fibers were examined as a function of growth time at two growth temperatures (800 °C and 750 °C) by high resolution SEM. Figure 3.14 displays typical CNT morphology as a function of growth time for 5, 10, 15 and 30 min at 800 °C and 750 °C, respectively. From these results, several trends can be inferred. Early nucleation and growth of CNT appears to be favored for the unsized T650 fiber in comparison to the sized

T650 as more growth occurs earlier in both cases. At 750 °C (Figure 3.14A (a & b)), it appears that very little CNT grows before 5 min. However, at 800 °C (Figure 3.14B (a & b)), the growth has progressed to the point that the unsized fiber 5 min morphology appears similar to that of the same fiber at 10 min at 750 °C. In the case of the growth at 800 °C, the enhanced early growth for the unsized fiber is consistent with the time required to

achieve uniform coverage (10 min for unsized vs. 15 min for sized fiber). At 750 °C, the time to achieve uniform coverage is earlier for the sized fiber than unsized fiber (15 min vs. 30 min). However, this may be due to the fact that unsized fiber grown for 15 min at 750 °C tended to grow relatively long CNT's at selective sites rather than uniformly across the entire surface. Though the fibers for this study grown at 750 °C were not as aligned as previously observed in Figure 3.13, they did maintain a more consistent length at 30 min than the disordered tubes grown at 800 °C which appeared denser and thicker. These trends are largely consistent with the enhanced flow rate and kinetics of the decomposing ferrocene for the CNT's grown at 800 °C. It also illustrates that with sufficient time, uniform coverage similar to that obtain for system which deposit catalyst directly onto the CF surface can be obtained [17].

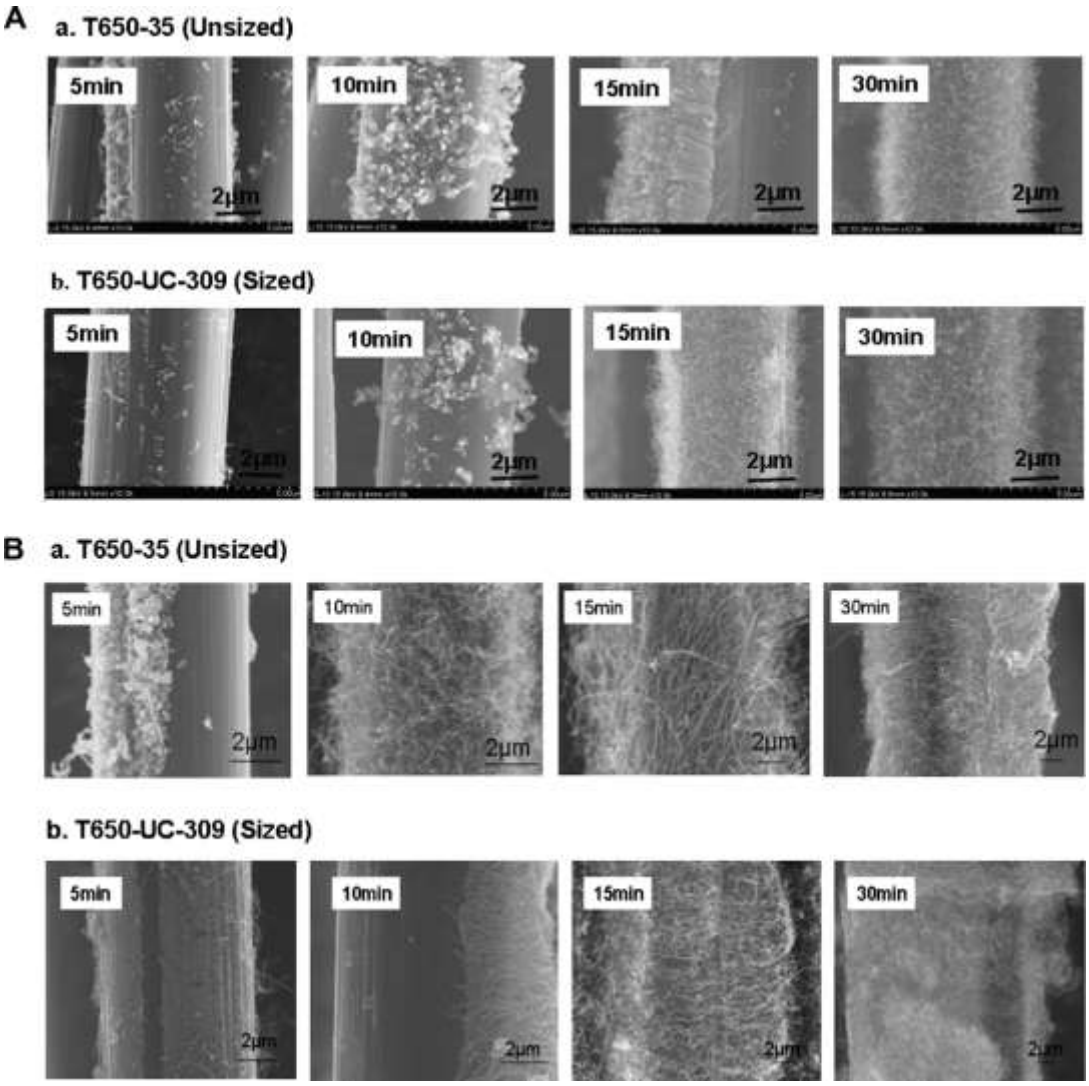

Figure 3.14.- CNT morphology as a function of growth time at (A) 750 C and 5 sccm for (a) T650-35 and (b) T650-UC-309, and at (B) 800 C and 10 sccm for (a) T650-35 and (b) T650-UC-309.

3.5.2. Anchorage of Carbon Nanotubes on Carbon Fibers

Hierarchical structure of CNTs on the carbon fiber surface could enhance the interfacial bonding between matrix and carbon fiber due to the significantly increase in surface area, morphology modulation, and chemical interaction. The presence of CNTs at the fiber–matrix interface is expected to enhance the reinforcement matrix bonding when the CNTs

are well attached to the fiber surface and resin has sufficiently penetrated into the CNTs array. The research result has shown that randomly oriented CNTs and aligned CNTs coated carbon fiber demonstrated a 71% and 11% increase in interfacial shear strength over unsized carbon fiber based on epoxy matrix. More detailed investigations on the interfacial shear strength of similar CF/CNT assemblies using a single fiber segmentation test in epoxy indicate shear strength values approaching those of highly optimized sized T650/35 fiber with good resin penetration. Another method for assessing the relative attachment strength of the CNTs to the CFs surface involves exposing the assemblies to a range of solvents while either in a low shear mixer or an ultrasonic baths. For example, it has been previously reported that CNTs which were grown on thin Ni films deposited by Plasma Vapor Deposition (PVD) were entirely removed with ultrasonic treatment in acetone due to the weak attachment strength. For this study, a small amount CNT/CF (about 2.0–2.5 mg) of unsized T650 fibers with CNTs grown at 800 °C with a flow rate of 10 sccm for 30 min were placed into four different liquids (10 ml of distilled water, acetone, methanol and isopropanol) and then placed in either an ultrasonic bath or a low shear (magnetic) mixer for 15 min. Before treatment, the fibers were uniformly coated with a dense and disordered CNT network as shown in Figure 3.13a. Aside from sample exposed to ultrasound in water which expanded slightly, the network of CNTs surrounding the carbon fiber were generally unperturbed as seen in Figure 3.15 and demonstrated good bonding between the CNT and the CF surface [17].

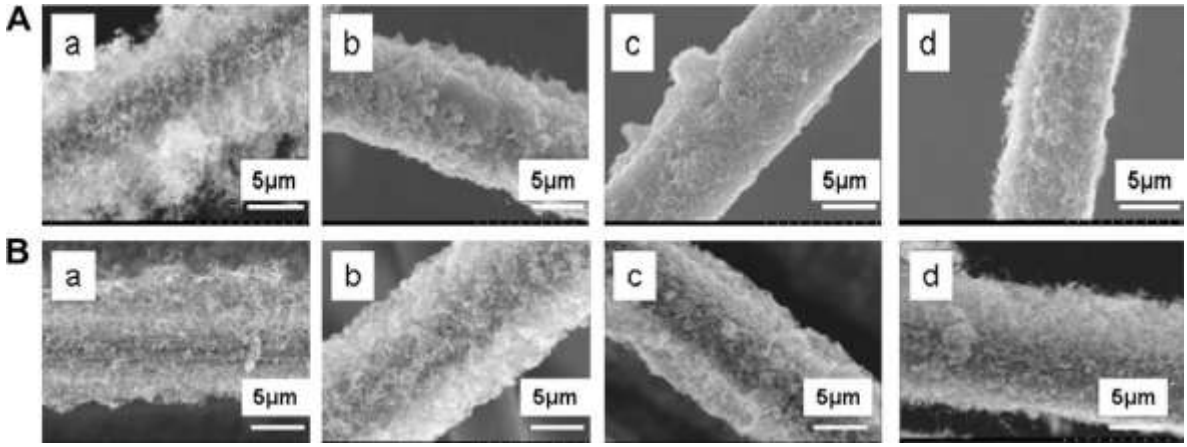

Figure 3.15.- SEM images of CNT/ CF after 15 min treatment A: 15 min in bath ultrasound in: (a) water, (b) acetone, (c) methanol, (d) isopropanol and B: 15 min in magnetic stirrer in: (a) water, (b) acetone, (c) methanol, (d) isopropanol.

The anchorage between CNTs and carbon fibers (via the Ni clusters) has also been tested after the growth process with simple immersion and ultrasonic bath treatment both with deionized water and acetone. The ultrasonic bath was a Sonica 5300 (with an estimated power density of 0.035 w/cm3 at the frequency of 45 kHz). All the treatments lasted for 5 min.

After the CNT growth process, the fiber bundle was fully infiltrated with a CNT network having a homogeneous and dense 3-dimensional distribution as seen in Figure 3.16.

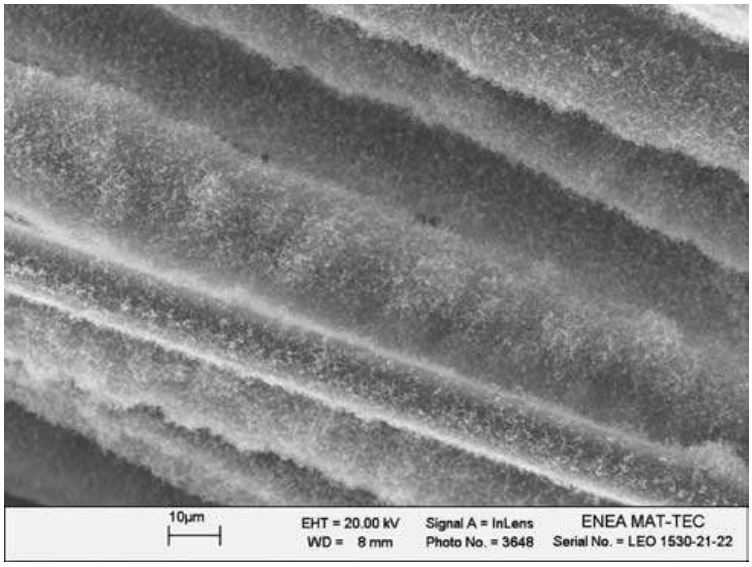

Figure 3.16.- CNT growth on carbon fibers.

The immersion of the coated fibers in deionized water and acetone for 5 min did not result in any significant morphological difference. The network of CNT was still surrounding the fiber, as shown by SEM micrograph Figure 3.17.

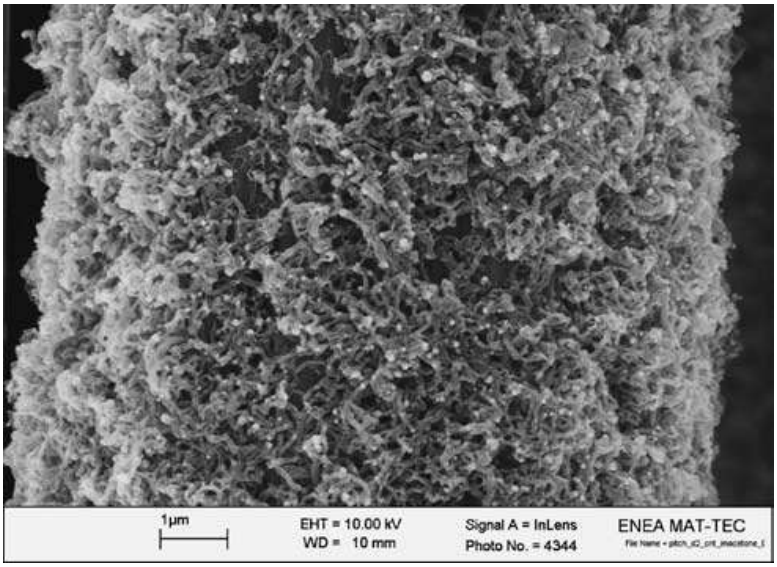

Figure 3.17.- CNT on carbon fiber after immersion in acetone for 5 min.

Samples were immersed and treated in ultrasonic bath for 5 min both in water and acetone. Figure 3.18 shows the CNT still anchored to the carbon fiber support, after ultrasonic bath in deionized water. On the lower panel of the picture, the cleanness and entanglement of the CNT network are shown at higher magnification. The CNT survived also the ultrasonic treatment in acetone.

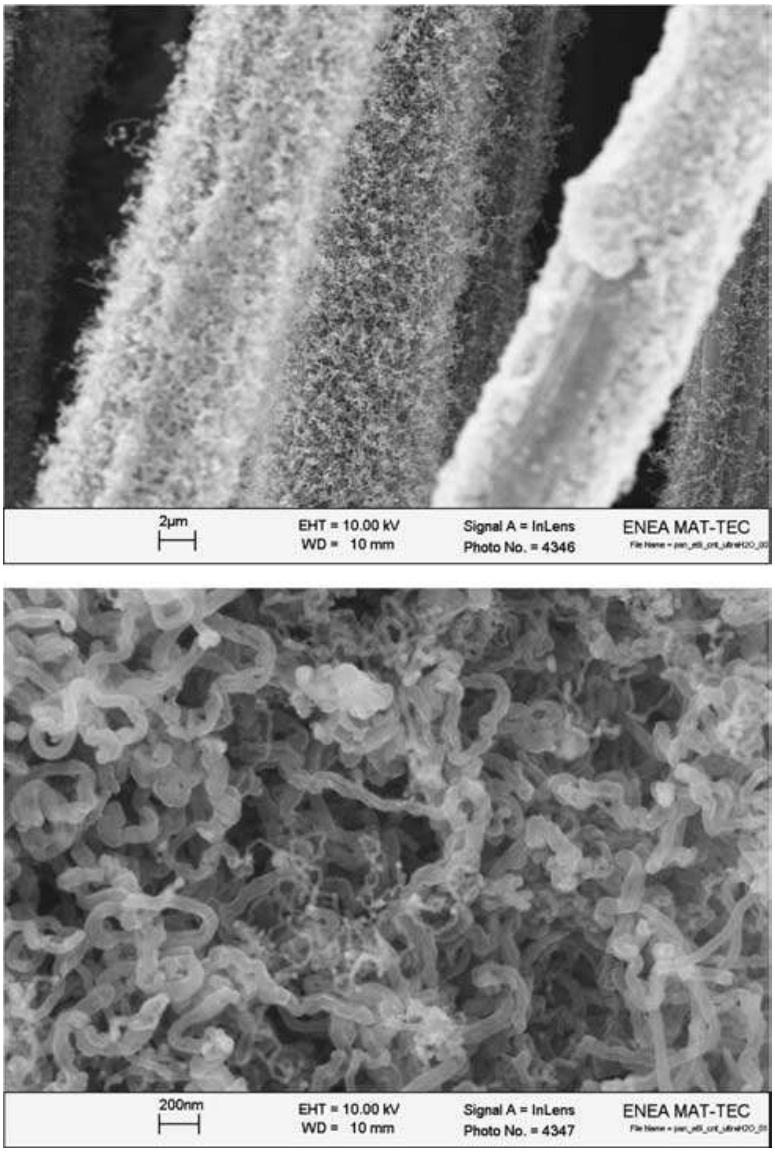

Figure 3.18. CNT on carbon fibers after ultrasonic bath in deionized water for 5 min.

Pseudo-mechanical tests performed on different samples, both before and after the CNT growth, revealed a good anchorage between CNT and carbon fibers The above results suggest the possibility to use the carbon fibers coated with CNT as reinforcement for low weight structural composites. This material, combining microscale (CFs) with nanoscale constituents (CNTs), allows in principle the dispersion of a high volume fraction of CNT throughout the composite and it is also expected to enhance the mechanical performance of polymeric matrix composite [17].

3.5.3. Thermogravimetric Analysis of Carbon Fibers with Carbon Nanotubes

The TGA run shown in Figure 3.19 suggests that there is no weight loss up to 500 °C, after which a sharp weight loss is observed with the DTG peak at 550 °C. The weight loss in this region is due to the oxidation of MWNTs present in the sample. Absence of any weight loss in the low temperature region, i.e. between 300 and 400 °C suggests the absence of amorphous carbon in the sample. However, we do not observe any weight gain in the temperature range <300 °C, which generally results from the oxidation of the catalyst present in the sample, suggesting the absence of bare catalyst particles, i.e. Fe in the deposits. No weight loss is observed beyond 600 °C. The total weight loss up to 1000 °C was calculated to be around 88% due to oxidation or burn out of CNTs. The remaining 12% weight could, therefore, be due to either iron catalyst or its oxide present in the sample as impurity [17].

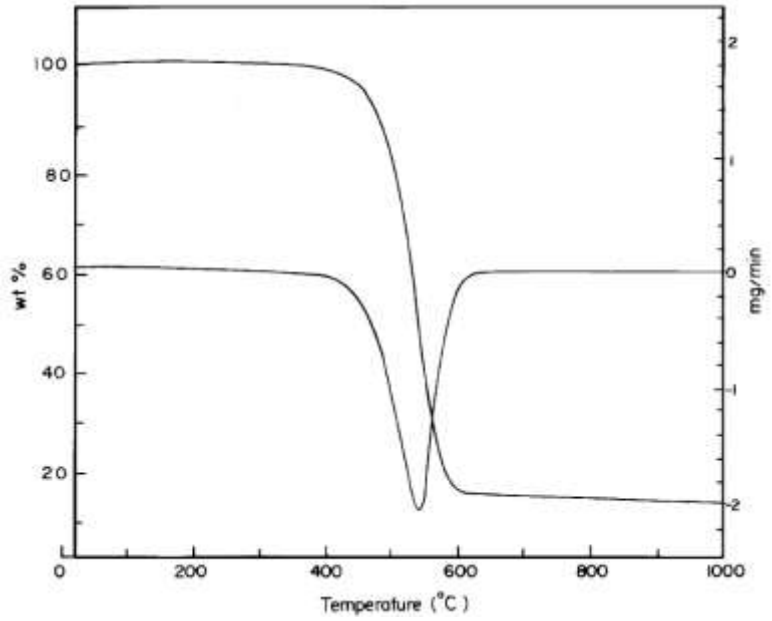

Figure 3.19.- TGA/DTA analysis of the as produced CNTs inside the reactor

Figure 3.20 displays the weight loss (left axis) and weight loss derivative (right axis) results for ‘‘as received” sized IM-7 in comparison to a carbon fiber with CNT grown at 800 °C for 30 min upon the surface. It was assumed that the pronounced weight loss near 580 °C involved the complete oxidation of CNT to gaseous products. Using the procedure previous discussed in the experimental section, CNT morphologies, such as the length and average diameter, can be determined by SEM imaging. The mass fraction of different materials can be measured on area under derivative weight loss curve by TGA testing. Assuming a regular array of CNTs having the measured average diameter, the measured average length, and an individual nanotube density of 1.4 g/cm^3; the CNT population density at the carbon fiber surface can be calculated to be as high as 8.0 x 109 tubes/cm^2. The results of SEM and TGA demonstrated that CVD can be successfully used to synthesize

CNTs on carbon fibers with high density, high coverage, and selectable CNT morphology by controlling growth conditions such as temperature, time and/or flow rate. [10]

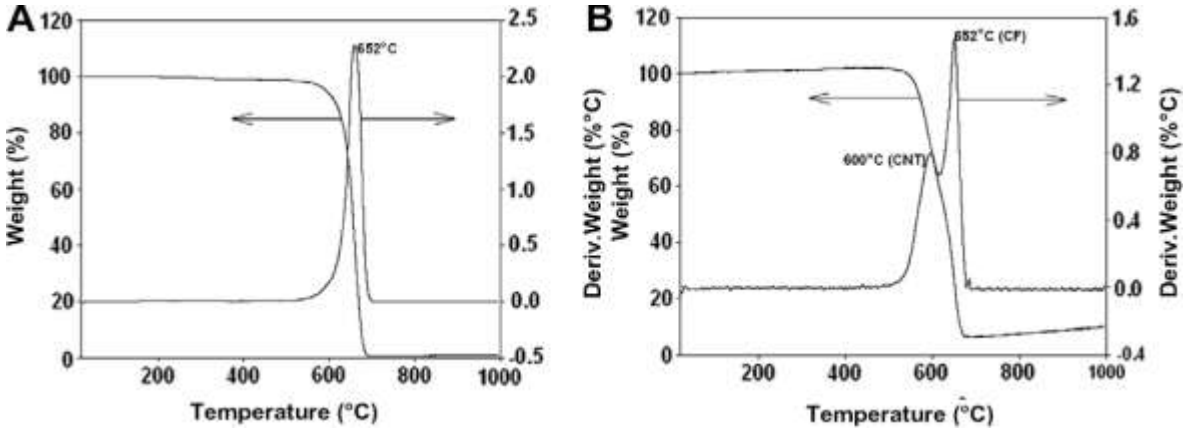

Figure 3.20.- TGA results for ‘‘as received” IM7 fiber (A) and CNT cover fiber (B) in air with a heating rate of 10 °C/min.

3.5.4. Mechanical Properties of Carbon Fibers with Carbon Nanotubes

The bonding between the fiber and the matrix is a crucial parameter controlling the load transfer between the composite constituents. The presence of CNT as filler of micro pores at the fiber–polymer interface could enhance the reinforcement–matrix bonding by providing mechanical interlocking between the fibers and the matrix by means of the nanotubes. This would also alleviate the problem of agglomeration when these are randomly introduced in the neat CNT–polymer composites.

Figure 3.21 shows the variation of flexural strength and flexural modulus of the UD hybrid composites with increasing amount of CNTs w.r.t carbon fibers as reinforcement. As shown in the Figure the flexural strength first decreases with respect to the single component (carbon fibers with 0% CNT) values with lower fractions of the CNTs and picks up with increasing volume or wt.% of CNTs. The initial decrease in the properties can be attributed to the fact that these low concentrations of the CNTs simply acts as defects rather than the true reinforcement. It is assumed that the growth of the tube is bottom up, i.e. the catalyst particle first deposits on the carbon fiber surface and becomes a nucleus for the growth of CNTs. It may also react with the carbon fiber surface at this temperature (750 °C) and create a defect. These defects then acts as stress concentration centers and thus leads to premature failure of the composites. The effect is offset with the higher concentration of the tubes so that the improvement in the strength of the composite is more than the loss in strength due to creation of defects on the carbon fiber surface. The observation suggests that in the first few minutes of deposition, most of the available carbon surface is used as substrate for the growth of CNTs. Further increase in deposition time results in the random growth of tubes between the filaments and finally starts wrapping up the bunch of tows. The improvement in the composite FS can therefore be attributed to the additional reinforcement of CNTs which also share the stress transfer along with the carbon fibers. As shown in the Figure the strength increases to 580 MPa for the hybrid composite as compared to only 471 MPa for the neat carbon fiber composites. The overall improvement is thus nearly 20%. The FM of the composites also show a similar initial dip before it picks up to a value of 56 GPa, an improvement of

~28% over the pure CF based composites. The improvement in the FM could be due to introduction of the CNTs in the structure possessing higher stiffness as compared to CFs (YM of MWNT ~1000 GPa, as compared to 230 GPa for T-300 grade CFs).

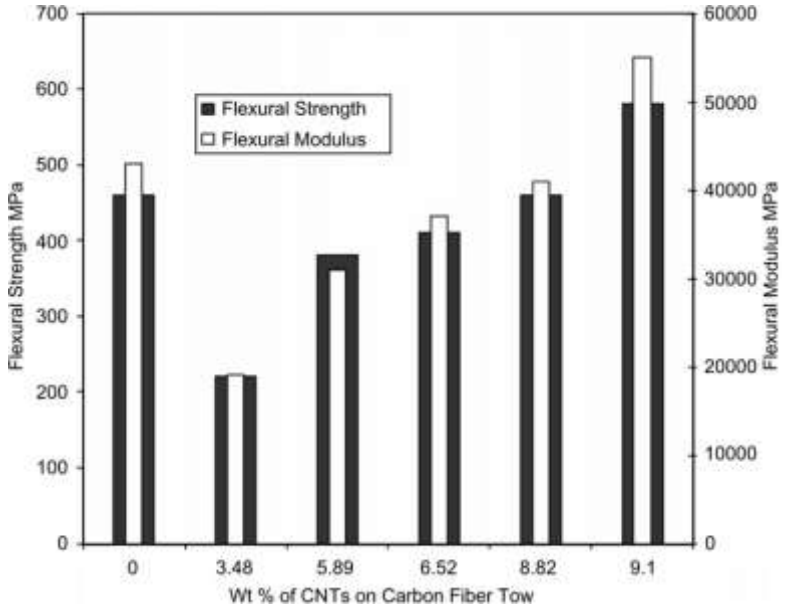

Figure 3.21. Mechanical properties of UD CF–CNT composites with increasing nanotube contents.

The mechanical properties of the CF cloth–CNT hybrid composites are plotted in Figure 3.22. As in the case of UD CF tows the strength of the hybrid composites first decreases up to 0.44 wt.% of CNT deposition and increases thereafter. The overall improvement in the flexural strength of the composite properties achieved in these samples is about 75% over the as produced cloth composites. This is quite unexpected since the weight of CNTs in both the cases, i.e. UD-CF tows and the cloth, is same, i.e. 8% only. It seems that the morphology of the carbon network is playing a major role in the translation of strength in the hybrid composites. As discussed earlier, in case of carbon fiber cloth there are spaces between the carbon fiber tows crossing each other (warp and wefts) and these become

favourable sites for CNTs to grow inside them. As such we do not find wrapping around of additional tubes as in case of UD tows, but additional growth of CNTs fill up these voids which are otherwise weak points in the cloth. The CNTs reinforcement at these sites seems to be responsible for such a high percentage increase in the FS value of CF cloth–CNT hybrid composites. It could be argued that the additional growth of CNTs with time on the cloth contribute usefully whereas similar addition in case of UD tows does not contribute significantly in the load transfer. The improvement in the FM is also higher comparatively, i.e. 54% over the neat CF cloth based composites.

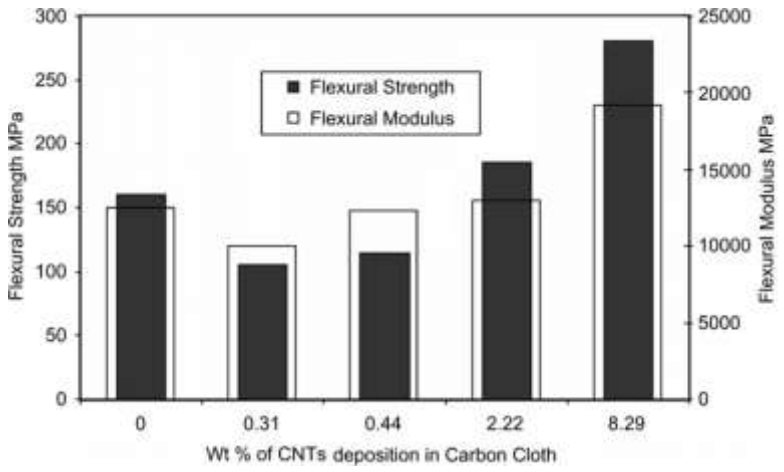

Figure 3.22.- Mechanical properties of carbon fiber cloth–CNT composites with increasing nanotube contents

The fracture behavior of the composites with low CNT contents and high CNT contents of the composites is shown in Figures 3.23 and 3.24. The carbon fiber pull out seems to be more in case of low loading of CNT than the one with higher amount of CNTs. We do not see any nanotube pull out or breakage as in case of neat CNT based polymer composites. It therefore confirms that the addition of nanotubes helped in creating interlocking

between the fibers and the matrix. The shear delamination of the hybrid composite is thus reduced and is reflected in their improved mechanical properties.

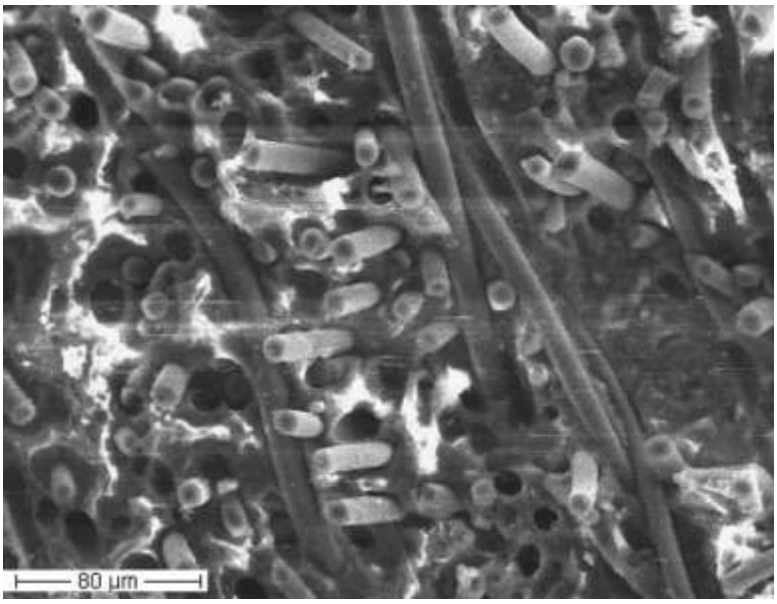

Figure 3.23.- Fracture behavior of carbon fiber cloth–CNT composites with 0.44 wt.% CNT.

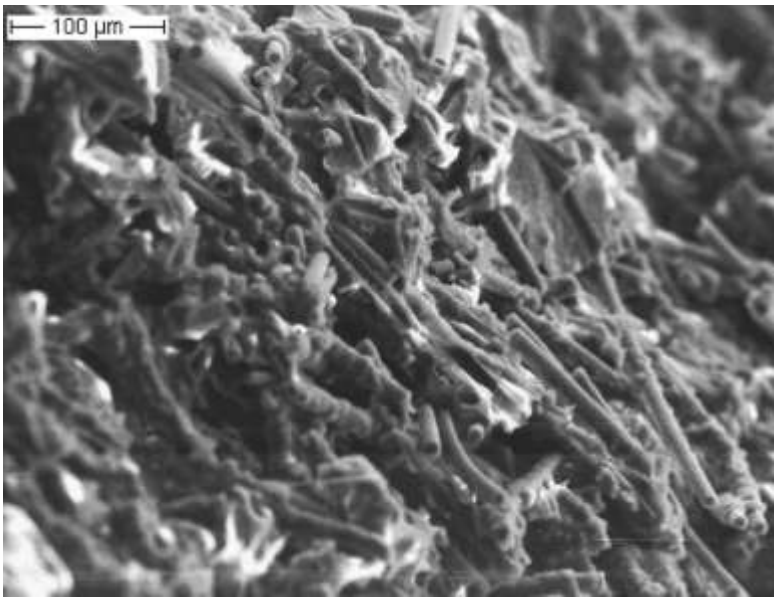

Figure 3.24.- Fracture behavior of carbon fiber cloth–CNT composites with 8.29 wt.% CNT.

The variation in the flexural strength and modulus of carbon fiber felt based hybrid composites is plotted in Figure 3.25. Interestingly the initial dip in the strength in these composites is much less as compared to the previous samples. As discussed earlier the rate of deposition/growth of CNTs on the felt is much higher as compared to other two substrates and the maximum amount of CNTs grown was found to be 18% which is almost double than that for UD and 2D networks. This can be attributed to the high porosity in the felt samples and a large exposed surface area of the carbon fibers as compared to previous two networks. The overall improvement in the strength of CNT grown felt composite is ~66% over the composite with only felt as the reinforcement. Such behavior shows that in case of carbon fiber felt a strong three dimensional network is introduced by the growth of CNTs which overcome the shear failure of the resulting composites

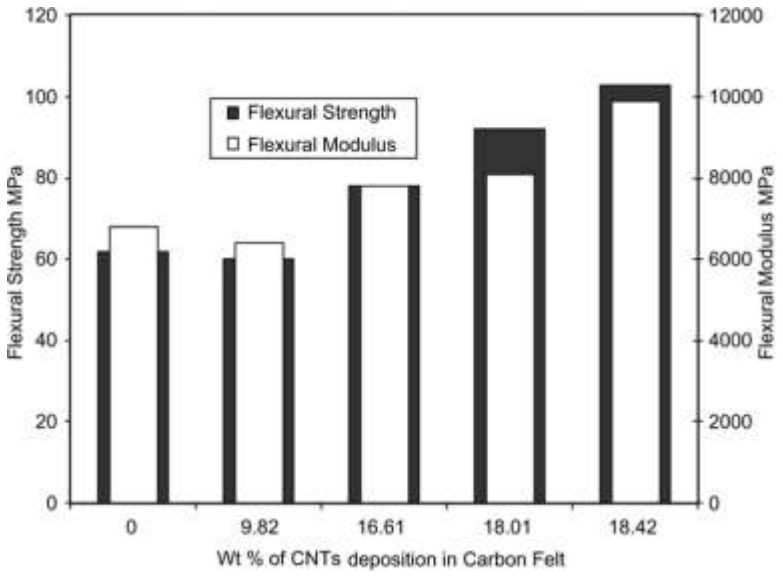

Figure 3.25.- Mechanical properties of carbon fiber felt–CNT composites with increasing nanotube contents.

. The hybrid composite also shows ~46% improvement in the FM over the neat felt based composites. Such high degree of improvement can be attributed to the higher amount of CNTs deposited in the felt [17].

As discussed above, the processing temperature is an important factor for controlling density and morphology of CNTs grown via the CVD method. High processing temperatures and oxidative environments can also affect the mechanical properties of carbon fiber. In order to investigate how quickly mechanical degradation is occurring during the CNT growth process for both sized and unsized T650 fiber, a series of single-fiber tension tests were made as a function of growth time. For each data point, over 50 samples have been tested. The results for tensile strength and tensile modulus are shown in Figures 3.26 and 3.27, respectively. IM-7 fibers were omitted due to their poor handling characteristics. The results in Figure 3.26 indicate that the average tensile strength for sized carbon fibers (T650-UC-309) is decreased within 15 min processing under CNT growth condition. This is attributed to the removal of the sizing layer, which otherwise can improve the tensile strength of the sized carbon fiber, and introduction of flaws. Note that the unsized T650 fibers experience a similar, but smaller, relative decrease at 800 °C. Perhaps the most encourage result from the perspective of maintaining tensile properties while growing a CNT array with uniform coverage and tailored morphology occurs for the unsized T650 with CNT grown at 750 °C. The results indicate that within the statistical variation of the measurements, the tensile strength, modulus, and ultimate strain is uncompromised and equivalent as a function of time. Similar results were obtained for ultimate strain (not shown) while the modulus remained less sensitive to conditions as

Figure 3.27 shown. Results for sized fibers grown at 700 °C for 30 min growth (limited growth) displayed no significant difference in tensile properties from those grown at 750 °C. In general, the sized T650 fiber simply had higher initial tensile strength (prior to CNT growth) and was reduced by nearly 40% due to exposure to the high temperature growth conditions. The final mechanical properties of the CNT/CF assemblies after growth at 750 °C were similar for the sized and unsized T650 fiber [11].

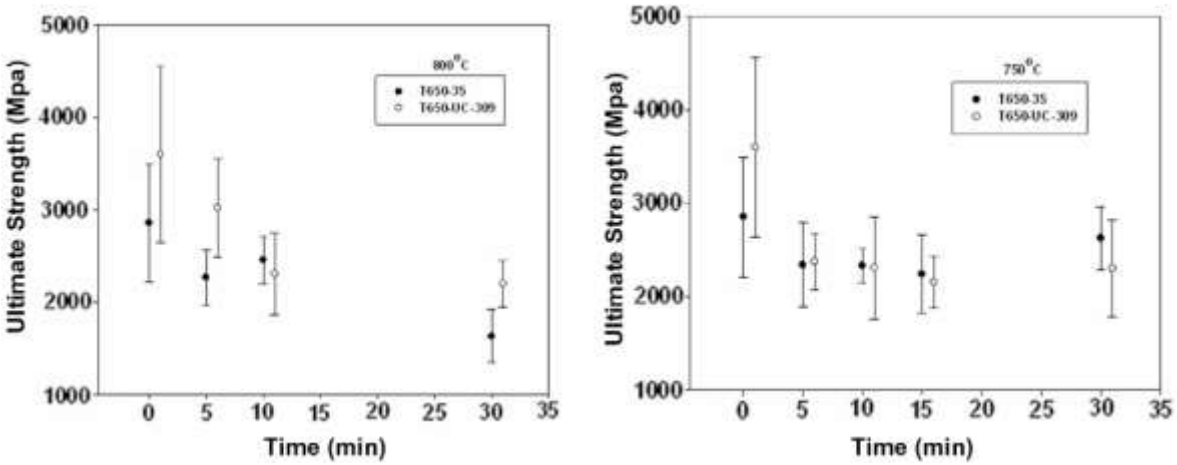

Figure 3.26.- Effect of CNT growth time in CVD chamber on single fiber tensile strength under procedure A at 800 °C (left) and procedure B at 750 °C (right) (symbols offset for clarity).

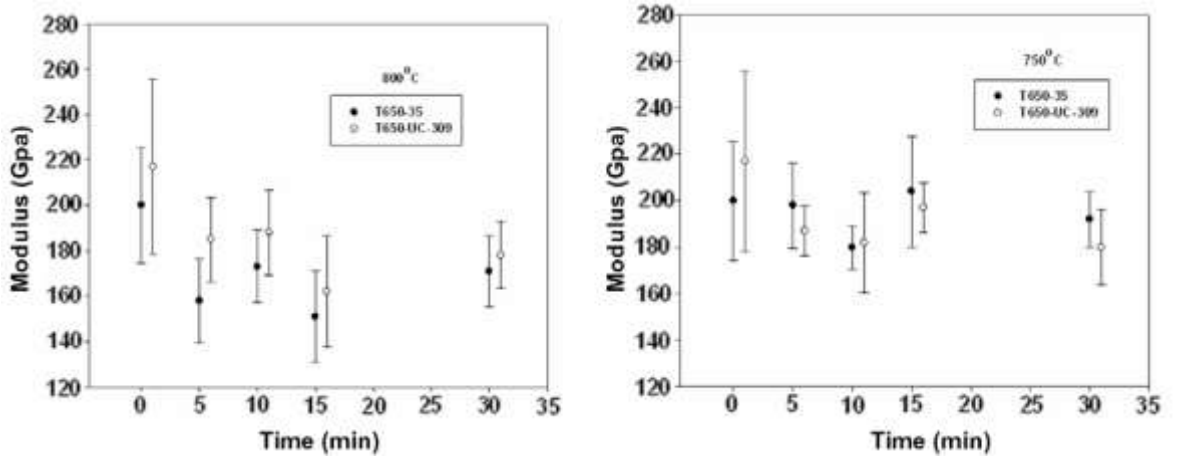

Figure 3.27. Effect of CNT growth time in CVD chamber on single fiber tensile modulus under procedure A at 800 °C (left) and procedure B at 750 °C (right) (symbols offset for clarity).

4. Experimental

4.1. Carbon Fiber Materials

Carbon Fibers were recovered from aerospace fiber-reinforced composites by pyrolysis at 480 °C for 45 minutes. The Recovered Carbon Fiber surface was characterized using high resolution field emission scanning electron microscope (FEI Nova NanoSEM 200).

4.2. Carbon Nanotubes Synthesized on Carbon Fibers by CVD - DOE

The experimental set up for growing CNTs on RCFs is shown schematically in Figure 4.1. Five different thermal CVD methods were employed to investigate the effect of growth condition. These procedures vary in three growth Temperature (800 °C, 750 °C, 700 °C, 650°C and 600 °C), the Catalyst concentration (Nickel (II) nitrate hexahydrate, $Ni(NO_3)_2 * 6H_2O$ and the Carbon Source (Ethanol or Isopropanol). RCFs were immersed in four mixtures for 30 minutes: dissolved in Ethanol 0.63, 1.25, 3.66 and 5.96 wt.% $Ni(NO_3)_2 * 6H_2O$ and dissolved in Isopropanol 0.63, 1.26, 3.68 and 5.98 wt.% respectively. CNTs were grown on RCFs surface kept inside the quartz reactor by thermal decomposition of Ethanol or Isopropanol in presence of Nickel catalyst obtained by the decomposition of the Nickel (II) nitrate hexahydrate.

A summary of the different growth experiments used, as well as the catalyst solution concentration, is shown in Table 4.1.

Table 4.1.- Design of Experiments

Carbon Source	Growth Temperature (°C)	$Ni(NO_3)_2 \bullet 6H_2O$ (g)	$Ni(NO_3)_2 \bullet 6H_2O$ wt. %
Ethanol	600	0	0
	650	0.05	0.61
	700	0.1	1.20
Isopropanol	750	0.3	3.61
	800	0.5	5.96

$Ni(NO_3)_2 \bullet 6H_2O$ was dissolved in 10 ml of ethanol.

Carbon source was carried in the reactor with Argon as carrier gas during the entire experiment. Growth began in the vapor phase and continued on Carbon Fiber substrates, and would last 30 minutes, with 3 ml alcohol consumed. Before the sample was removed, the tube and sample was cooled under flowing argon to room temperature.

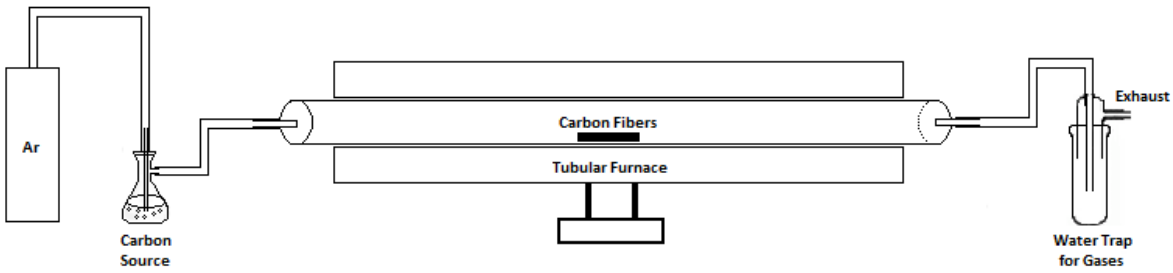

Figure 4.1.- Schematic representation of Chemical Vapor Deposition Process

4.3. Analysis of Solids Products from CVD

The morphology of CNTs on the RCFs surface was characterized using a high resolution field emission scanning electron microscope (FEI Nova NanoSEM 200). Raman measurements were performed using a MicroRaman Thermo 532nm

5. Results and Discussion

The effect of CVD growth conditions on the CNTs morphology, structural and relative tube density was quantified using SEM and RAMAN.

5.1. Scanning Electron Microscopy

Carbon nanotubes were successfully by CVD method using nickel as catalyst, Ethanol and Isopropanol as carbon source . In all experiments were added in a carbon tape and then cover with a gold conductor layer by sputtering (≤100Å) to characterizes the morphology of CNTs. The results of each experiment are showed in Figure 5.1 to Figure 5.39. The growth of CNTs on carbon fiber surface by CVD method was varied by changing three parameters: (1) carbon source, (2) growth temperature, and (3) nickel concentration. The combination of these parameters not only affect CNTs morphology, but also can change the density and coverage of CNTs/CF. CNTs were mostly found as bundles.

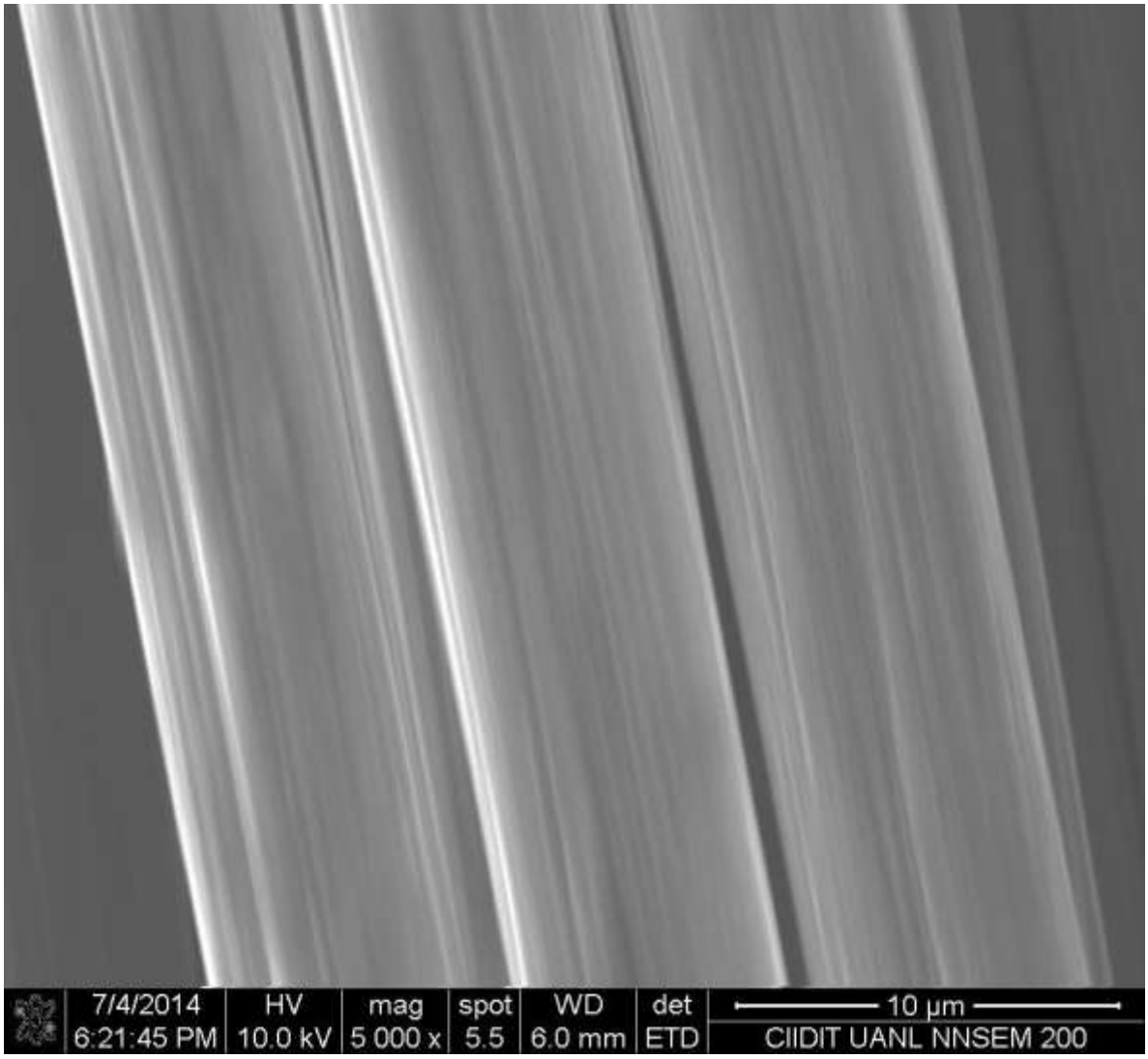

Figure 5.1.- Carbon Fiber after pyrolysis

In the Figure 5.1 show SEM image of recovered CF after pyrolysis sample using before to grown CNTs. According to the CNT growth mechanism, the CNT morphology and density on the carbon fiber surface could be influenced by nickel concentration or/and temperature. In Figures 5.2, 5.3, 5.4 and 5.5 shows SEM images of CNTs on surface CF "as-grown" samples that were grown for 30 min at 600°C with a variation of nickel concentration, using ethanol as carbon source. From these images, we can see that CNTs

are not visible at low nickel concentration (Figures 5.2 and 5.3 with 0.6 and 1.2 wt. % nickel concentration, respectively). This can be attributed to the low activity of the nickel as a catalyst at this temperature because the nickel concentration is not enough to synthesized the carbon nanotube on the carbon fiber surface.

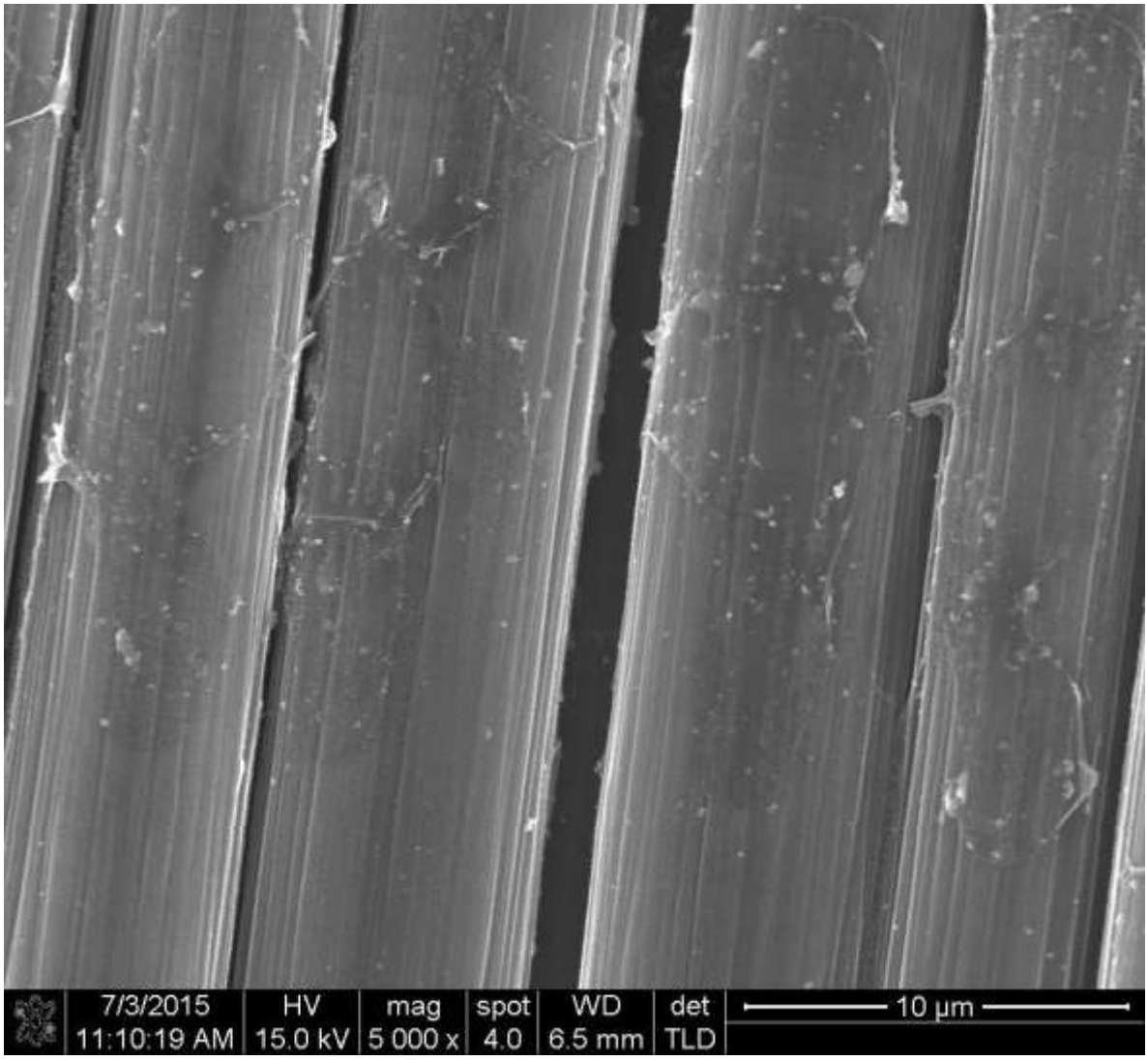

Figure 5.2 ETOH_600°C_05g30m

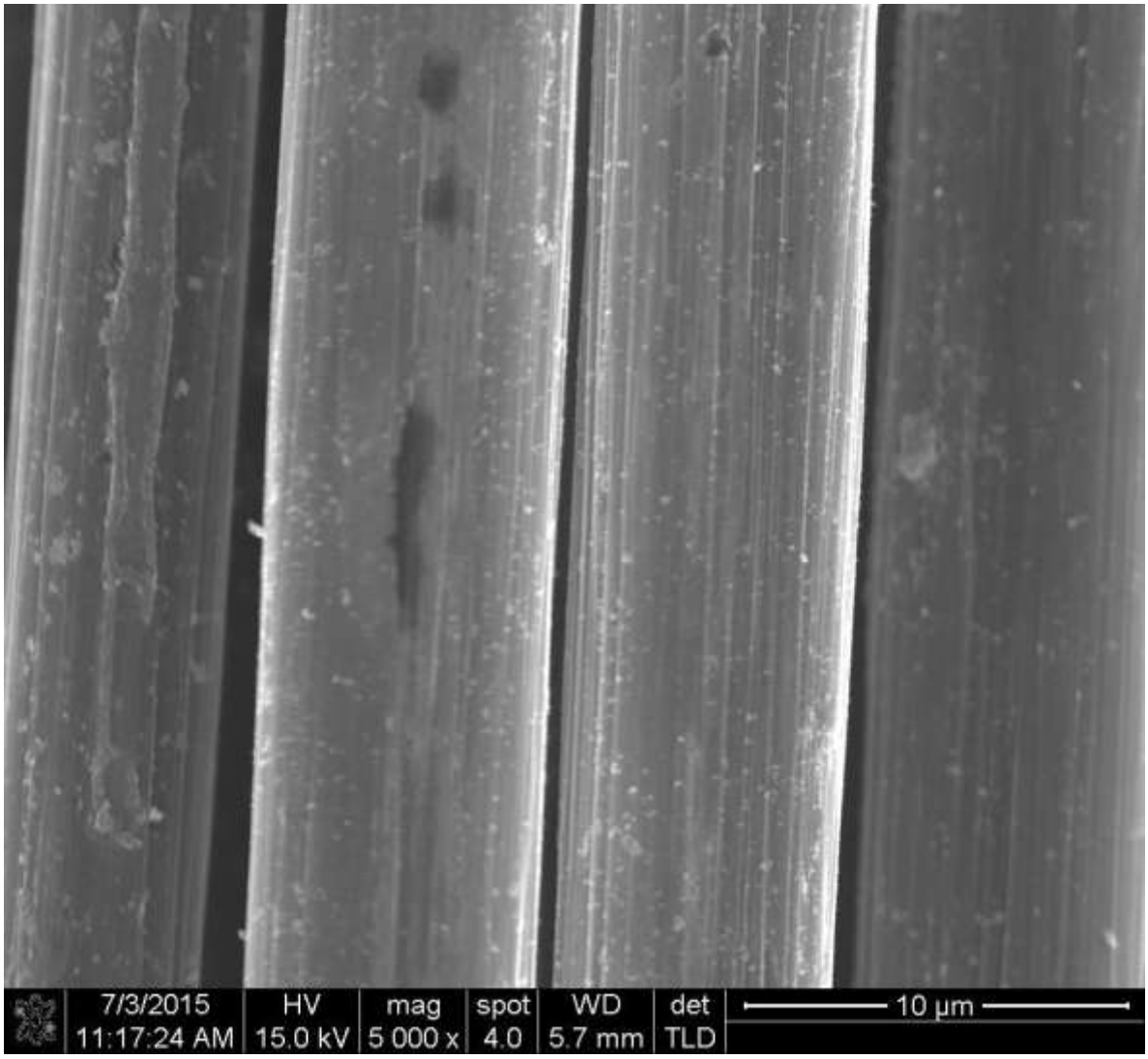

Figure 5.3 ETOH_600°C_1g30m

Figure 5.4 show SEM image of CNTs/CF sample with a high density of the CNTs, but when the nickel concentration increase the CNTs are not covering all CF surface, as show in Figure 5.5.

CNT morphologies, such as the length, average diameter and density, are affected by the nickel concentration to synthesize CNTs on carbon fibers in these condition by controlling the nickel concentration.

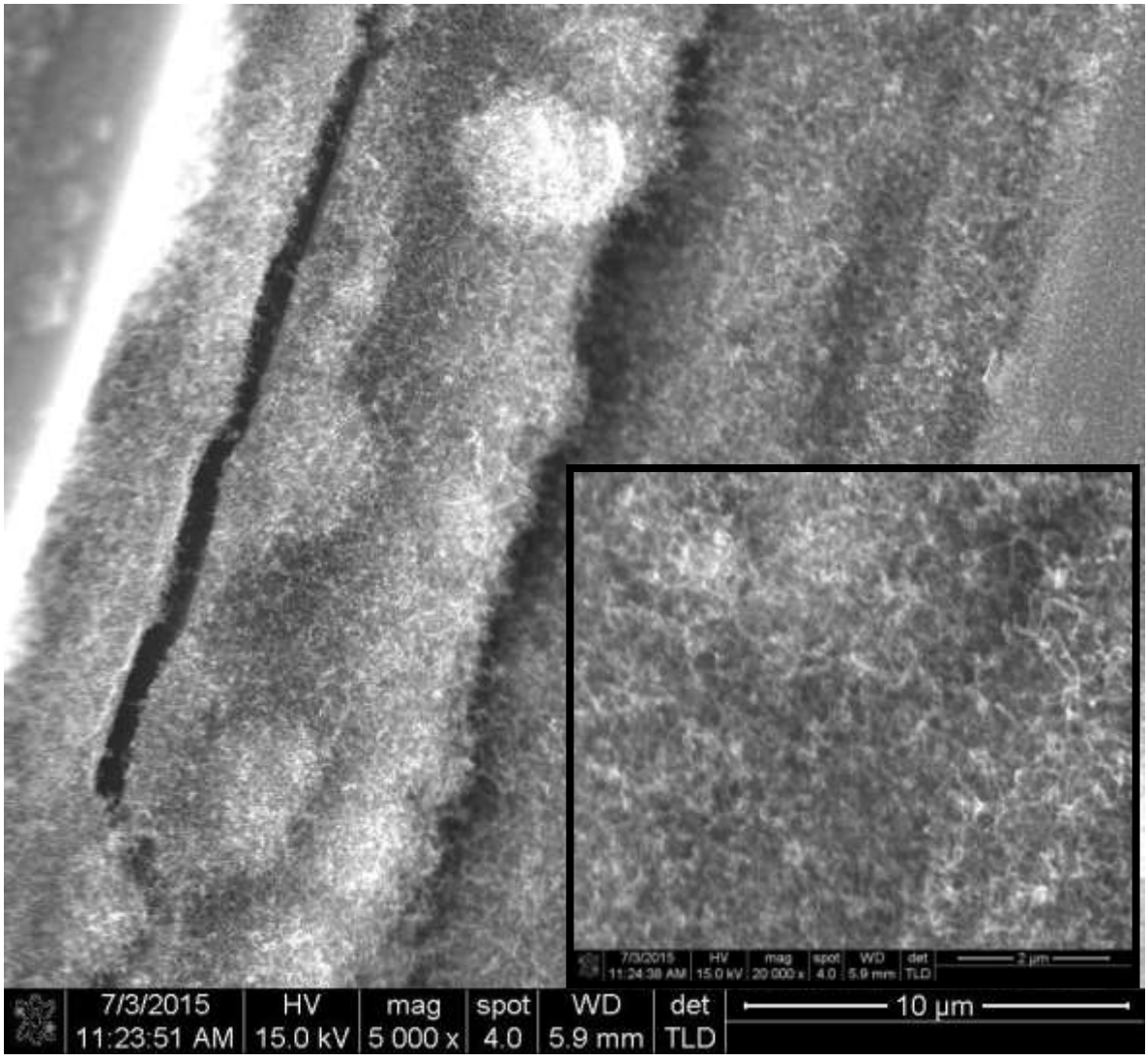

Figure 5.4 ETOH_600°C_3g30m

For this reason, we made the same experiments increasing the temperature to 650°C to study the synthesis of CNTs on CFs substrate. The results are showed in the Figures 5.6, 5.7, 5.8 and 5.9.

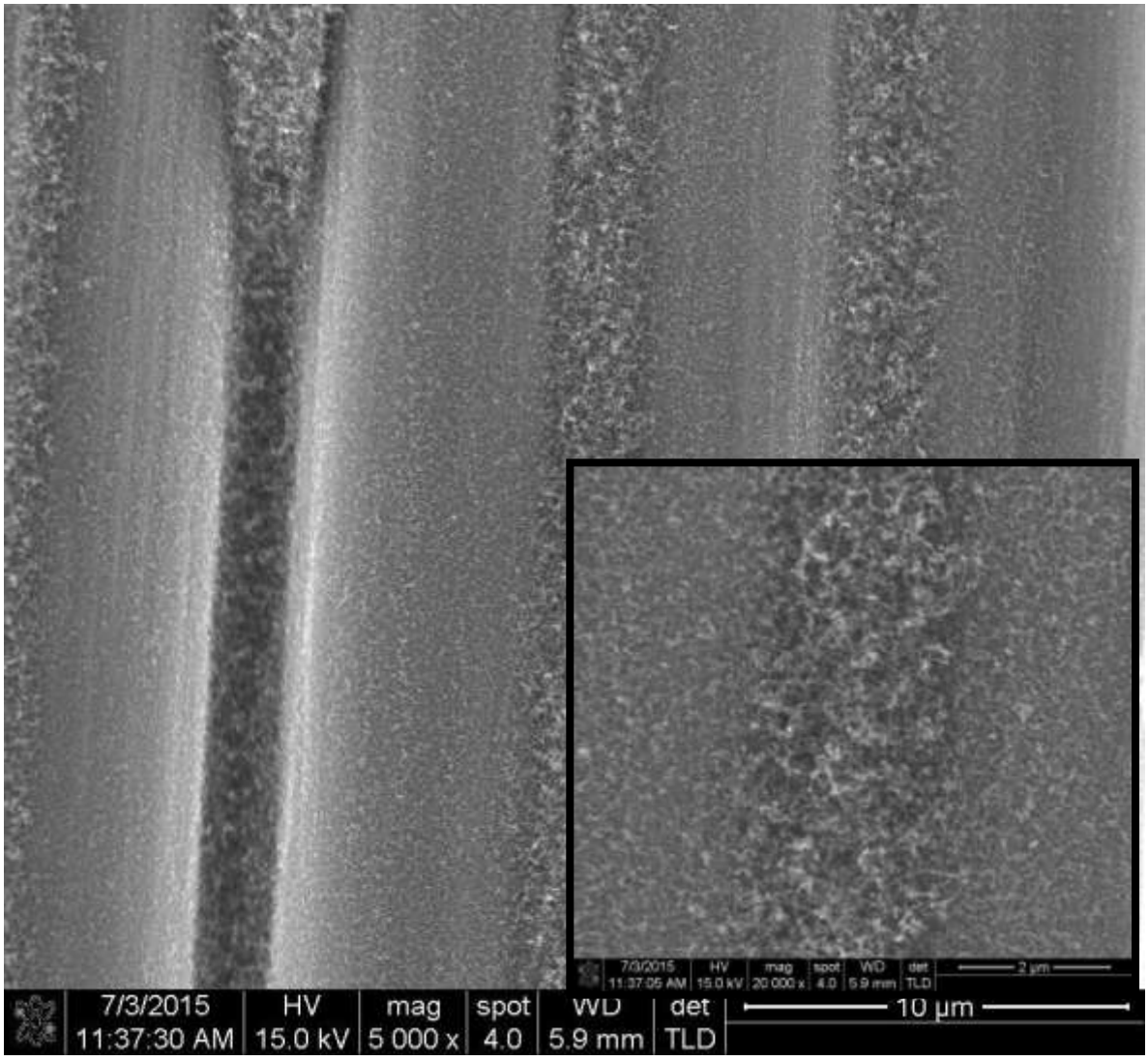

Figure 5.5 ETOH_600°C_5g30m

In the Figures 5.6 y 5.7 we observe that there are not CNTs on carbon fiber substrate, same case in the last experiment (Figures 5.1 y 5.2). At these conditions (low

concentration of nickel concentration and low temperature) wasn't possible to obtain CNTs.

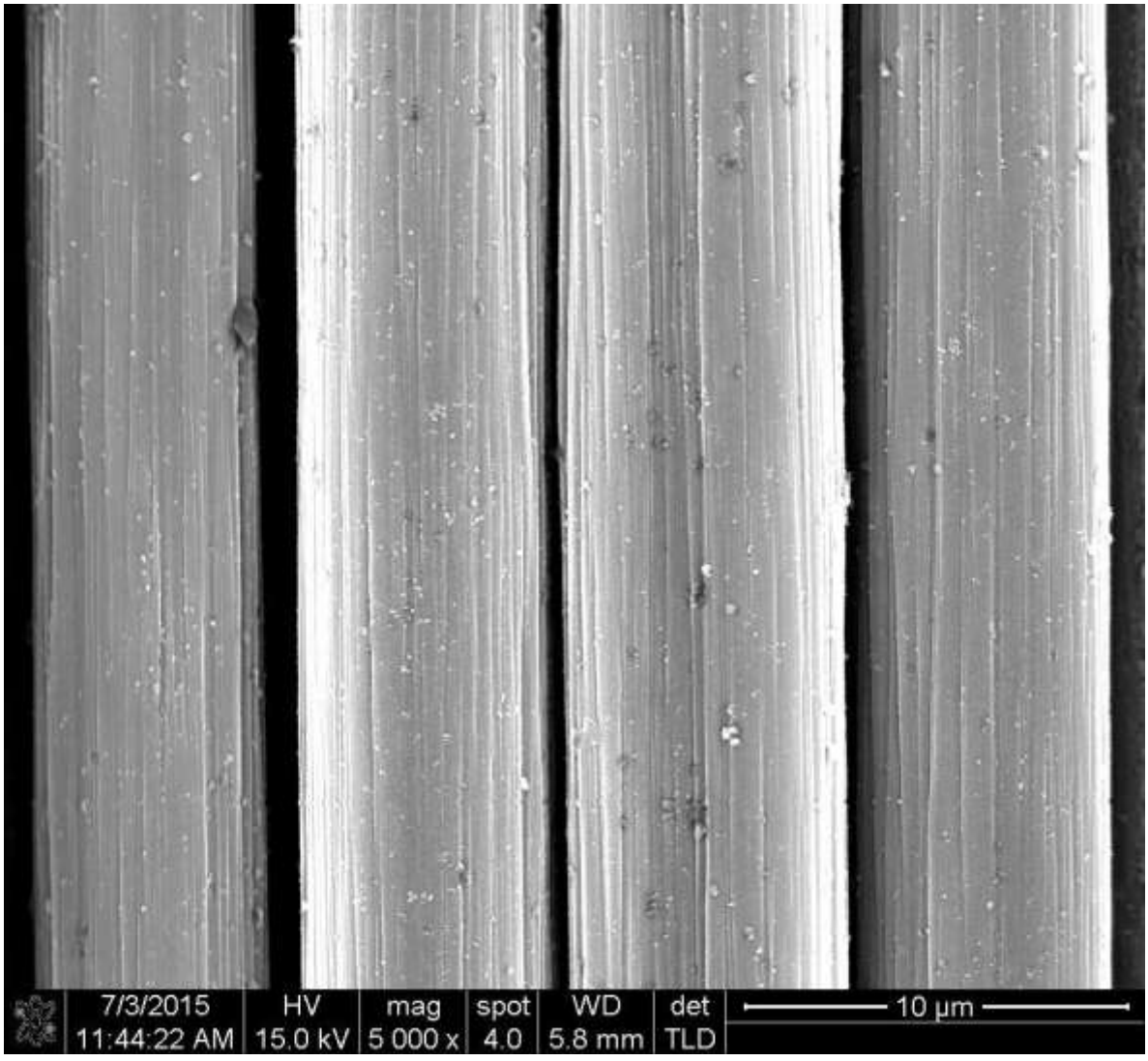

Figure 5.6 ETOH_650°C_05g30m

The effect of CNT growth nickel concentration could be influenced by the insufficient thermal activation on the carbon fiber surface, and for that reason there's not enough nucleation's spots available to the growth process.

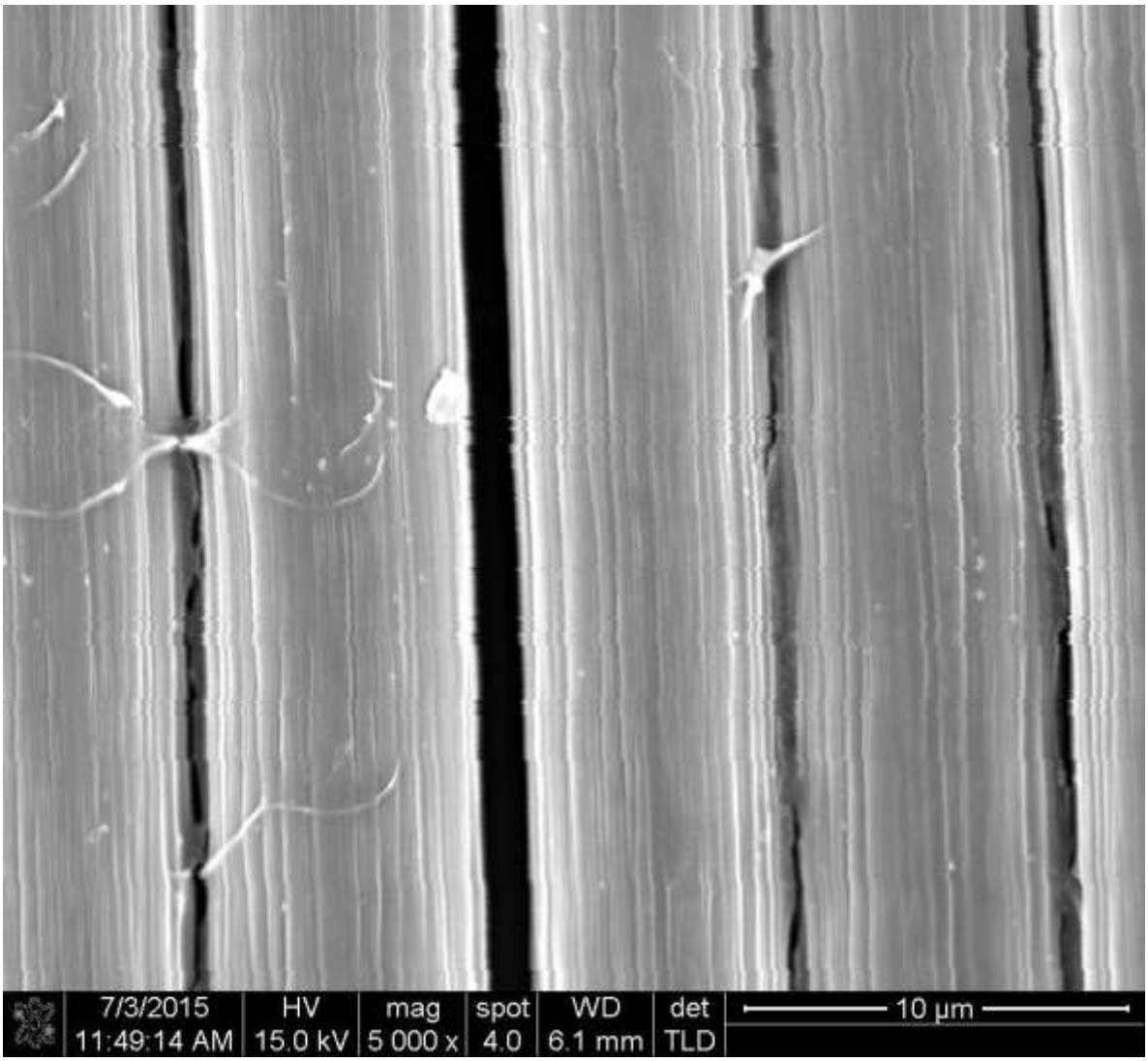

Figure 5.7 ETOH_650°C_1g30m

The Figures 5.8 and 5.9 shows a successfully CNT growth on CF substrate. From these experiments, the CNT are more bigger in length and diameter than in the experiments in the Figure 5.4 and 5.5. Also we can see, the density and coverage are better in these conditions.

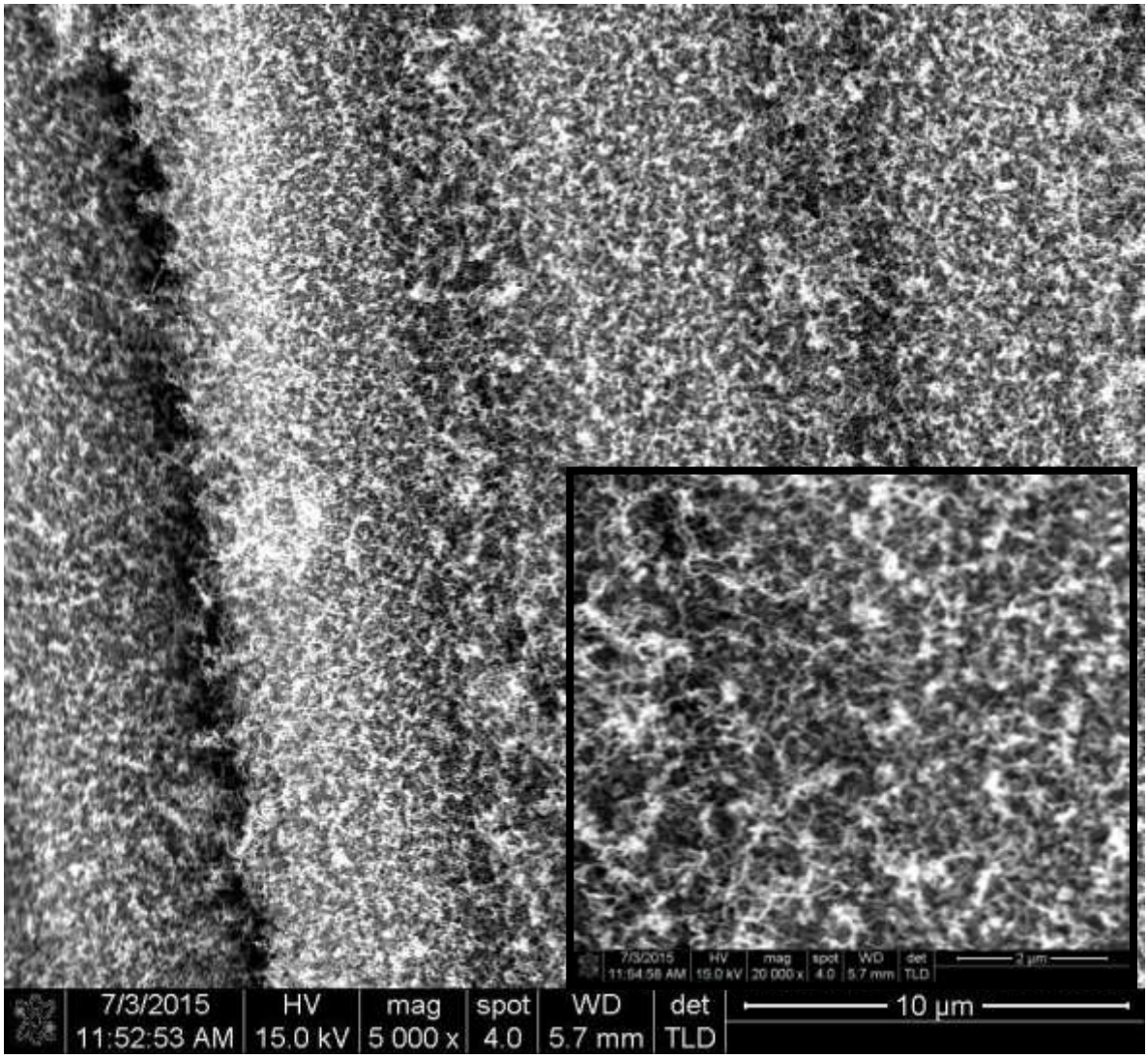

Figure 5.8 ETOH_650°C_3g30m

The effect of CNT growth temperature is also an important factor for controlling density and morphology of CNT grown. When the temperature is increasing in 50°C, is possible to obtain better results in the synthesis of CNTs.

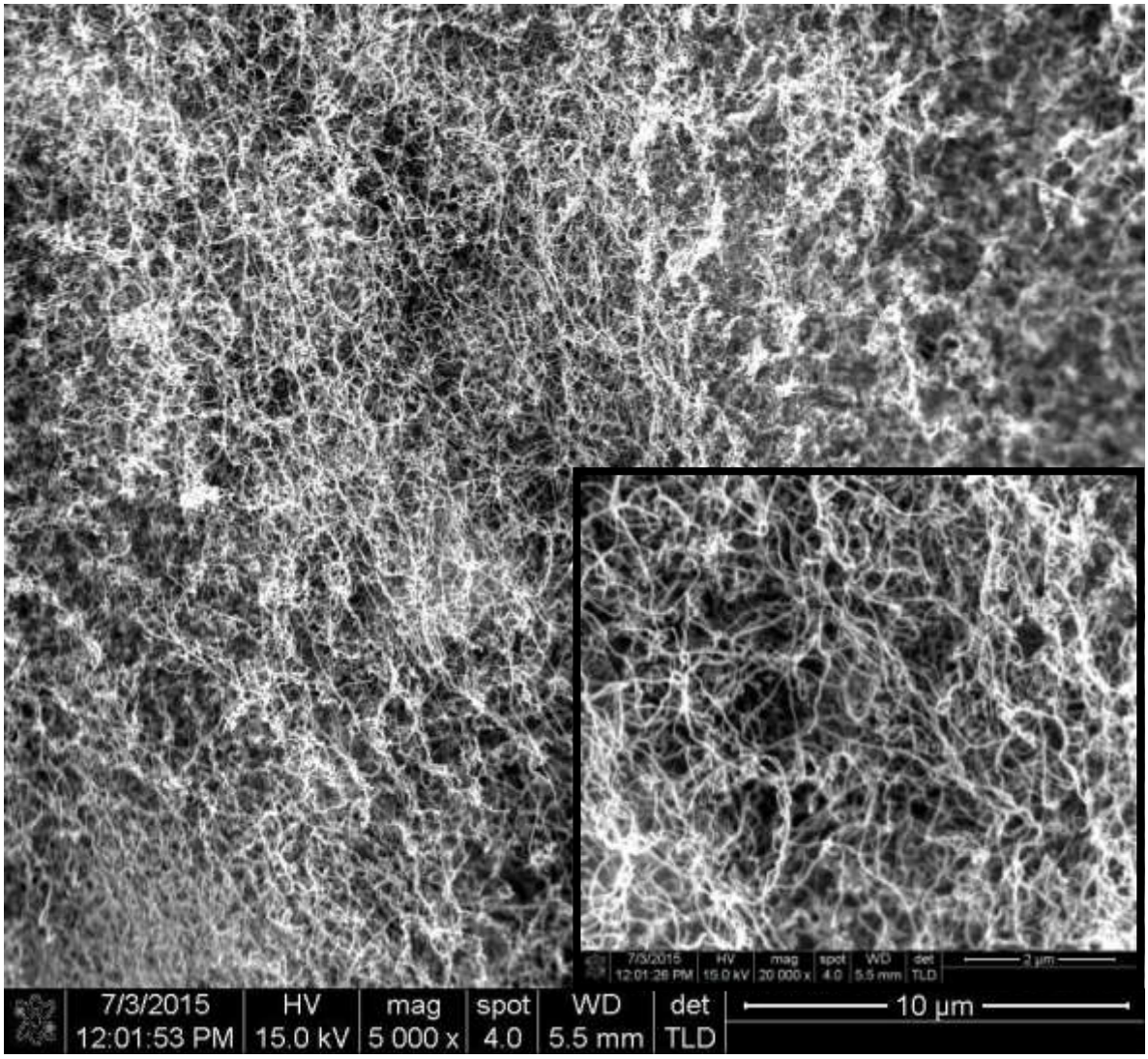

Figure 5.9 ETOH_650°C_5g30m

The synthesis of CNTs on CFs at 650 °C with 3.6 and 5.9 wt. % of nickel concentration (Figures 5.8 and 5.9) shows CNTs with more density and length growth than the CNTs synthesized at 600 °C with the same wt. % (Figures 5.4 and 5.5). The best results obtained at 650° C were with a high nickel concentration (3.6 and 5.9 wt. %). The results at 700 °C are showed in the Figures 5.10 - 5.13. Riccardis et al [17] synthesized CNTs on CF yarns by a deposition of nickel cluster onto the CF surface using electro-deposition technique (ELD)

and the CNTs growth process was performed with the hot filament chemical vapour deposition (HFCVD) technique. The synthesis conditions .... H2 and CH4 as precursors The aim was to reinforced CF to improve anchorage with the polymeric matrices. The results of this study of the Ni clusters by ELD demonstrated to be a good technique to provide a strong anchorage between the Ni clusters and the CF surface, after the CNTs growth process on the CF surface was fully infiltrated with a CNT network having a homogeneous and dense distribution. Those results are very similar with the results obtained in the Figures 5.8 and 5.9, but in this experimentation were obtained the same results in one step, Ni clusters and CNTs network.

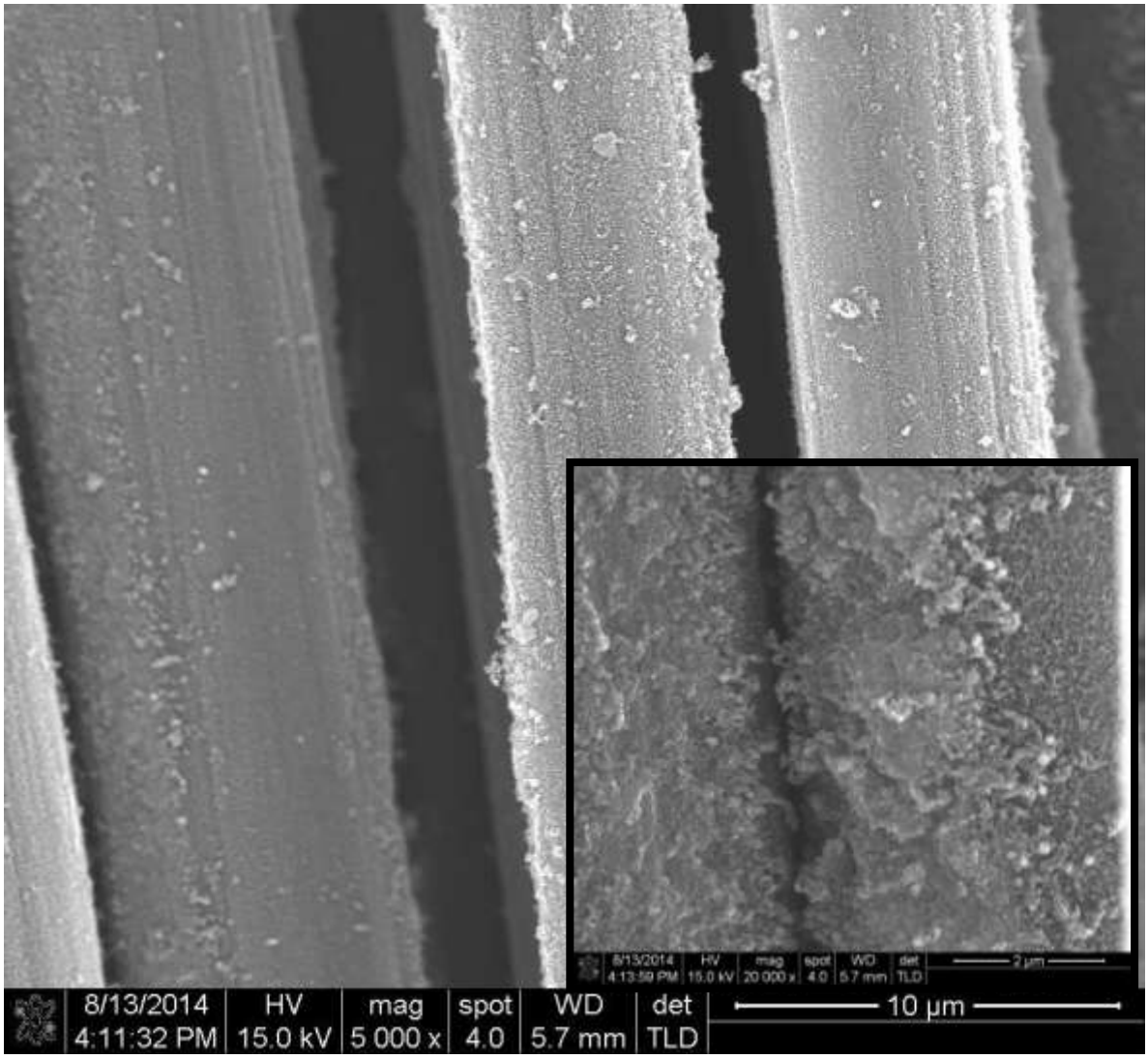

Figure 5.10 ETOH_700°C_05g30m

The Figure 5.10 shows the synthesis of CNTs with 0.61 wt. % of nickel concentration. In this experiment, it was obtained CNTs a medium density with short length, the CNTs covers all the CF surface. The effect of CVD growth increasing 50 °C of this experiment had an impact in this synthesis. Growth temperature could be influenced the synthesis of CNTs.

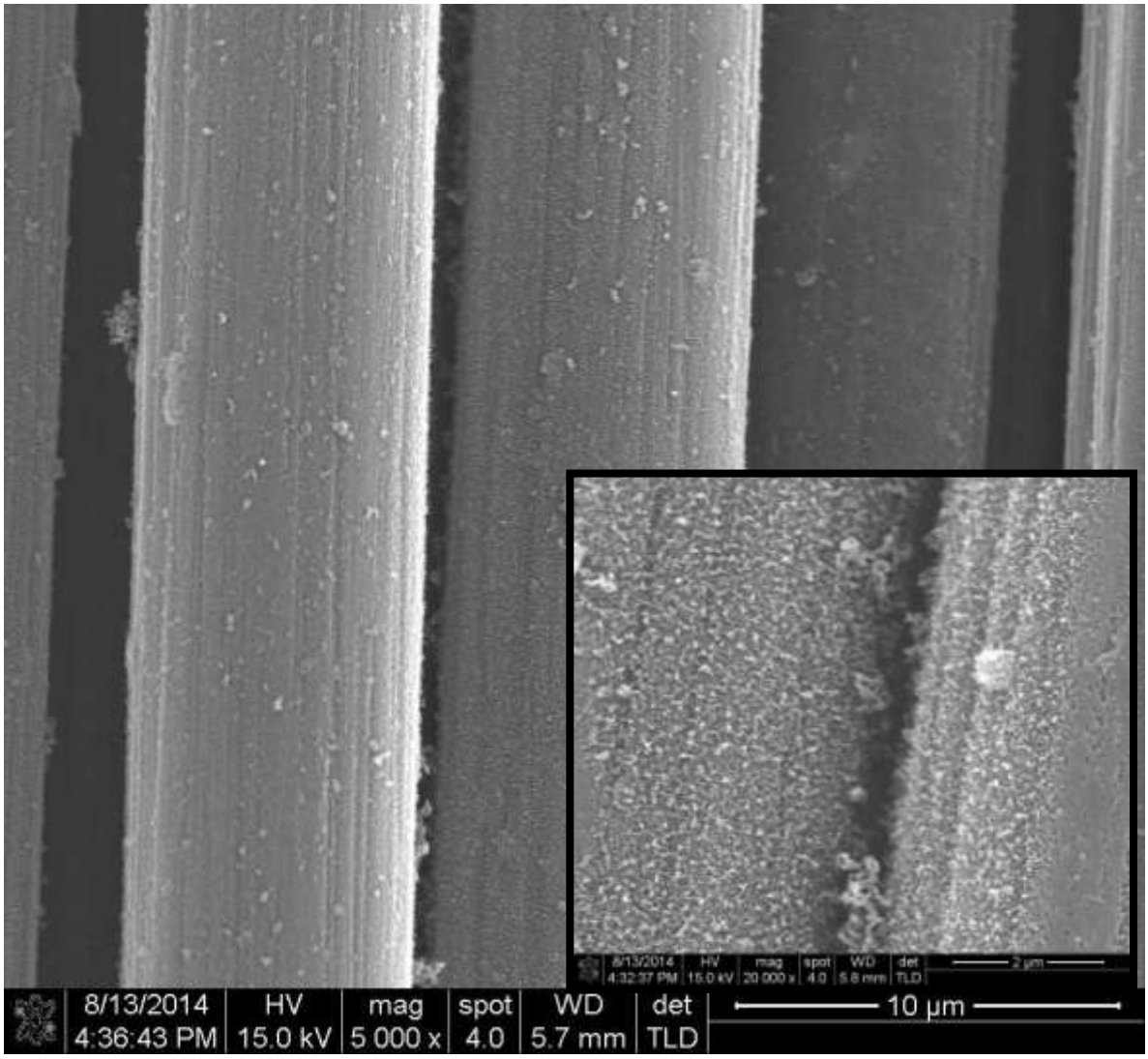

Figure 5.11 ETOH_700°C_1g30m

In the Figure 5.11 shows the result of the synthesis of CNTs at 700°C with 1.2 wt.% of nickel concentration with a similar growth of CNTs than in Figure 5.10.Then, the nickel concentration was increased to 3.6 wt. % (Figure 5.12) and shows that the CNTs are longer than the last two experiments.

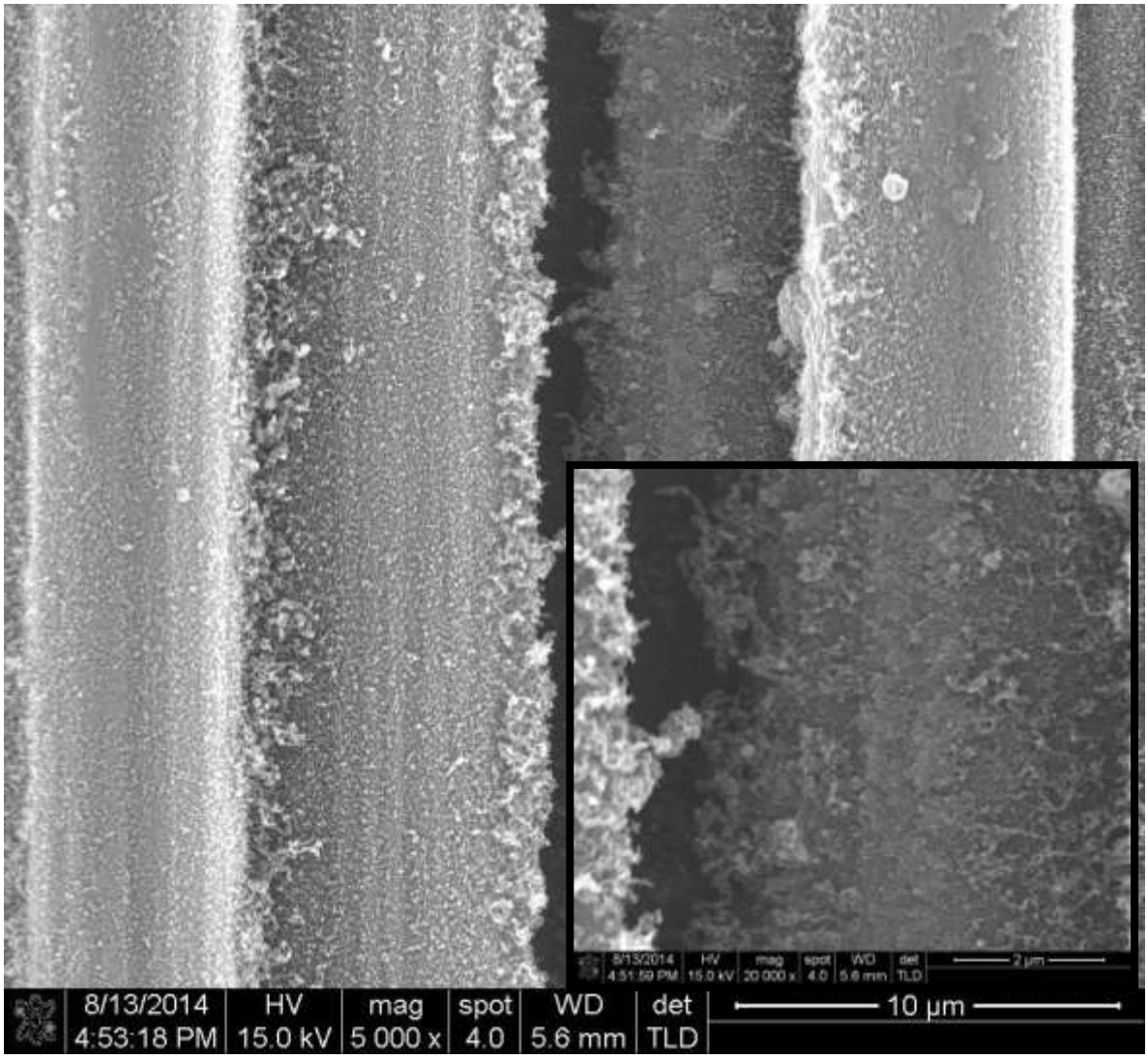

Figure 5.12 ETOH_700°C_3g30m

In the last experiment at 700°C was increased the nickel concentration to 5.9 wt.% and the result is showed in the Figure 5.13. In this experiment, the CNTs synthesis had a preferential growth between CFs, but decrease the mass of CNTs synthesized on the CF surface. The best results at 700° C are showed with a 3.6 wt. % of nickel concentration.

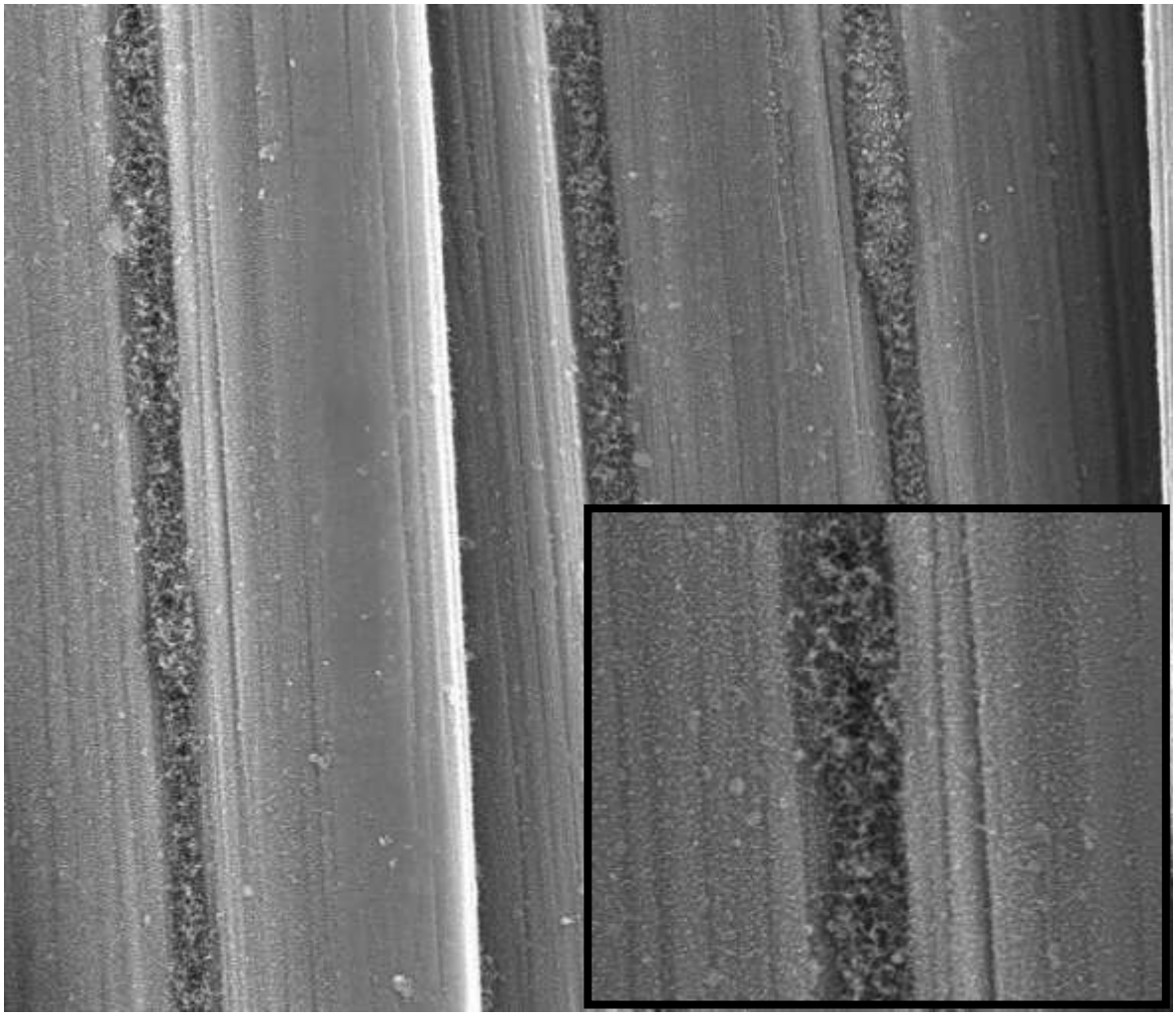

Figure 5.13 ETOH_700°C_5g30m

For now, has been presented the synthesis of CNTs at low temperatures, in the next results we increased the temperature until 750° C y 800° C and the analysis are showed in below. In the Figures 5.14 to 5.17 shows the results obtained at 750 °C. The Figure 5.14 shows the experiment that contains 0.61 wt % of nickel concentration, in this case, there is not CNTs on CF surface.

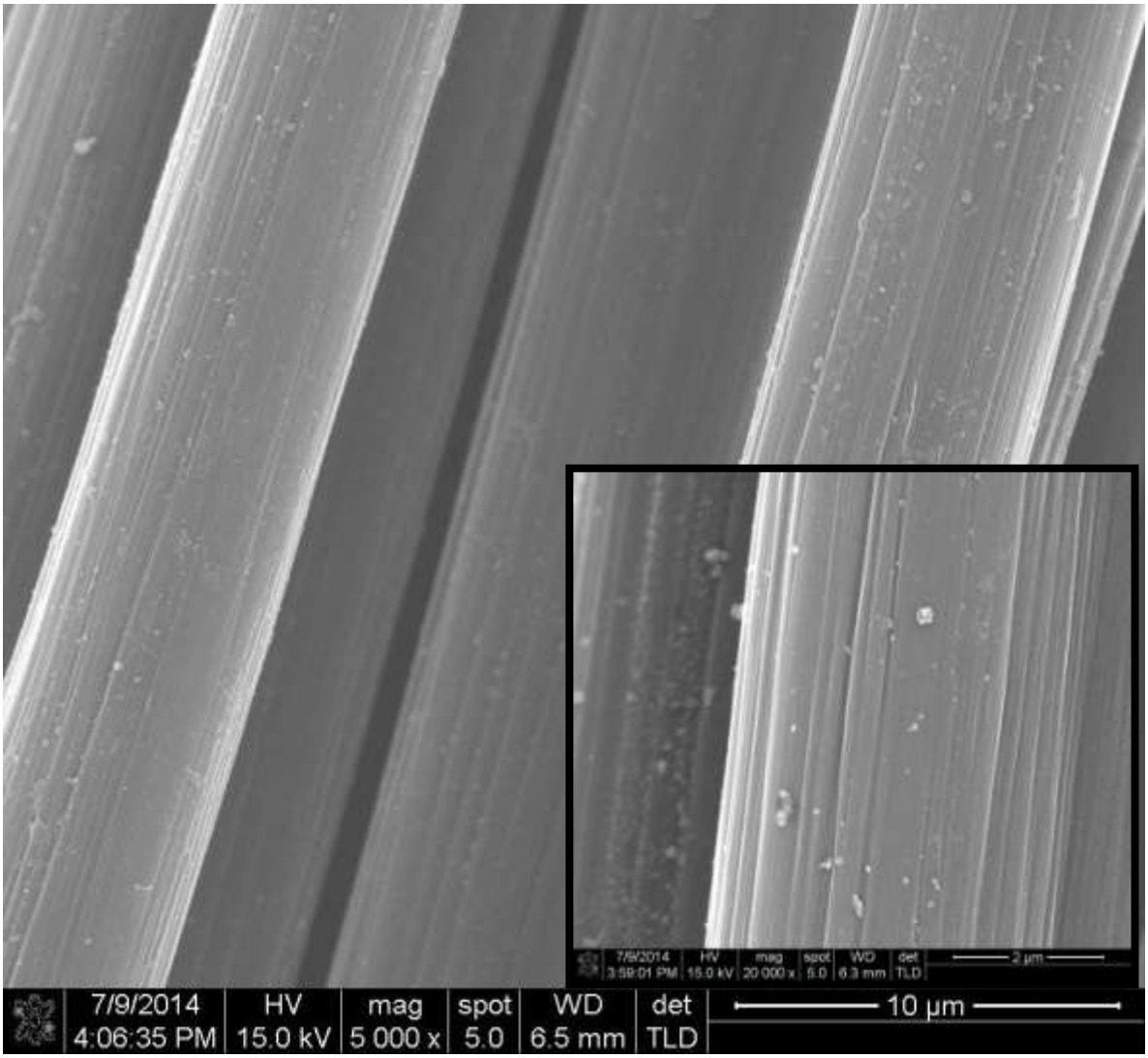

Figure 5.14 ETOH_750°C_05g30m

Figure 5.15 shows growing CNTs on CF surface with 1.2 wt. % of nickel concentration, there is just fewer of them, CTNs are small and the grown is very randomly.

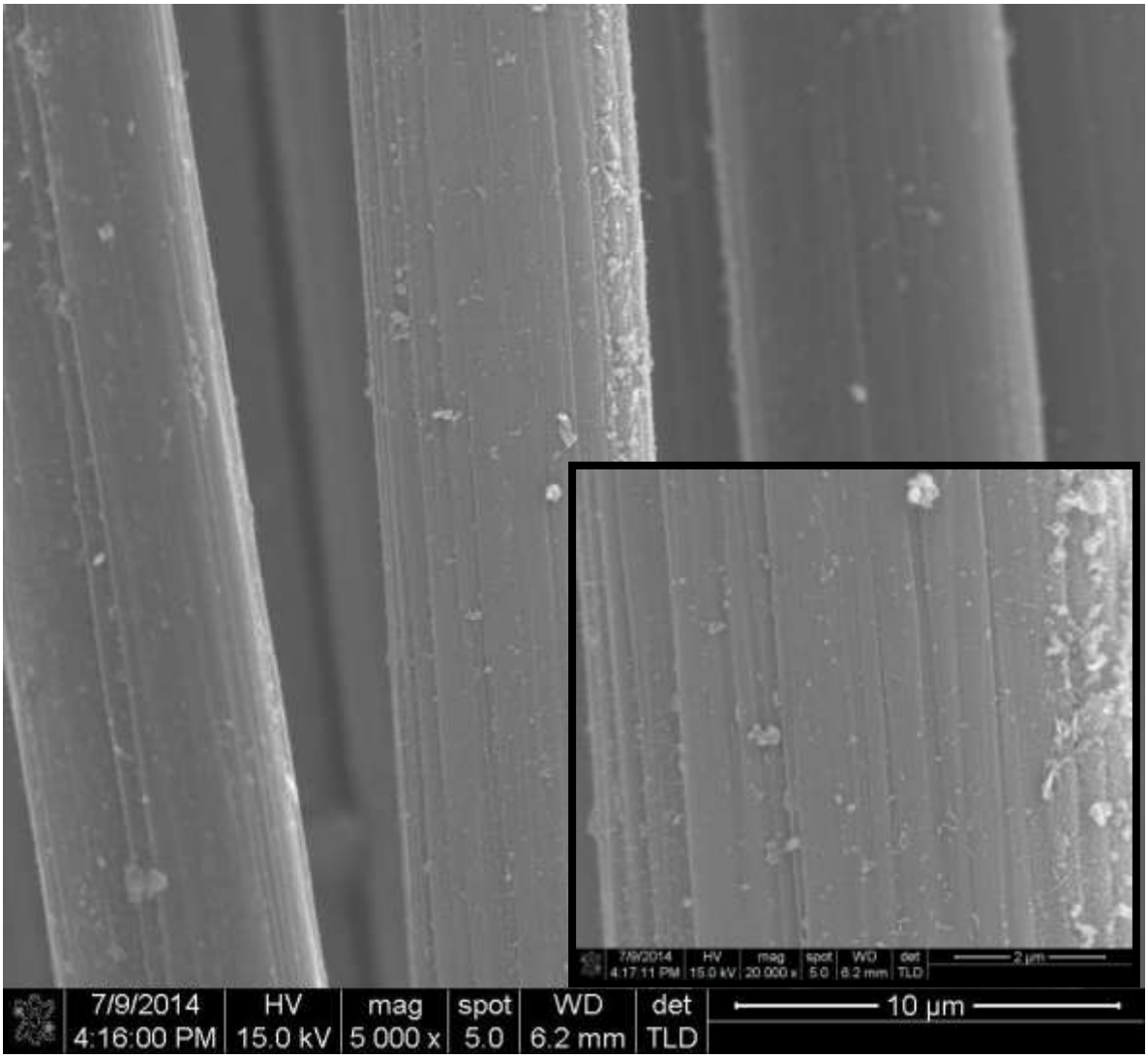

Figure 5.15 ETOH_750°C_1g30m

Figure 5.16 and 5.17 it is observed that the amount of CNTs increased with nickel concentration (3.6 and 5.9 wt% of nickel concentration, respectively), but these experiments are not the best results.

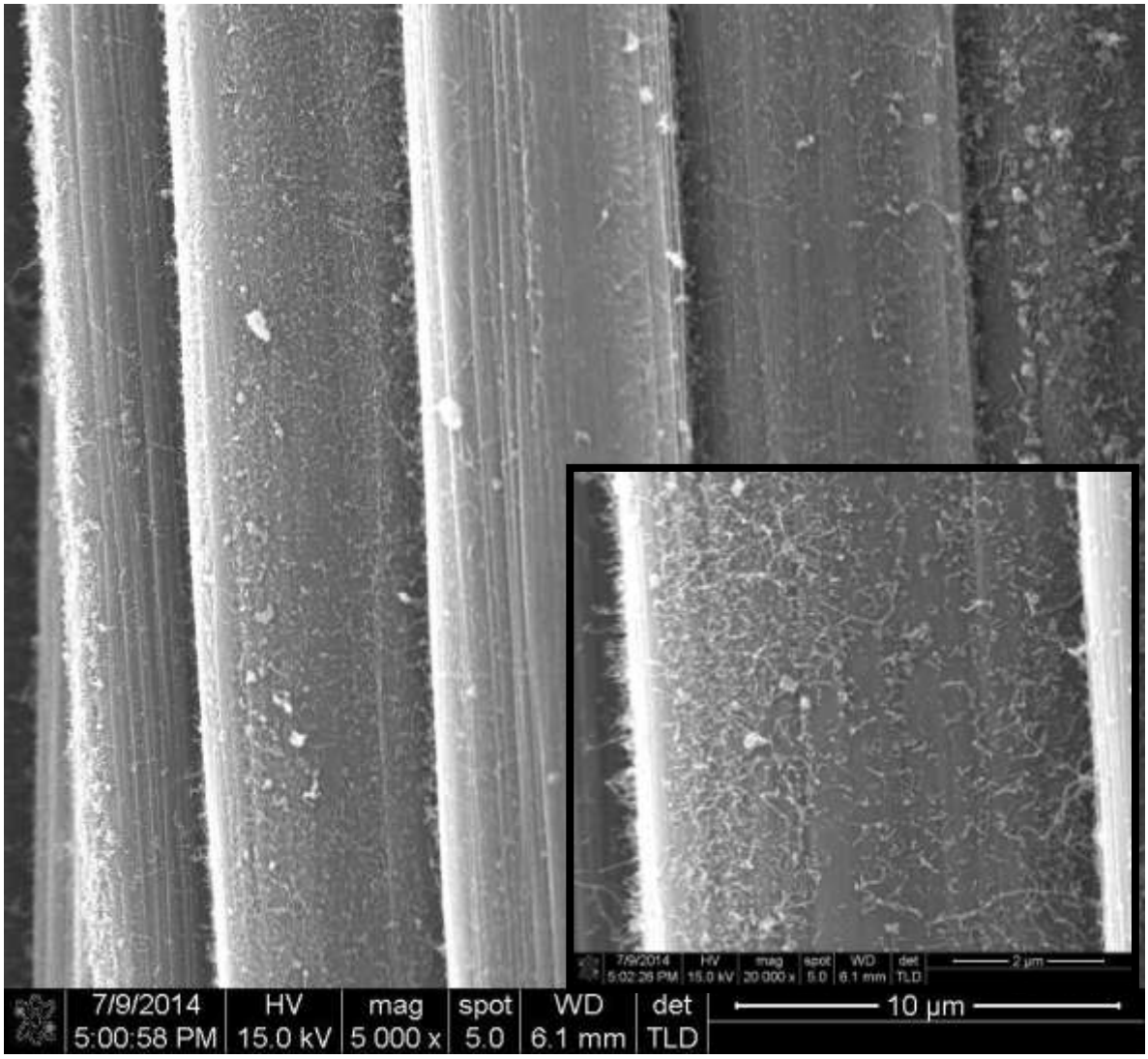

Figure 5.16 ETOH_750°C_3g30m

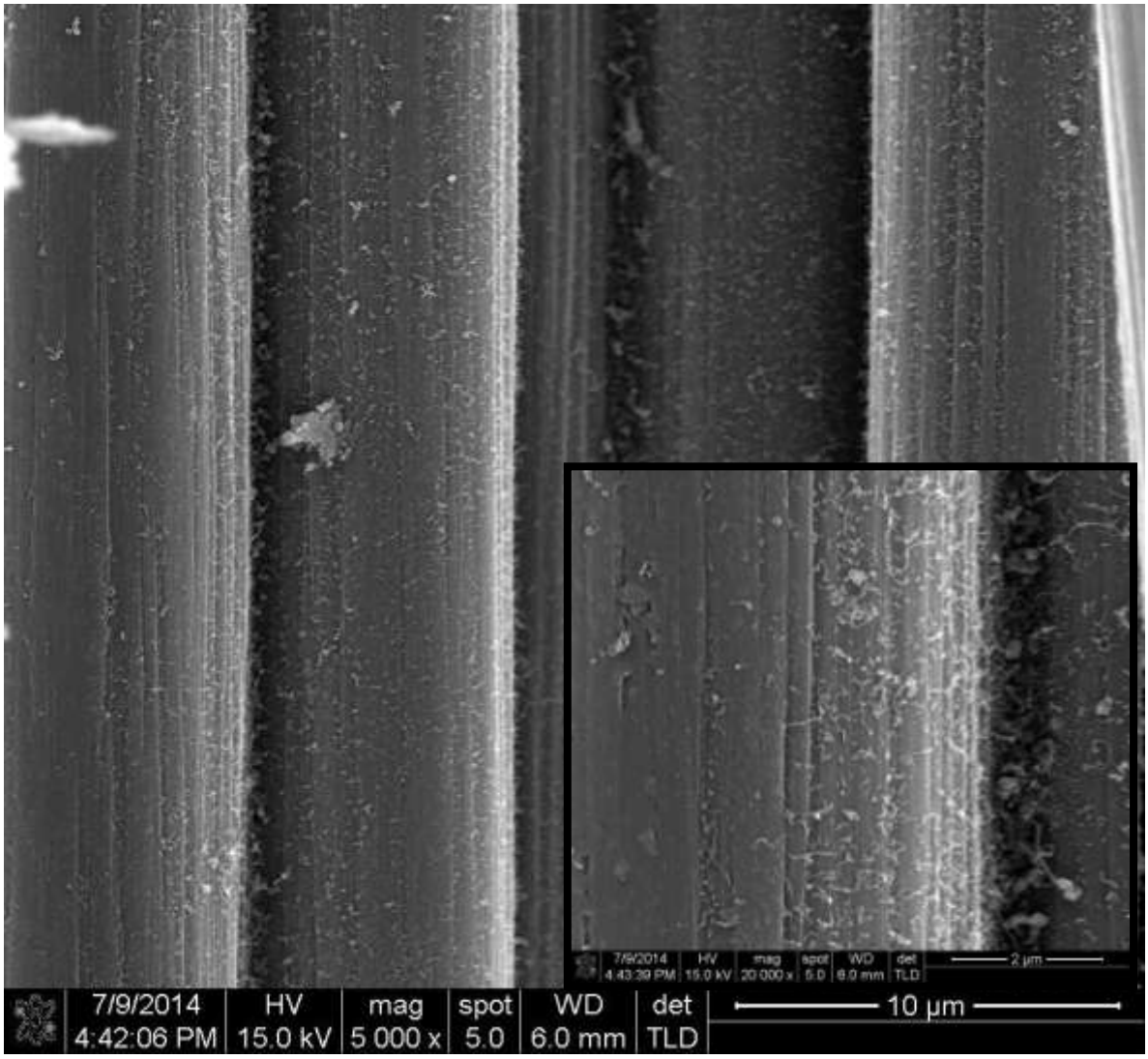

Figure 5.17 ETOH_750°C_5g30m

The results at 800 °C are showed in the Figures 5.18 to 5.21. Figure 5.18 shows a successful CNTs synthesis with a very high density and cover surface CF at low nickel concentration (0.61 wt.%) and a higher temperature of synthesis.

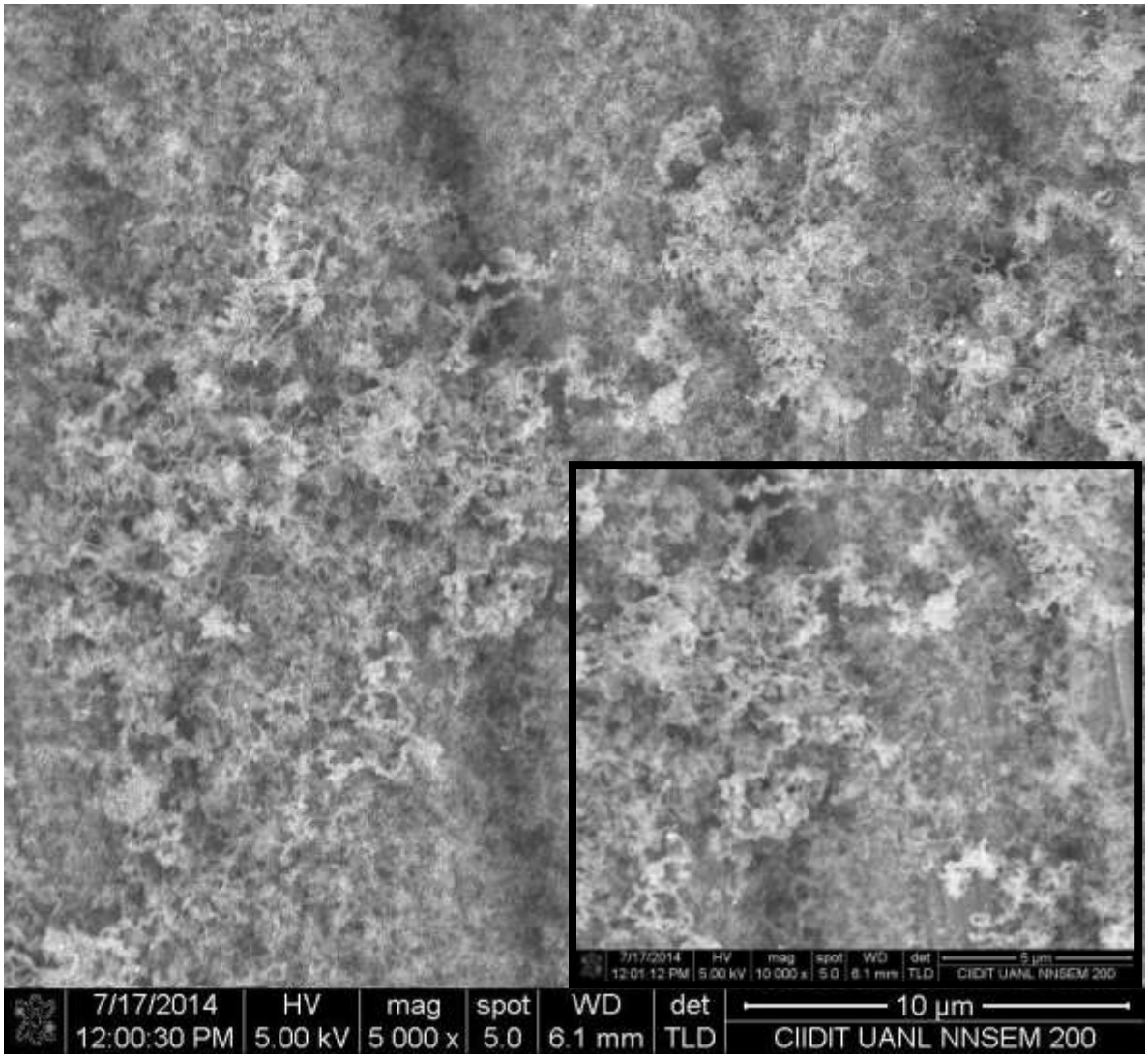

Figure 5.18 ETOH_800°C_05g30m

When the nickel concentration increase to 1.2 wt.% (Figure 5.19) the density of CNTs decrease, in this image shows that CNTs have a preferential in growing between CFs. In the Figure 5.20 shows the result with 3.6 wt. % nickel concentration, in this experiment CNTs grows on CF surface, but was not better than Figure 5.18. Zhang *et al* [10] synthesized CNTs on a fabric CF surface with and without sizing by CVD method. The sized fibers are produced with thin epoxy-based materials formulated to enhance tensile and interfacial properties. They used xylene/ferrocene mixture as carbon source/catalyst and

700 °C, 750 °C and 700°C growth temperature. They report very low density of CNTs at 700 °C, because insufficient thermal activation of ferrocene decomposition by the iron catalyst needed for the nucleation of growths processes on the carbon fiber surface. In our study, the results obtained at 600 °C and 650 °C temperatures of synthesis (Figure 5.8, 5.9, 5.25, 5.26) shows the CNTs network with a high density, the Ni catalyst for the nucleation of growths process occurred during the synthesis process at lower temperatures.

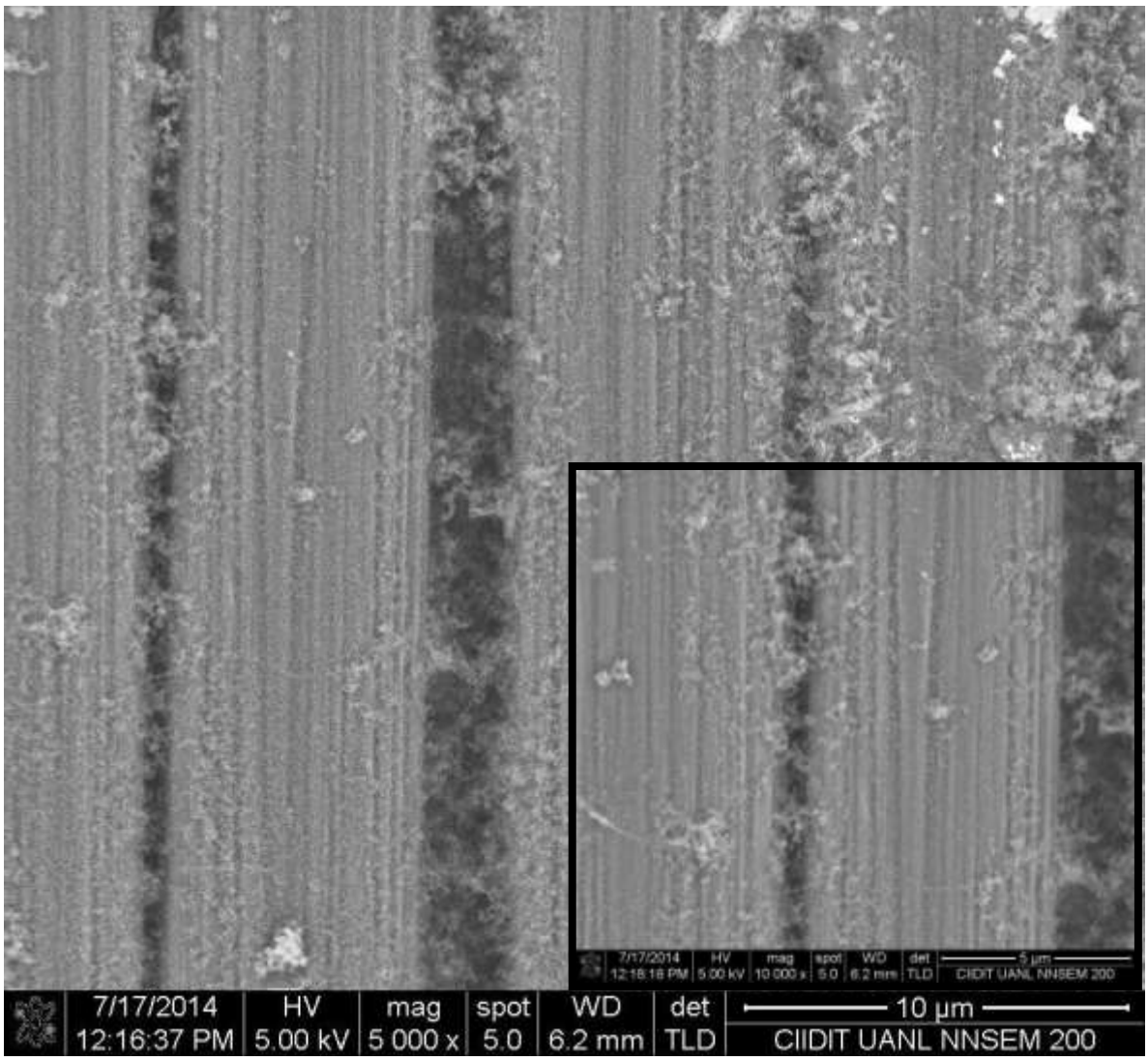

Figure 5.19 ETOH_800°C_1g30m

Figure 5.21 shows the results obtained with 5.9% of nickel concentration. In this image shows CNTs with a high density and cover surface on CFs. The best results at 800 °C were with 0.61 and 5.9 wt. % of nickel concentration.

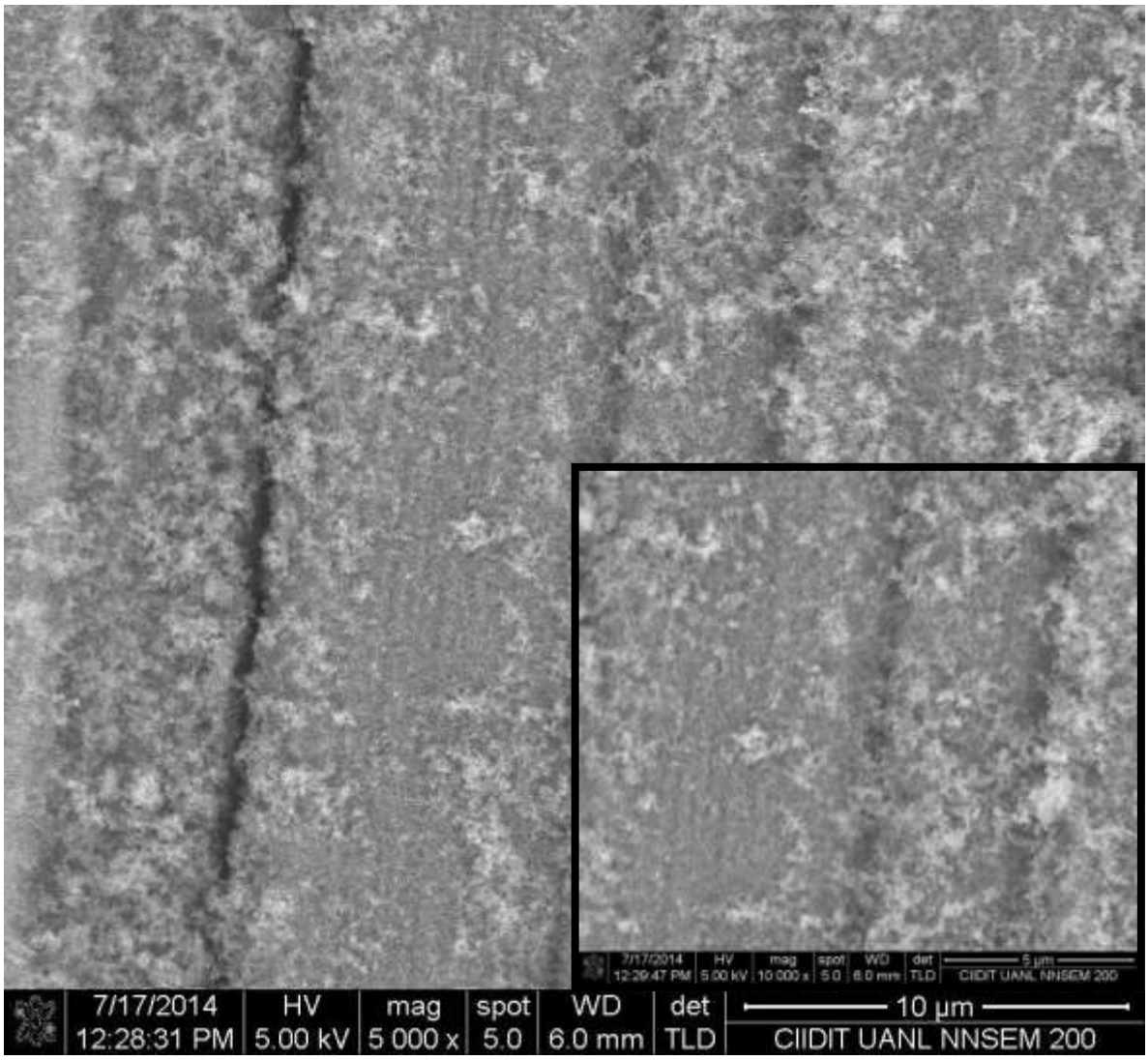

Figure 5.20 ETOH_800°C_3g30m

The last experiments shows the results of the CNTS synthesis using Ethanol as carbon source. Now it is present the results obtained of the CNTs synthesis using Isopropanol as

carbon source, temperature synthesis at 600 to 800 °C and 0.61 to 5.9 wt. % of nickel concentration.

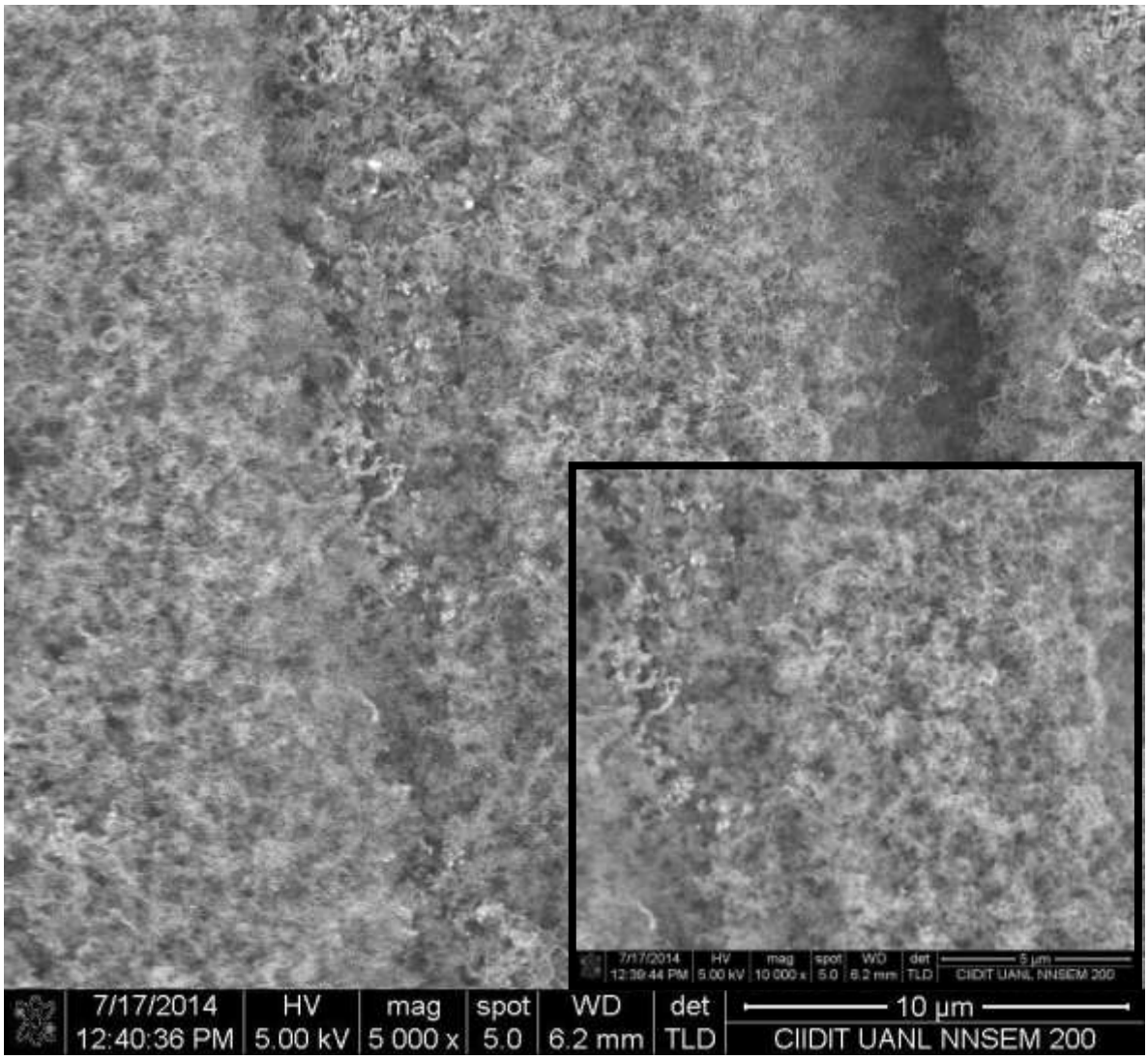

Figure 5.21 ETOH_800°C_5g30m

The first results at 600 °C are showed in below. Figure 5.22 shows that there are not CNTs, with these conditions (low concentration of nickel concentration and low temperature) was not possible to obtain CNTs.

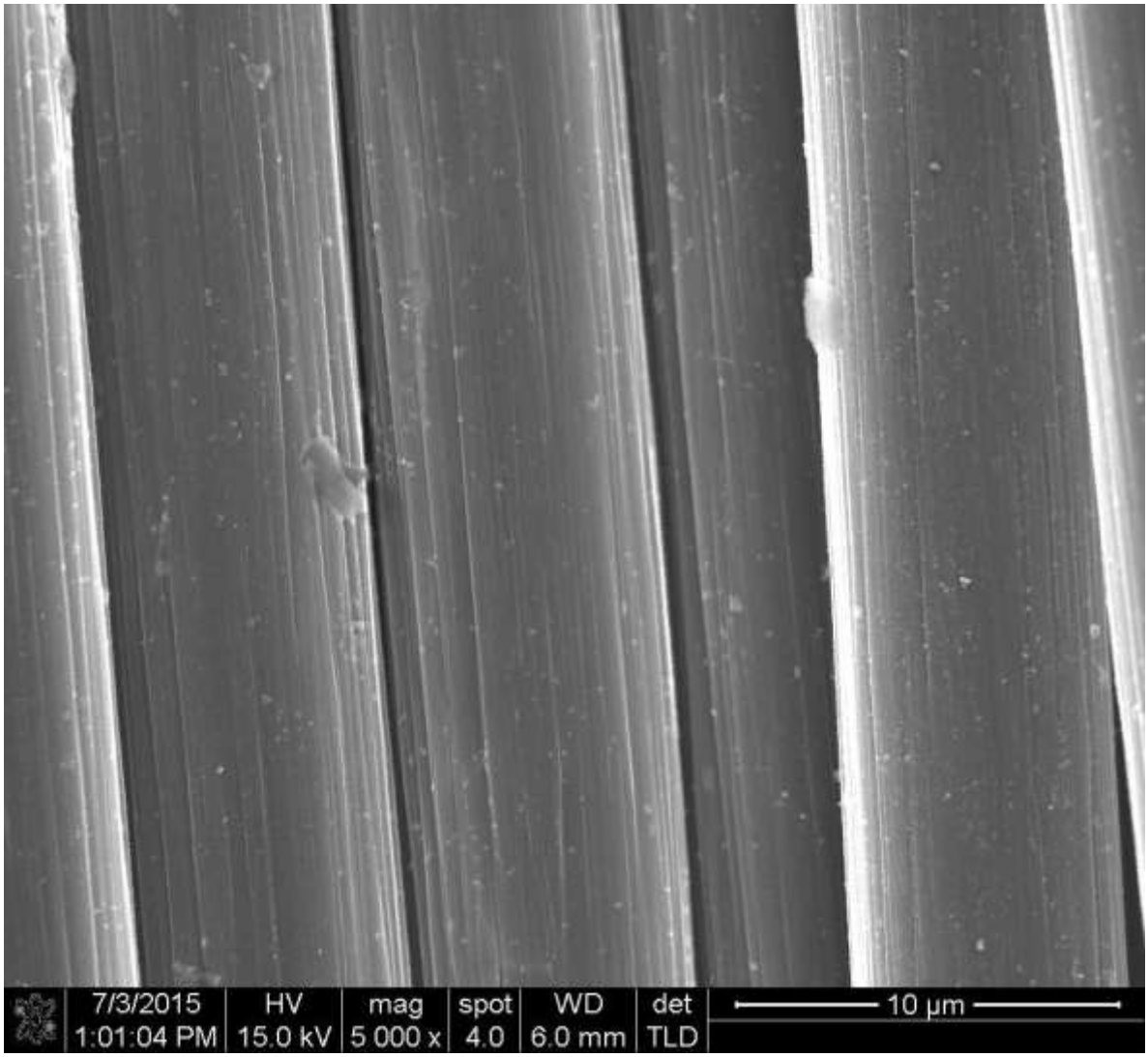

Figure 5.22 ISOH_600°C_05g30m

Figure 5.23 the CNTs synthesized with 1.2 wt. % of nickel concentration, the image shows a high growing between CFs but not on CF surface.

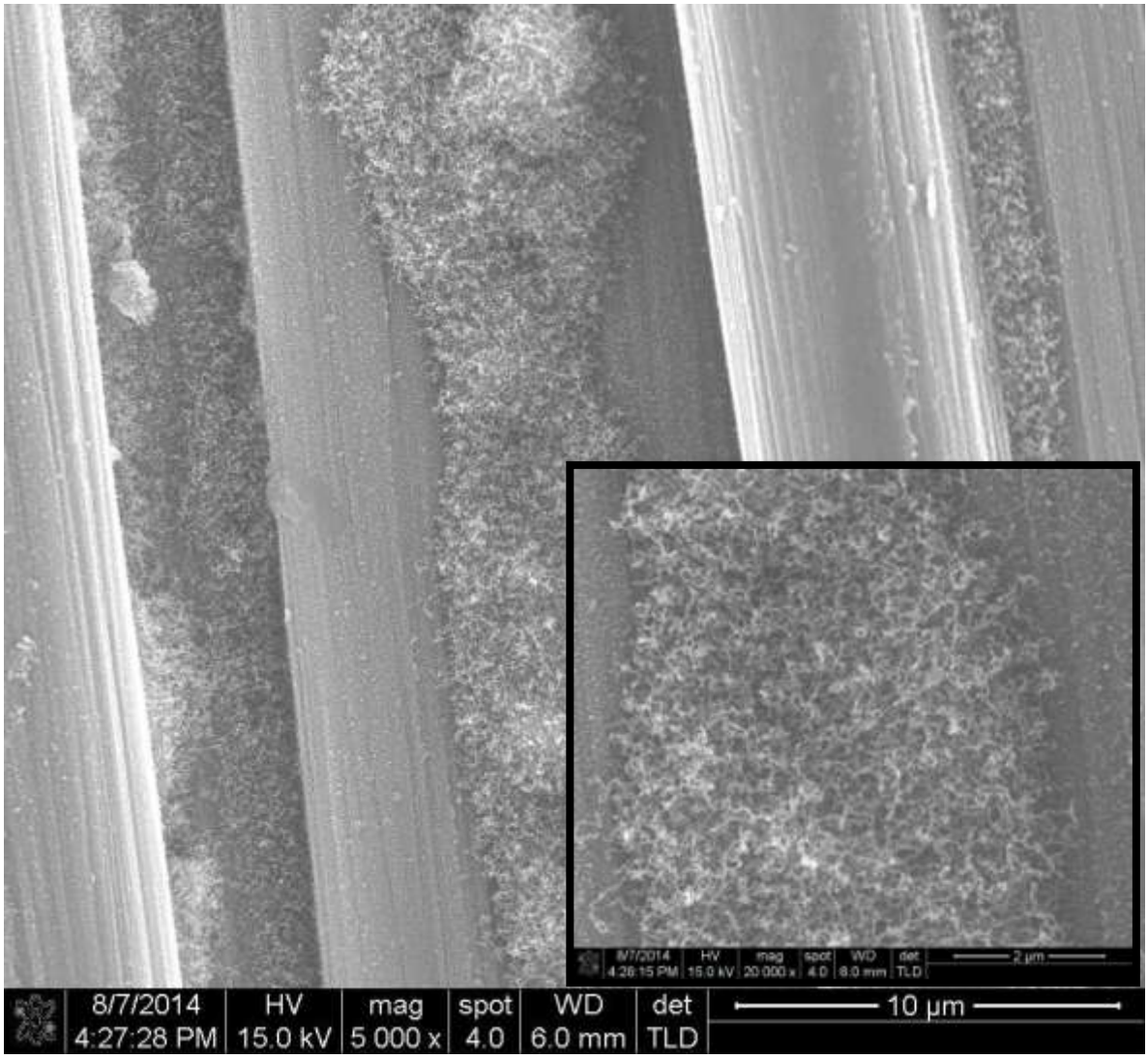

Figure 5.23 ISOH_600°C_1g30m

The results of the experiment with 3.6 wt. % of nickel concentration it is shows in Figure 5.24. In this image, relatively small CNTs compared to those in Figure 5.23 are shown.

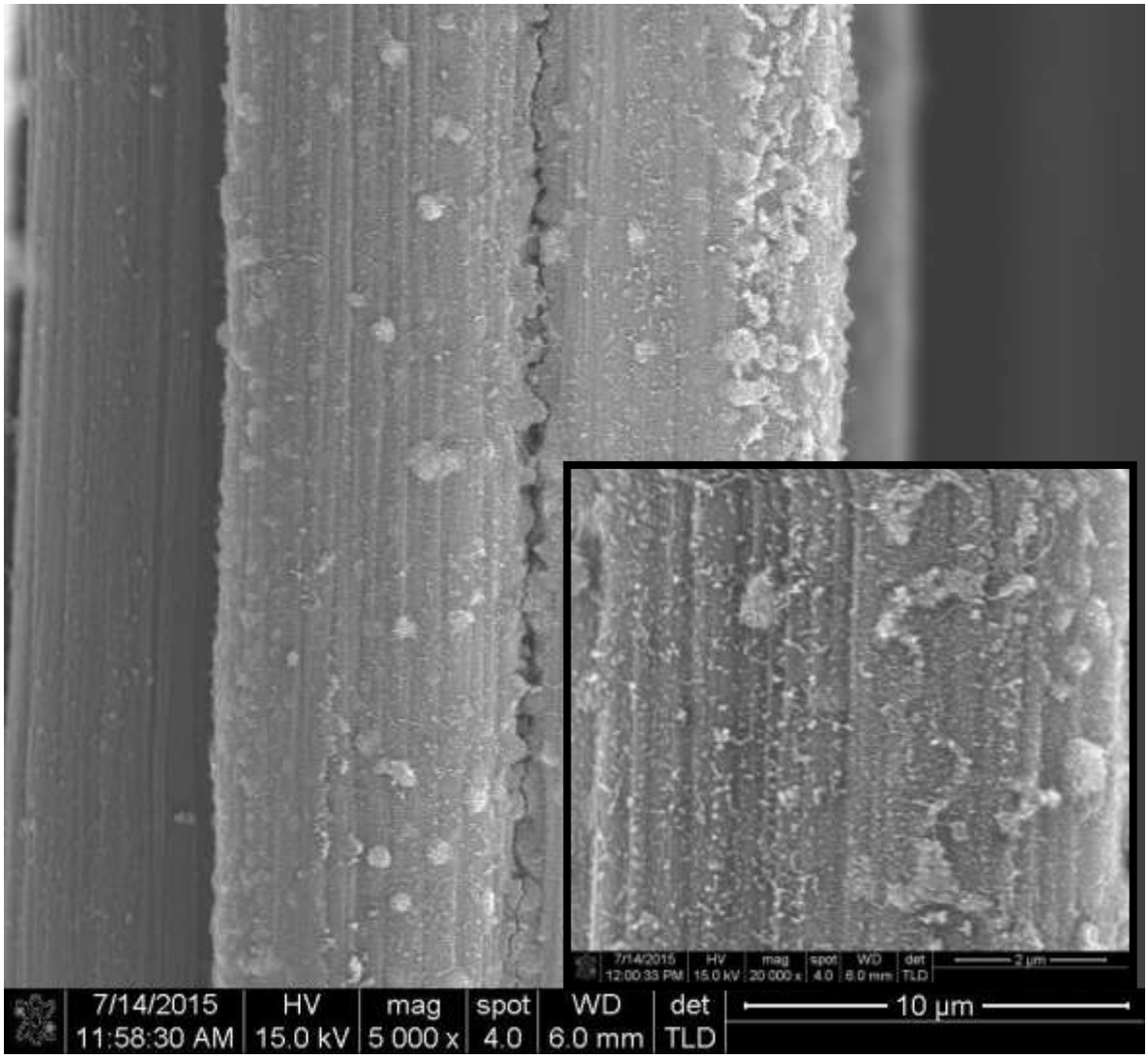

Figure 5.24 ISOH_600°C_3g30m

Figure 5.25 shows the results of the CNTs with 5.9 wt.% of nickel concentration, with a high CNTs density and high cover CFs surface. This is the best result at 600 °C with 5.9 wt.% of nickel concentration.

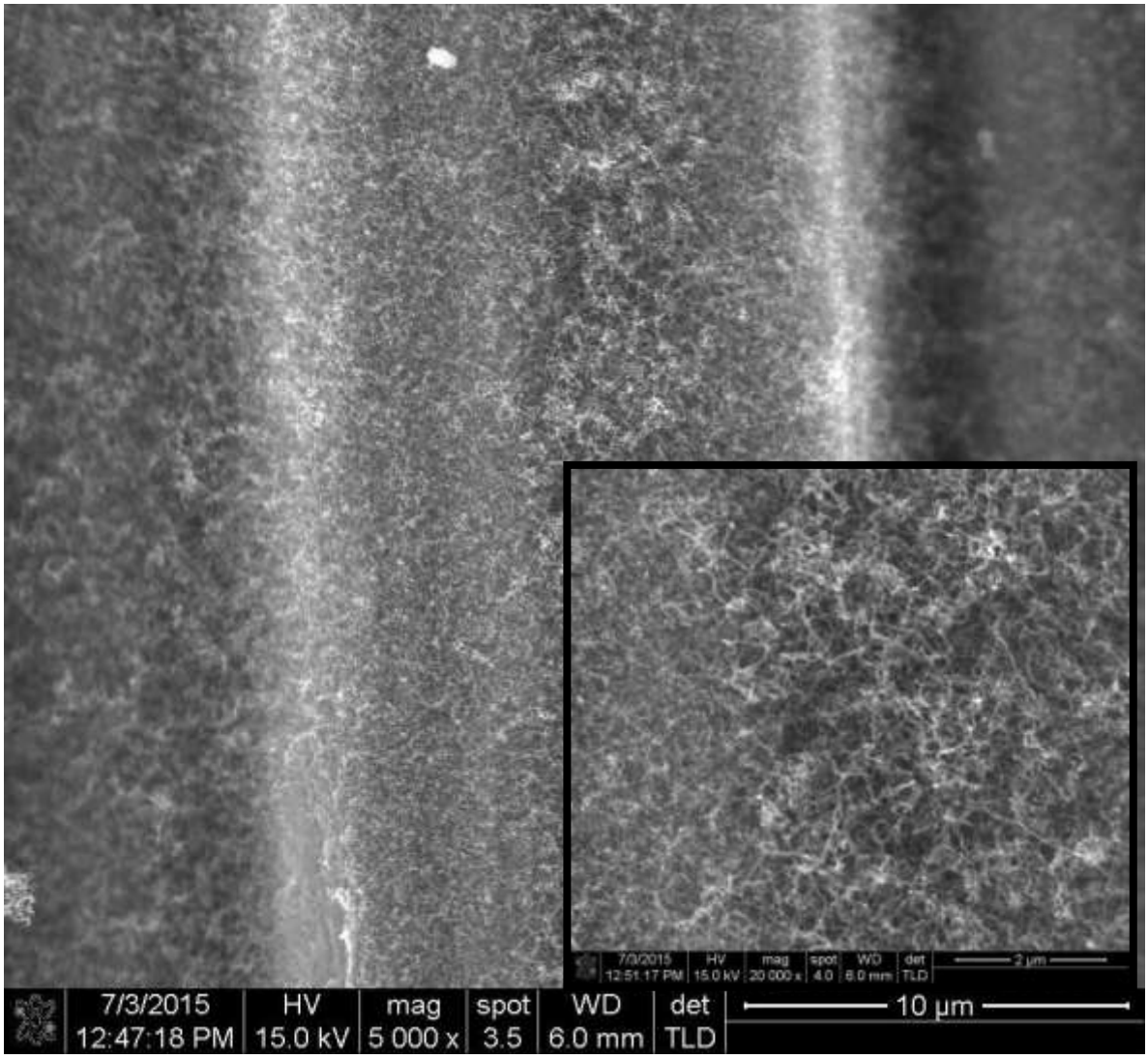

Figure 5.25 ISOH_600°C_5g30m

The next experiments were synthesized at 650 °C increasing the nickel concentration. In the Figure 5.26 shows the experiment with 0.61 wt.% of nickel concentration, with a very high density of CNTs and high cover CFs surface. Naito reports CNTs grafted on surface of CF (Pitch and PAN) by CVD under vacuum using ferrocene as catalyst at 700 °C and 750 °C. Before synthesis CFs were treated in vacuum by 1h at 750 °C to remove sizing. CNTs were found to grow uniformly and densely. The outer diameters of the CNTs ranged

from 30 to 80 nm. [17] We have similar results as showed in this Figure, the CNTs were interconnected with one another at several locations, forming a three dimensional network structure on the fiber surface.

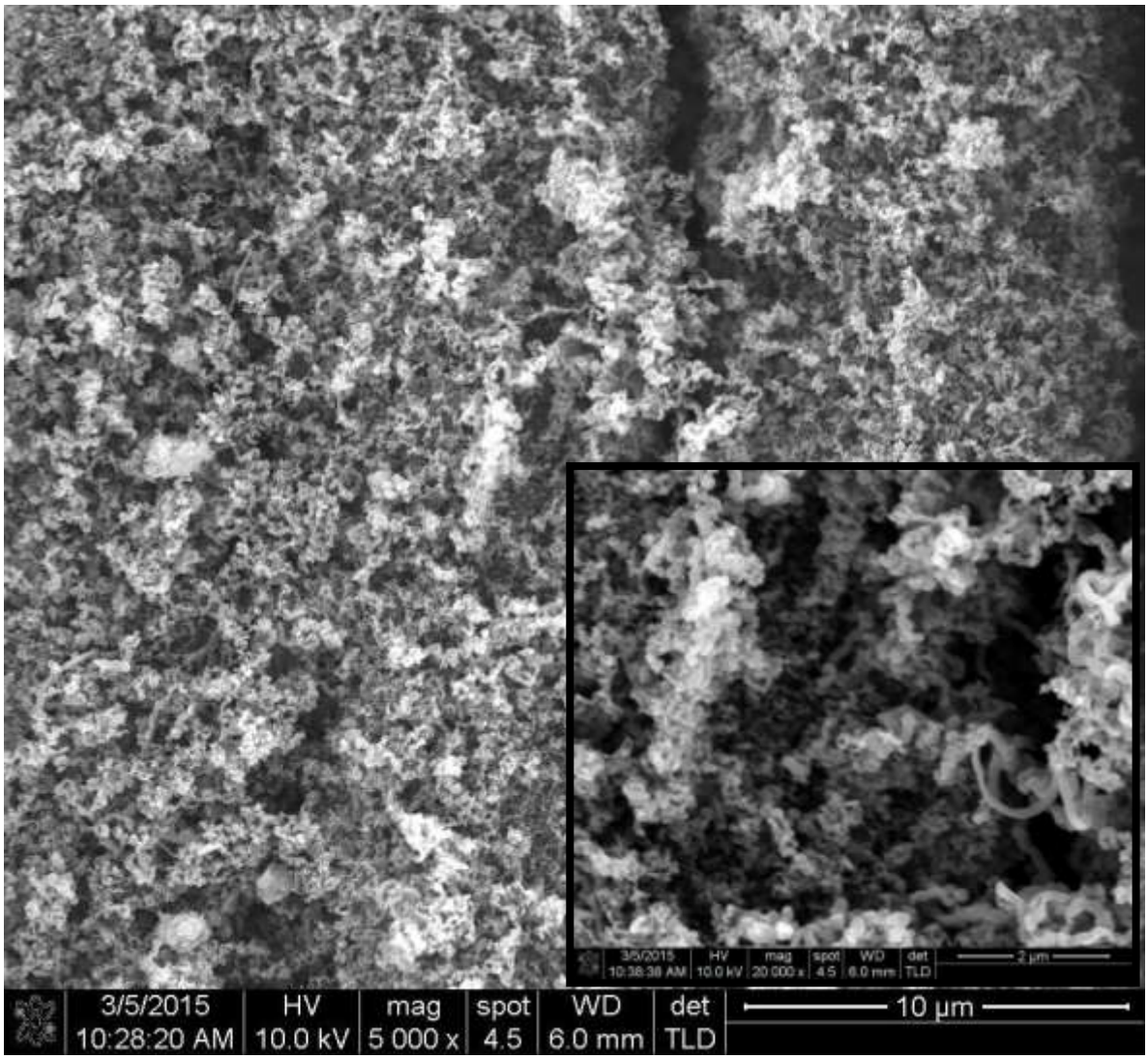

Figure 5.26 ISOH_650°C_05g30m

Figure 5.27 shows the synthesis of CNTs with 1.2 wt.% of nickel concentration, with a very small CNTs on CFs surface but with high cover surface. The CNTs form bundles

between CFs. Is possible that CNTs don't grown enough because there is a lot of nucleation spots and maybe needs more reaction time to obtain bigger CNTs.

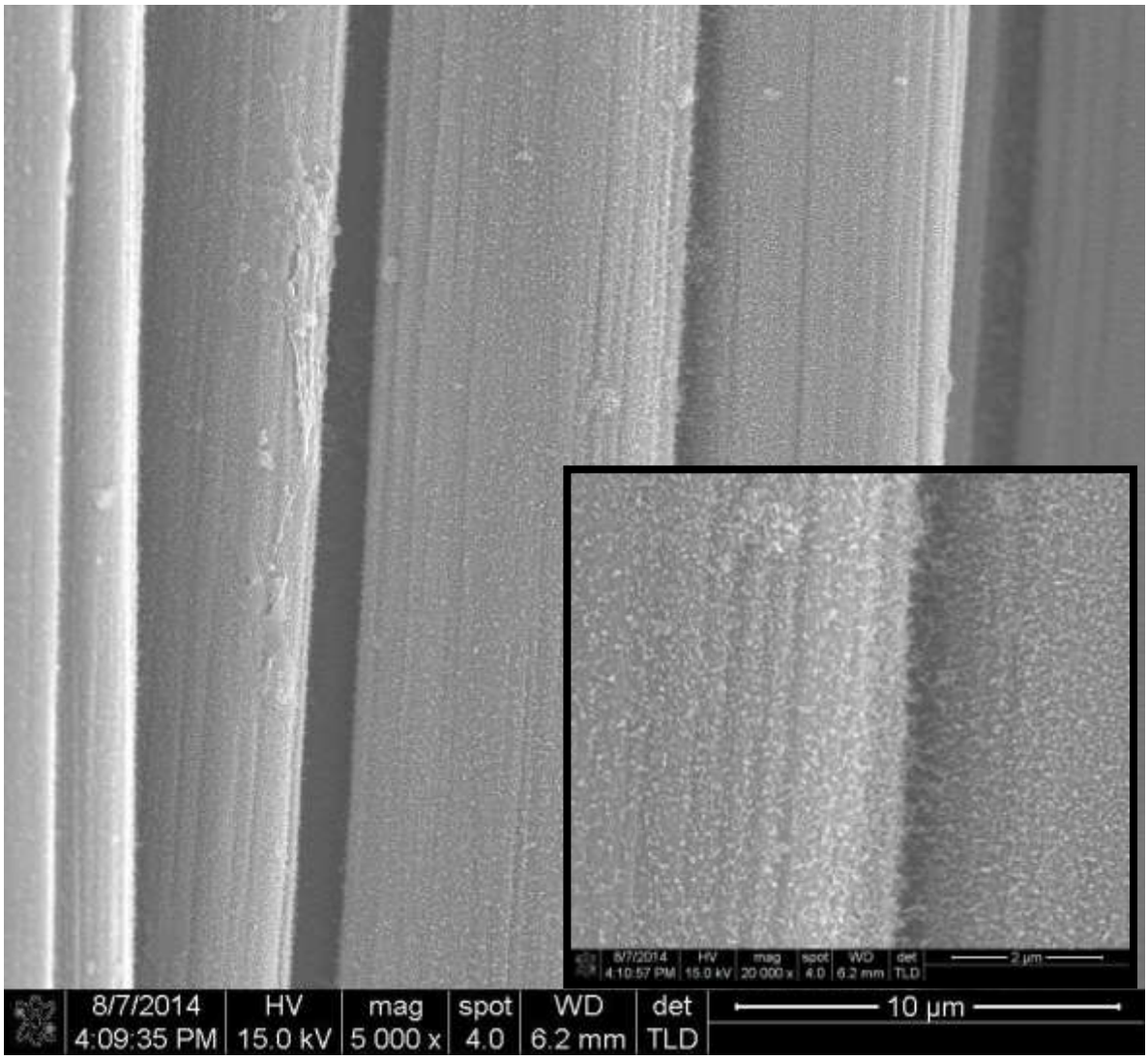

Figure 5.27 ISOH_650°C_1g30m

Figure 5.28 shows the result obtained with 3.6 wt.% of nickel concentration, with a big and small CNTs on CFs surface and a high cover surface. Is possible that big CNTs had a preferential growth because the high nucleation spots in some CFs areas.

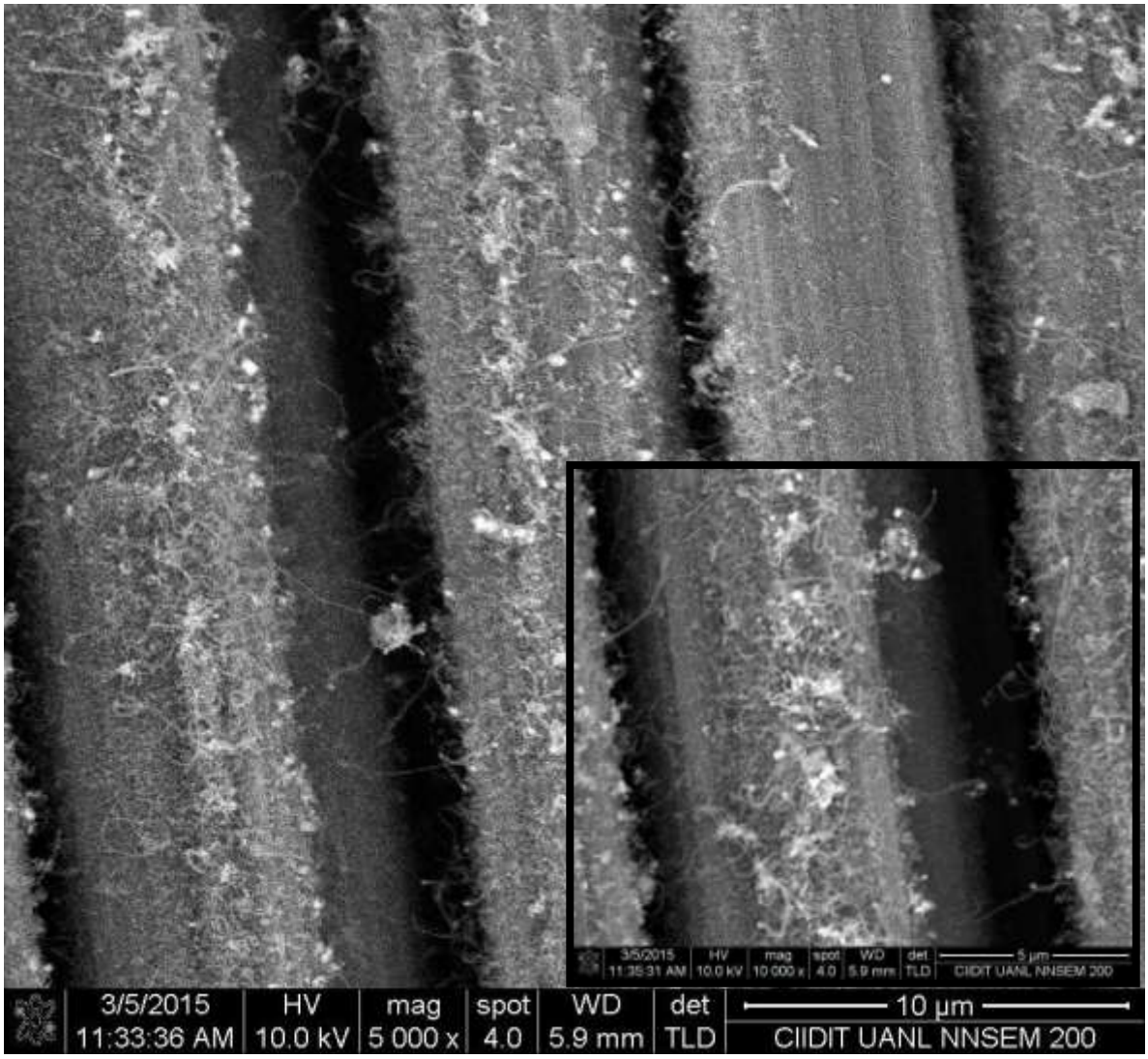

Figure 5.28 ISOH_650°C_3g30m

Figure 5.29 shows the results obtained with 5.9 wt.% of nickel concentration. It is observed a small CNTs on CFs surface. In this experiment was not favorable the growing of CNTs (a high nickel concentration).

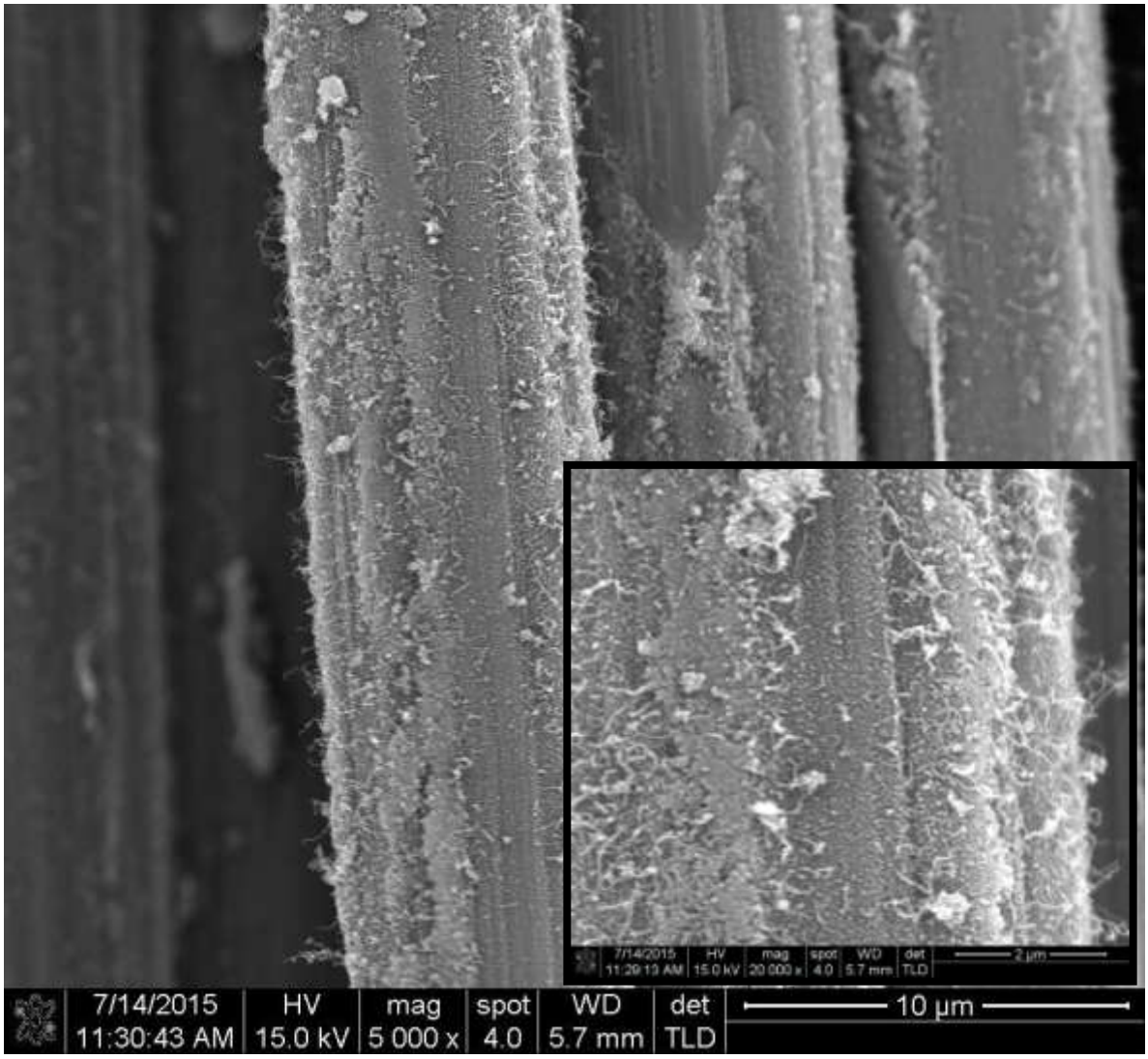

Figure 5.29 ISOH_650°C_5g30m

In the next images (Figures 5.30 to 5.33) shows the results obtained at 700 °C. Figure 5.30 is observed the result of the experiment at 700 °C with 0.61 wt.% of nickel concentration. There is CNTs in all CFs surface with a high density, but the CNTs are small, these CNTs form bundles between CFs.

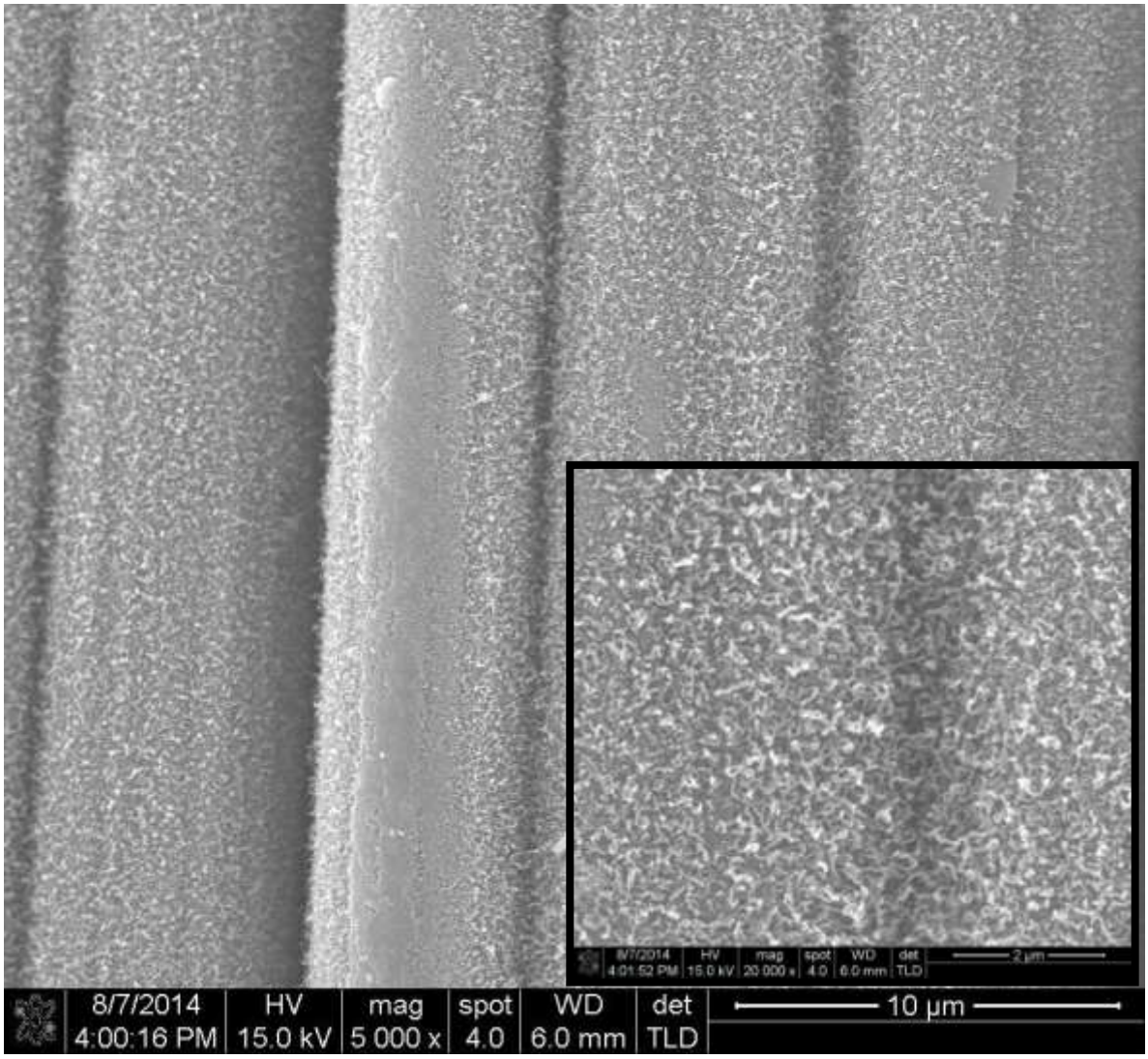

Figure 5.30 ISOH_700°C_1g30m

In Figure 5.31 (with 1.2 wt.% of nickel concentration) is observed similar results than Figure 5.30, high density and small CNTs on CFs surface. In this experiment, when we increase the nickel concentration the CNTs is not improvement apparently.

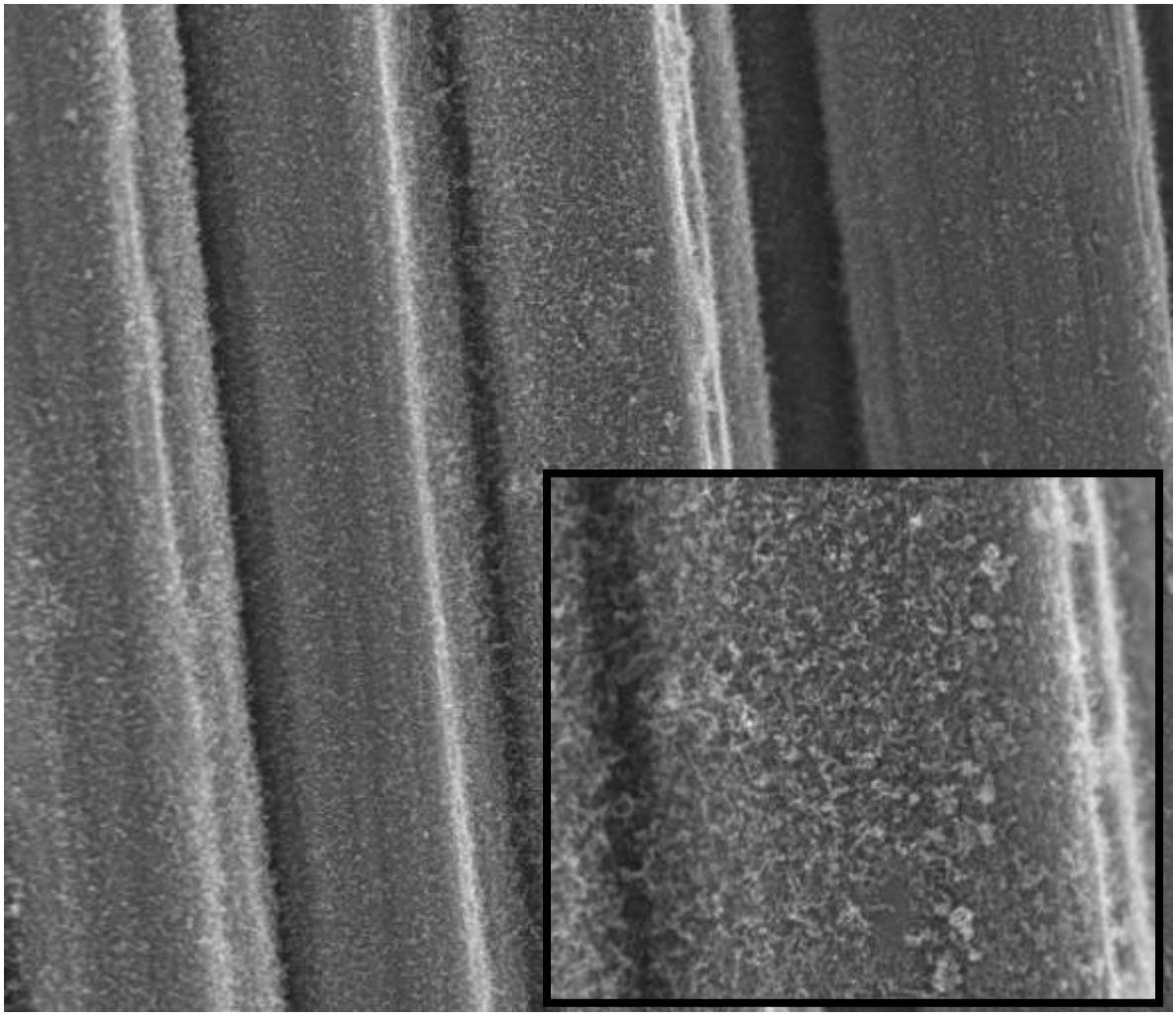

Figure 5.31 ISOH_700°C_3g30m

Figure 5.32 is showed the result obtained with a high Ni concentration. It is observed that the CNTs are very similar with the last experiment in distribution, density and size.

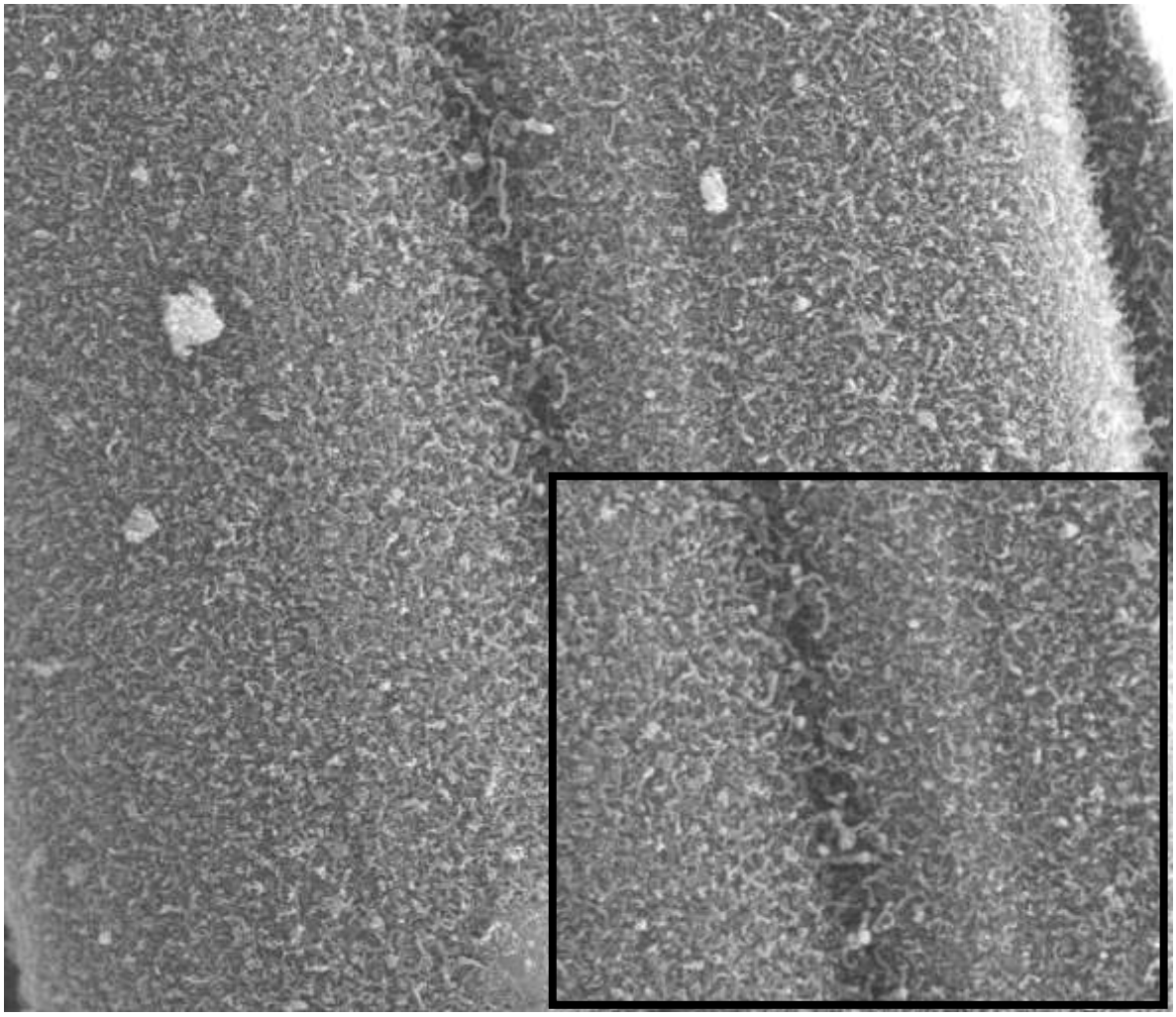

Figure 5.32 ISOH_700°C_5g30m

In the next images (Figures 5.33 to 5.36) shows the results obtained at 750 °C. Figure 5.33 and 5.34 shows the CNTs obtained at lower Ni concentrations. The CNTs grafted to the surface of CFs grow uniformly and with a high density forming a three dimensional network structure. Feng An *et al* synthesized CNTs by CVD on surface of unsized CFs (PAN) at 750 °C using ferrocene as precursor for catalyst, C_2H_2 as carbon source and N_2 or 50% H_2/N_2 mixture. Their results shows CNTs with a high density, closely compact and

interconnected with each other. These results match perfectly with our results in this experiment with different conditions and some variations in the method.

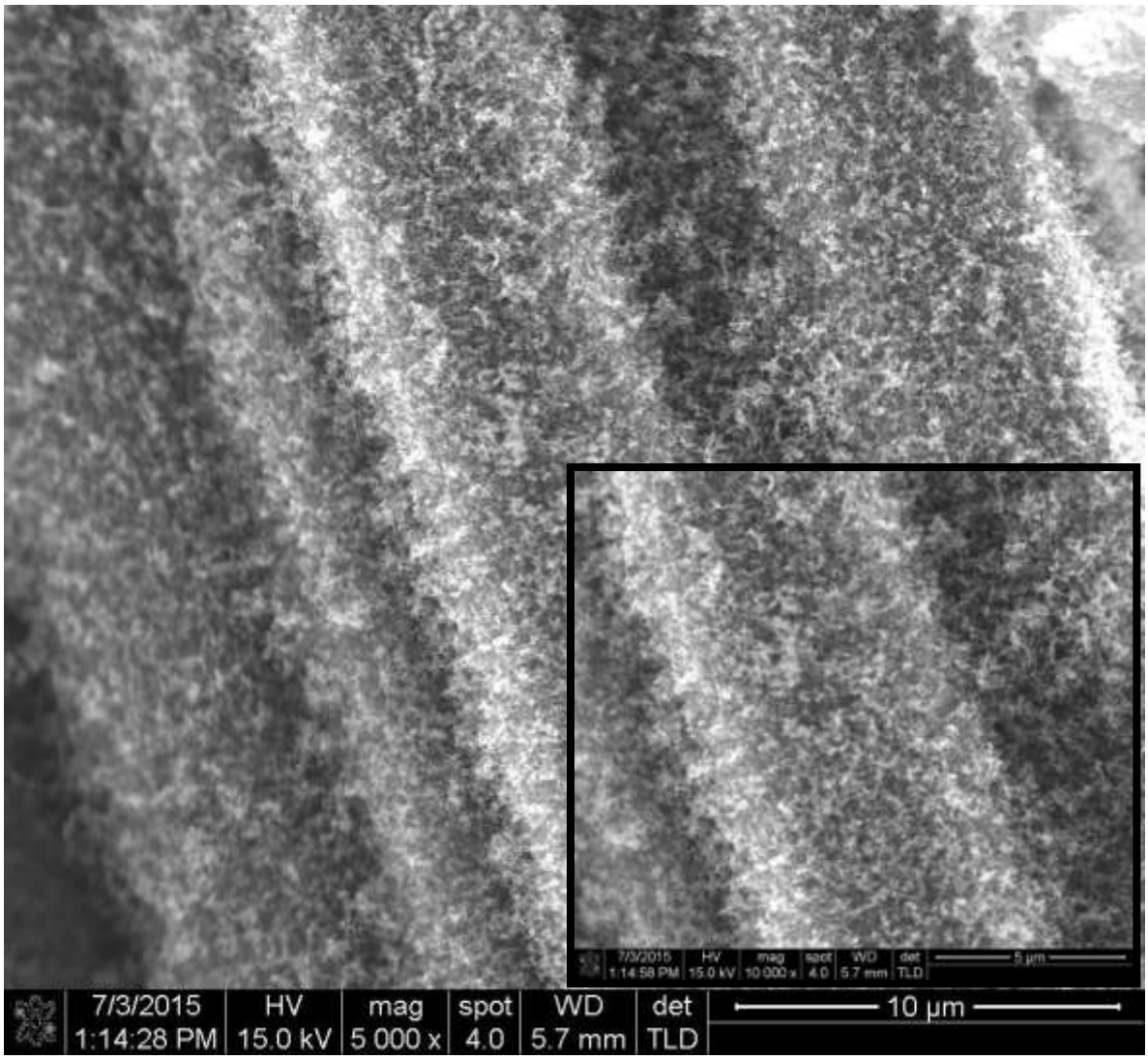

Figure 5.33 ISOH_750°C_05g30m

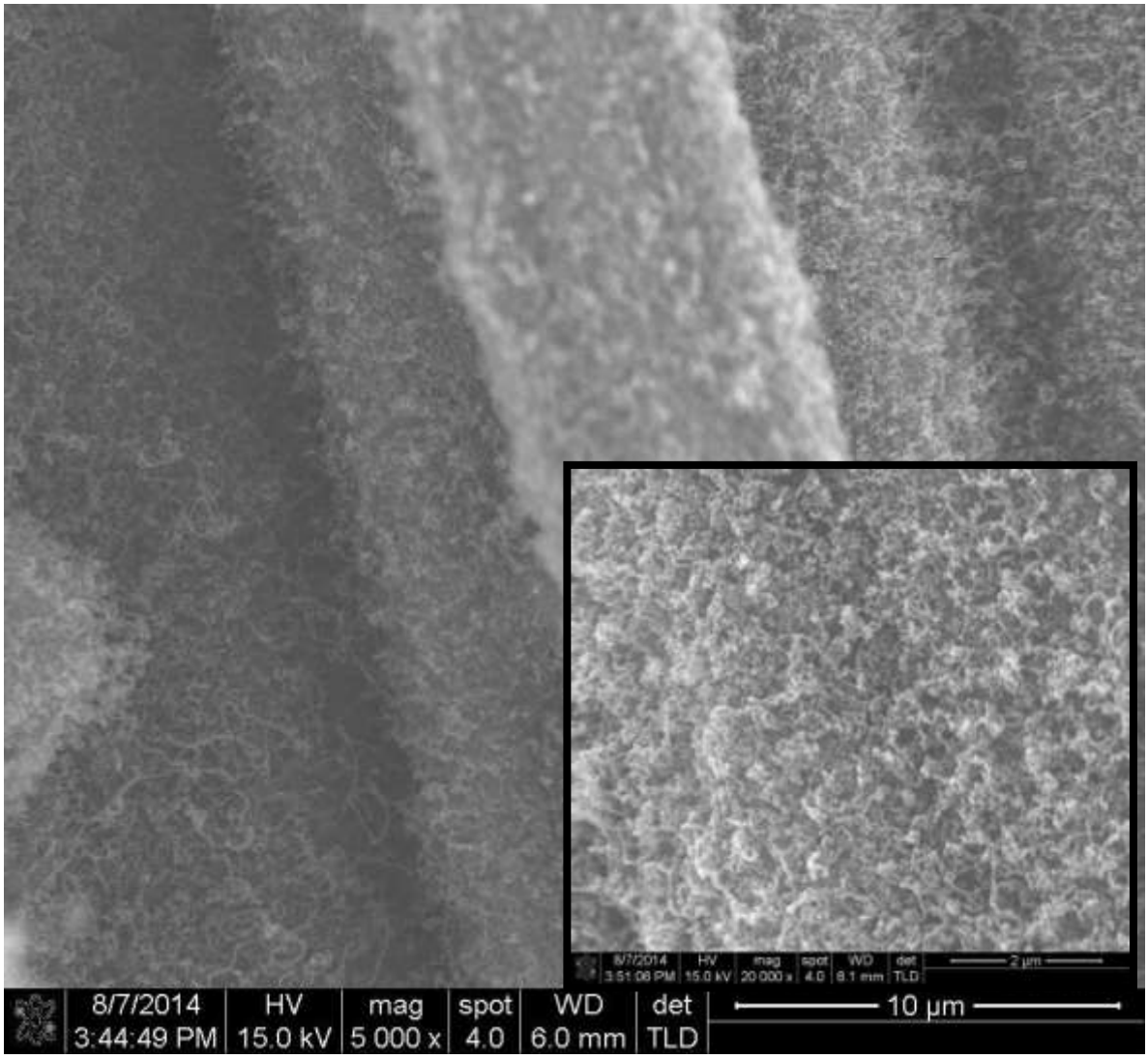

Figure 5.34 ISOH_750°C_1g30m

Figures 5.35 and 5.36 shows the results obtained at the highest Ni concentrations. Increasing the catalyst concentration the density of CNTs decrease. The best results are obtained at lower catalyst concentration, is desirable because the cost is lower.

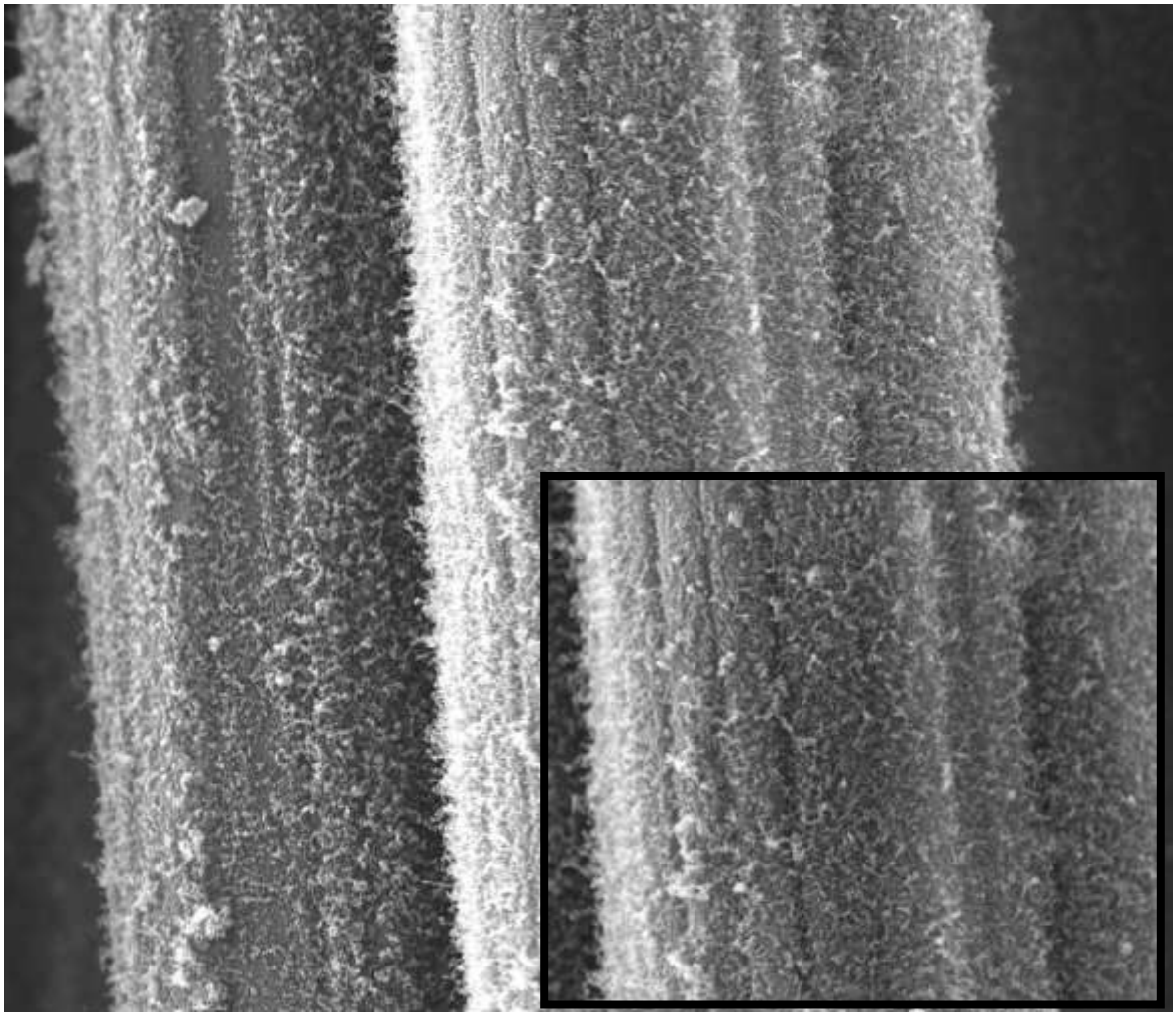

Figure 5.35 ISOH_750°C_3g30m

Figures from 5.37 to 5.39 shows the last results obtained by SEM CNTs analysis at 800 °C. In this conditions, the best results obtained are showed in the Figure 5.37, that results correspond to the lower Ni concentration.

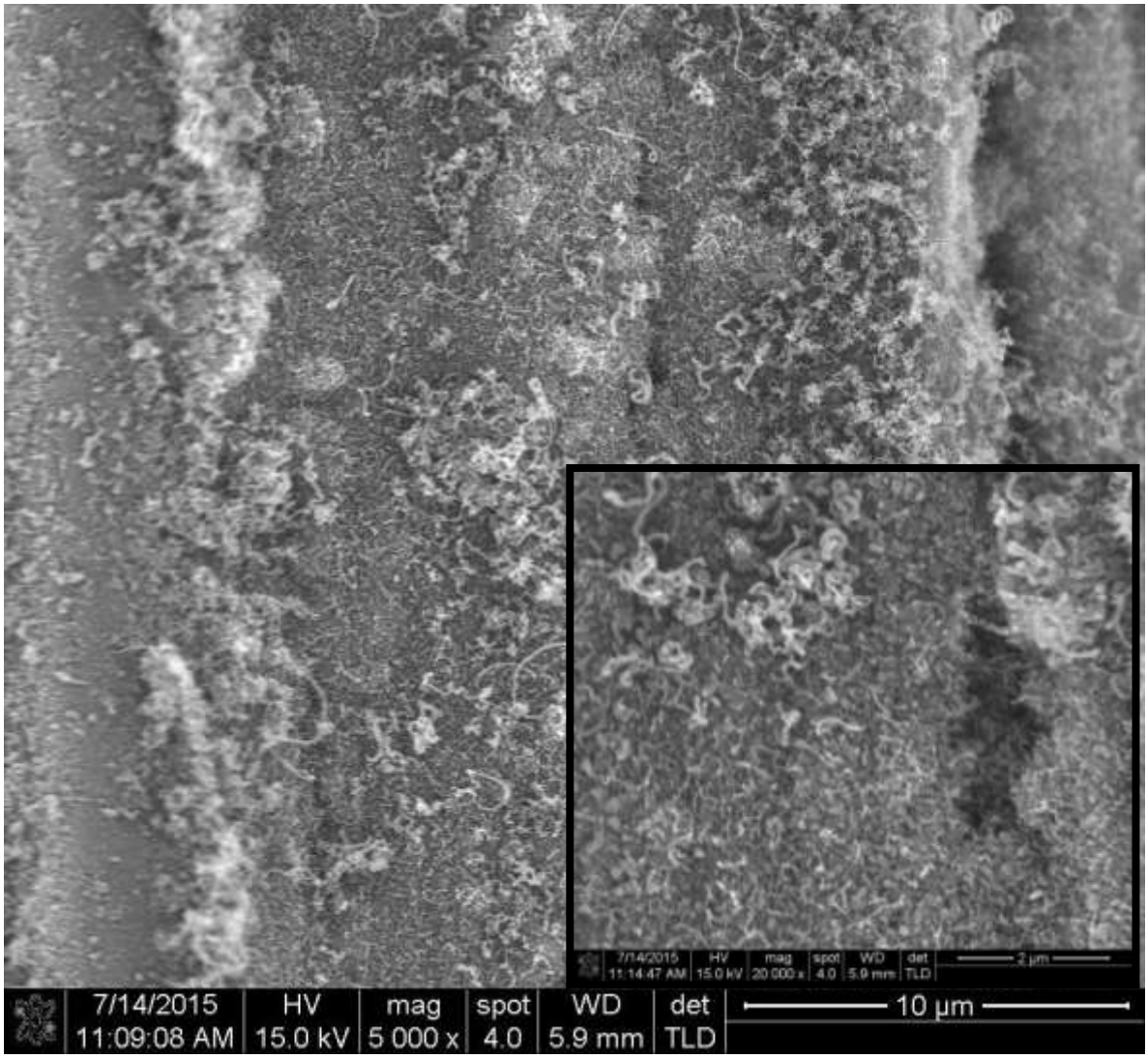

Figure 5.36 ISOH_750°C_5g30m

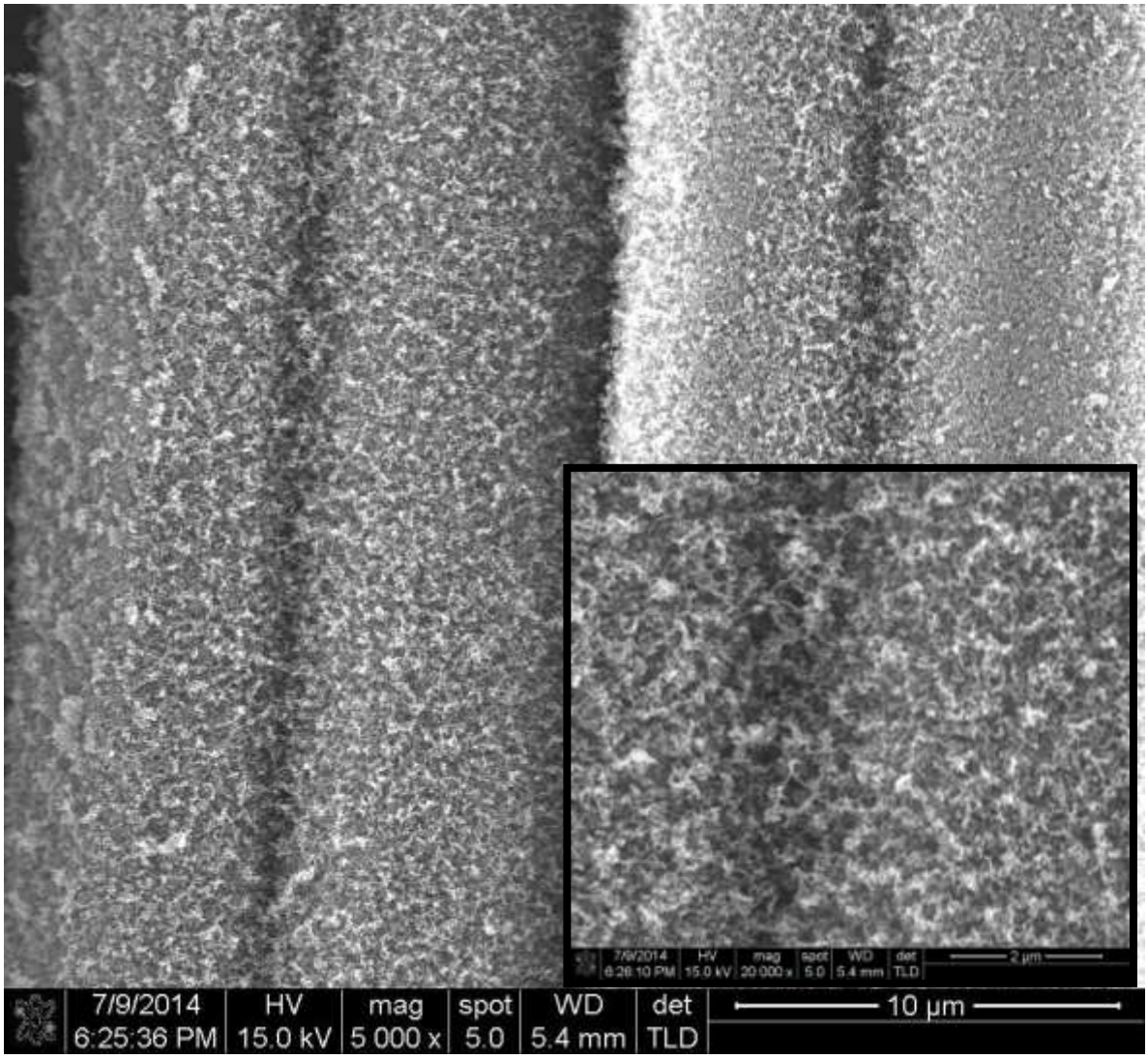

Figure 5.37 ISOH_800°C_1g30m

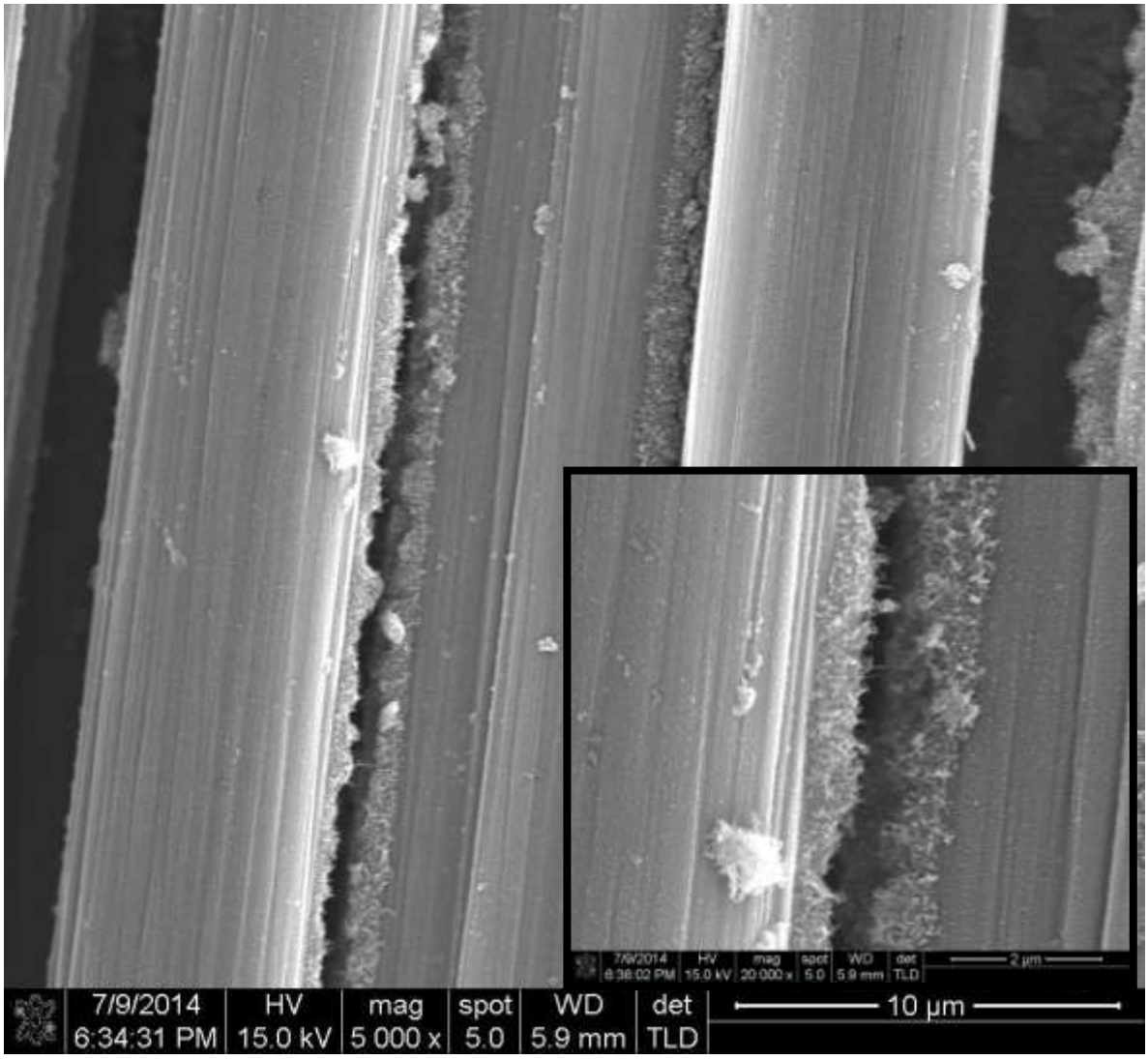

Figure 5.38 ISOH_800°C_3g30m

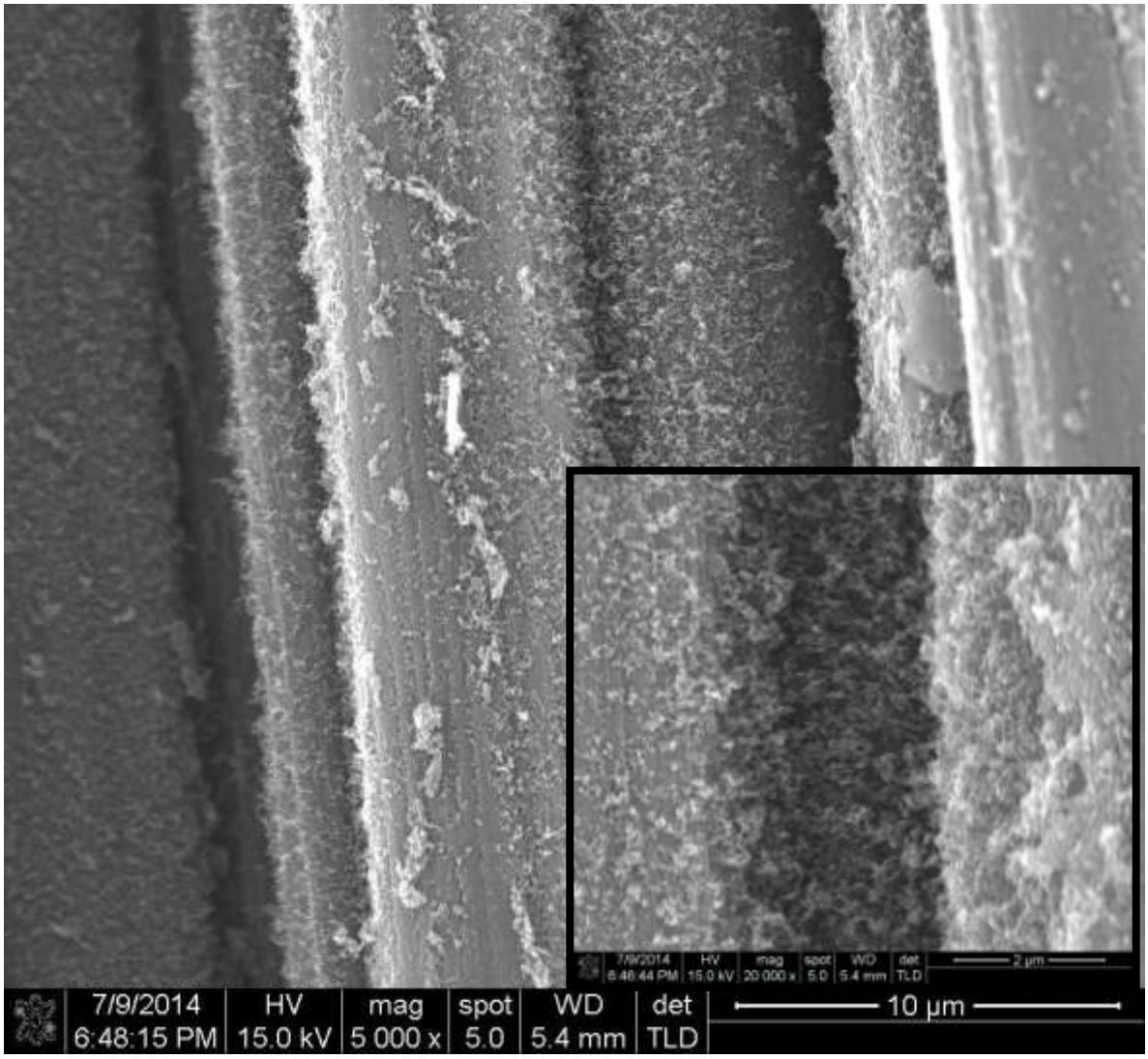

Figure 5.39 ISOH_800°C_5g30m

5.2. RAMAN Spectroscopy

The Raman spectra of synthesized CNTs on carbon fibers are shown. Figure 5.40 shows the different spectra obtained with different reaction temperatures using ethanol as carbon source. Figure 5.41 shows the different spectra obtained with different reaction temperatures using isopropanol as carbon source. These spectra show characteristic carbon D band from the sp3 bonds and G band from sp2 bonds. While these bands are

also present in the RCF samples (clean recovered carbon fibers, with no attached CNTs), the samples with CNTs anchored to the CF surface show more pronounced bands in the Raman intensity. We can infer that Multiwall CNTs (MWCNTs) are being synthesized since there is no band present in the RMB zone.

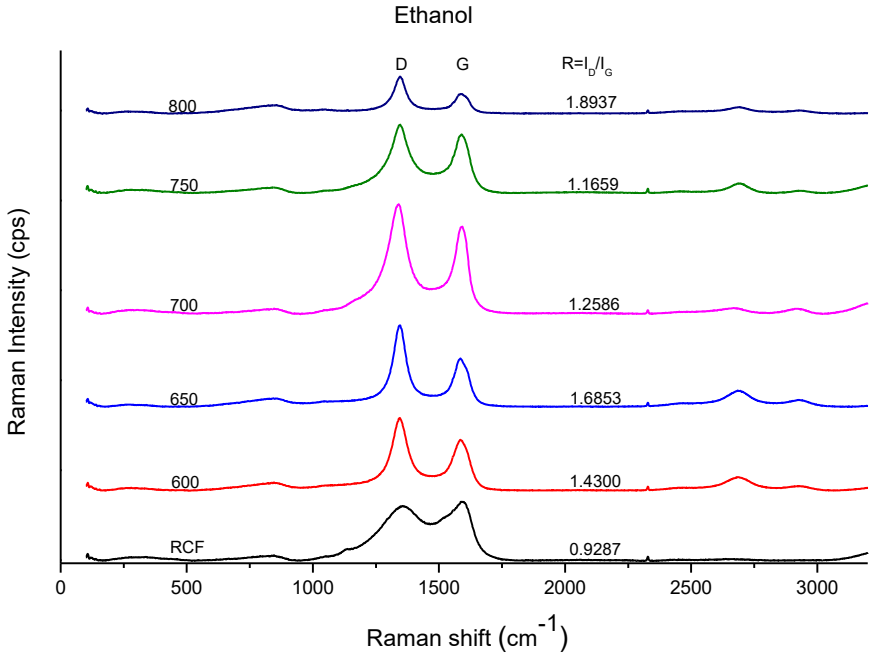

Figure. 5.40 Raman spectra of synthesized CNTs on carbon fibers using ethanol as carbon source. In each Figure, the Raman spectra of different reaction temperatures are shown.

The ratio of intensities between D and G bands is below 1 in the RCF sample; the intensity ratio between D and G bands is above 1 in the samples with MWCNTs on the CF surface except from experiments with isopropanol as carbon source at 800 °C and 600 °C which can be interpreted as a result of less structurally defective MWCNTs synthesized with those parameters. Moreover, high ratio of intensity of the discussed bands is also a characteristic of MWCNTs.

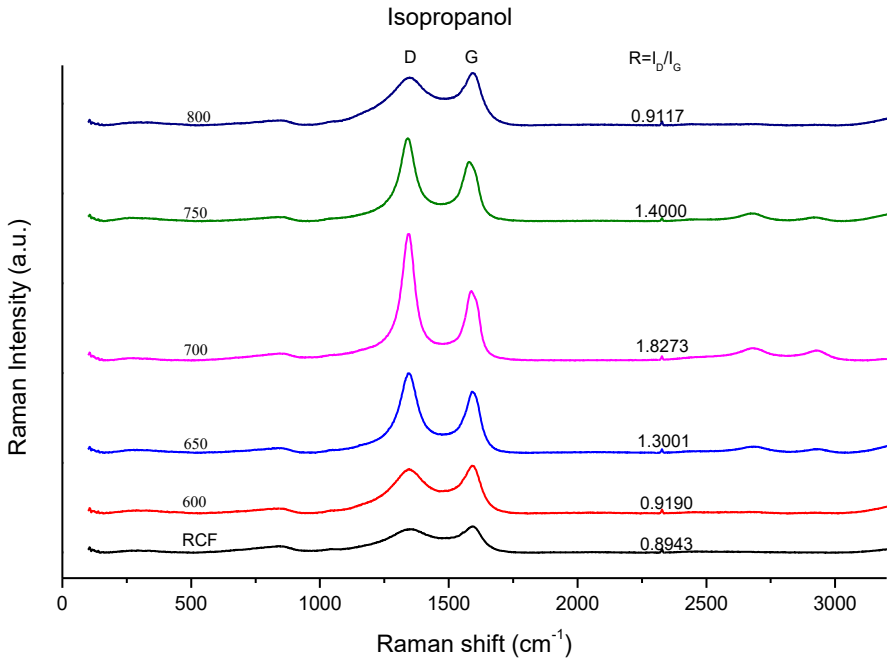

Figure 5.41 Raman spectra of synthesized CNTs on carbon fibers using Isopropanol as carbon source. The Raman spectra of different reaction temperatures are shown.

5.3. Pseudo-Mechanical Characterization

In this study, a small amount of CNT/CF were placed into three different liquids and then placed in and¿ ultrasonic bath and magnetic stirring for 5 and 15 minutes. Figures 5.42 and 5.43 show the SEM micrographs of the results of the pseudo-mechanical testing of anchorage of the CNTs to the CFs surface, tests submitted in different solvents, namely acetone, ethanol and water; specifically, Figure 5.42 shows the results of mechanical stirring testing and Figure 5.43 shows the results of ultrasonication testing of samples.

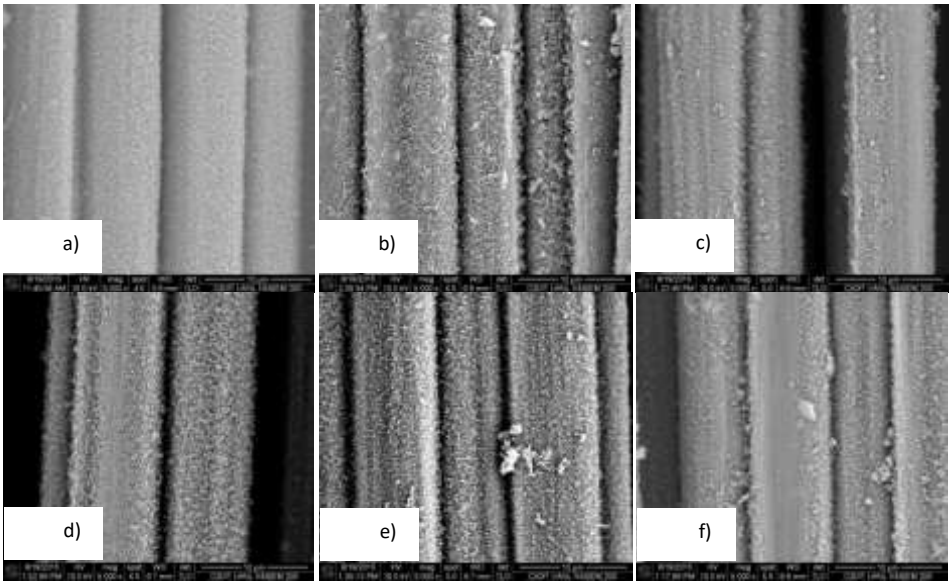

Figure 5.42. SEM images of samples obtained after submission to pseudo-mechanical stirring testing with: a) Acetone, 5 min; b) Acetone, 15 min; c) Ethanol, 5 min; d) Ethanol, 15 min; e) Water, 5 min; f) Water, 15 min.

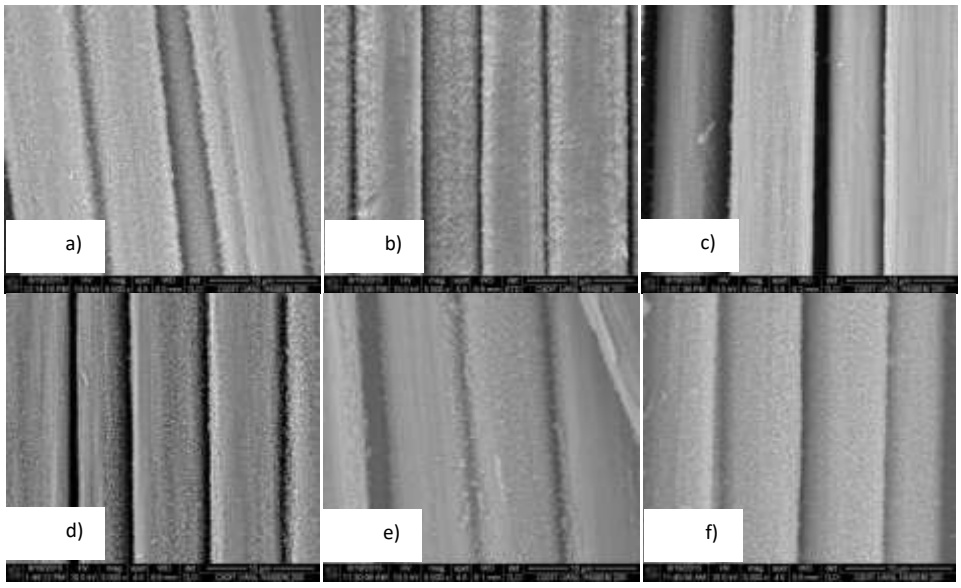

Figure 5.43.- SEM images of samples obtained after submission to pseudo-mechanical ultrasonication testing with: a) Acetone, 5 min; b) Acetone, 15 min; c) Ethanol, 5 min; d) Ethanol, 15 min; e) Water, 5 min; f) Water, 15 min.

The results of both, mechanical stirring and ultrasonication show that the CNTs are strongly anchored onto the CF surface, since, after the pseudo-mechanical testing the

CNTs are still visible in the SEM micrographs; the implication of these results mean that carbon fibers with synthesized CNTs can be handled in new processes to form new composite materials. There is basically no significant difference between the images obtained from synthesized CNTs on the carbon fibers and those obtained after submission to pseudo-mechanical testing, whether mechanical stirring or ultrasonication with any solvent.

Zhang *et al* [17] report a sizing approach to fabricate CNT/CF hybrid fiber by exploring a sizing agent containing MWCNTs. MWCNTs were purchased from Shenzhen Nanotech, Port. Co. Ltd. and acid treated with HNO3 and H2SO4. CF tow (unsized) was supplied by Hengshen Co. Ltd. The CF tow was passed through the sizing agent suspension, baked in an oven and then rolled. The results of the fabrication of CNT/CF hybrid fiber shows a lower density of CNTs and a poor distribution. They found that the effect of the coating layer on the interfacial shear strength of CNT/CF reinforced with a polimer composite is higher than that of untreated CF. This process take more the one step, also to buy the MWCNTs is expensive. In our study, recovered CF with CNTs as sizing and reinforcement is a candidate for hybrid composites materials. The introduction of CNTs offers potential for selective reinforcement, where nanoscale reinforcement can be included in matrix-rich interlaminar regions to improve through-thickness properties of polymer composite.

Carbon nanotubes were successfully anchored to carbon fibers by CVD method using nickel as catalyst and ethanol or isopropanol as carbon source. Pyrolysis used as a recycling technology has the advantage of recovering most of the material introduced in the reactor in the forms of solid, gas, and liquids. Clean carbon fibers can be recovered for

potential reuse in new composites. After the experimental development of the CVD method of synthesizing CNTs onto CF surface, the Raman spectroscopy confirms the apparition of CNTs and the pseudo-mechanical testing confirms the anchorage of the CNTs to the CF surface.

6. Conclusions

Through this research, an experimental method of revalorization of recovered/recycled carbon fibers has been developed through the anchorage and growth of carbon nanotubes directly onto the carbon fibers surface via chemical vapor deposition. Clean carbon fibers were recovered using pyrolysis as a recovery method. Chemical vapor deposition method for synthesis of carbon nanotubes was implemented using ethanol or isopropanol as carbon source in the catalytic presence of Ni nanoparticles. It was demonstrated that the carbon nanotubes and Ni nanoparticles can be synthesized in one step at the same time onto the carbon fibers surface at different temperatures while obtaining an interesting ratio of coverage of the carbon fiber surface with CNTs. Multiwall carbon nanotubes are being synthesized through this method which has been corroborated with the Raman spectroscopy. Relatively good structured MWCNTs are being synthesized using isopropanol as a carbon source at 800 °C and 600 °C.

Pseudo-mechanical testing confirms that the CNTs have a good anchorage to the CF surface making this novel revalorized recovered carbon fibers with CNTs a potentially good reinforcement for new high performance composite materials.

Growing CNTs on CF surface could provides to tailor the thermal, electrical and mechanical properties of the fiber-resin interface of a composite. To obtain in one step the metal catalyst and CNT network at low temperature is a big advantage. This process not required any pretreatment of the fiber before CNTs synthesis, however is possible to increase the performance of CNT with a functionalization pretreatment of the CF. According with the results showed for Riccardis et al and Zhang et al, this material based on CF coated with CNTs, shows potential for applications as sizing material in polymeric matrix composites.

7. References

[1] Christian P. Deck, Kenneth Vecchio, Growth mechanism of vapor phase CVD-grown multi-walled carbon nanotubes, , Carbon 43 (2005) 2608–2617.

[2] R. Morales Ibarra, M. Sasaki, M. Goto, A. T. Quitain, S. M. García Montes, J. A. Aguilar-Garib, Carbon fiber recovery using water and benzyl alcohol in subcritical and supercritical conditions for chemical recycling of thermoset composite materials, Journal of Materials Cycles and Waste Management (2014 Online), DOI 10.1007_s10163-014-0252-z.

[3] L.Y. Sun, G.L. Warren, J.Y. O'Reilly, W.N. Everett, S.M. Lee, D. Davis, D. Lagoudas, H.J. Sue, Mechanical properties of surface-functionalized SWCNT/epoxy composites, Carbon 46 (2008) 320–328.

[4] A.G. Osorio, I.C.L. Silveir, V.L. Bueno, C.P. Bergmann, $H_2SO_4/HNO_3/HCl$—functionalization and its effect on dispersion of carbon nanotubes in aqueous media, Appl. Surf. Sci. 255 (2008) 2485–2489.

[5] Nanotube bundles and tube-tube orientation: A van der Waals density functional study, Heiko Dumlich* and Stephanie Reich, PHYSICAL REVIEW B 84, 064121 (2011).

[6] Z. Ren et al., Aligned Carbon Nanotubes, NanoScience and Technology, DOI: 10.1007/978-3-642-30490-3_2, © Springer-Verlag Berlin Heidelberg (2013).

[7] Carbon nanotubes : science and applications / edited by M. Meyyappan. NASA Ames Research Center Moffett Field, CA. pag 8-22. (2005).

[8] Wei-Wen Liu, Siang-Piao Chai, Abdul Rahman Mohamed, U. Hashim, Synthesis and characterization of graphene and carbon nanotubes: A review on the past and recent developments, Journal of Industrial and Engineering Chemistry 20 (2014) 1171–1185.

[9] Large Scale Synthesis of Carbon Nanotubes, S. Karthikey, P. Mahalingam, M. Karthik, E-Journal of chemistry, 2009, 6(1), 1-12.

[10] S.-J. Park, Surface Treatment and Sizing of Carbon Fibers, Chapter 4, pp 101-133, Carbon Fibers (2014), Springer Series in Materials Science 210.

[17] Qiuhong Zhang, Jianwei Liu, Ryan Sager, Liming Dai, Jeffery Baur, Hierarchical composites of carbon nanotubes on carbon fiber: Influence of growth condition on fiber tensile properties, Composites Science and Technology 69 (2009) 594–601.

[17] M.F. De Riccardis, D. Carbone, Th. Dikonimos Makris, R. Giorgi, N. Lisi, E. Salernitano, Anchorage of carbon nanotubes grown on carbon fibers, Carbon 44 (2006) 671–674.

[17] R.B. Mathur, Sourav Chatterjee, B.P. Singh, Growth of carbon nanotubes on carbon fibre substrates to produce hybrid/phenolic composites with improved mechanical properties, Composites Science and Technology 68 (2008) 1608–1615

[17] Dikonimos Makris Th, Giorgi R, Lisi N, Pilloni L, Salernitano E, De Riccardis MF, et al. Carbon nanotubes growth on PAN and Pitch based carbon fibers by HFCVD, Fullerenes. Nanotubes Carbon Nanostruct 2005; 13(Suppl. 1):383–92.

[17] Wenbo Liu, Shu Zhanga, Lifeng Hao, Fan Yang, Weicheng Jiao ,Xiaoqin Li , Rongguo Wang. Fabrication of carbon nanotubes/carbon fiber hybrid fiber in industrial scale by sizing process. Applied Surface Science 284 (2013) 914– 920.

[17] Tensile Properties of Polyimide Composites Incorporating Carbon Nanotubes-Grafted and Polyimide-Coated Carbon Fibers. Kimiyoshi Naito. JMEPEG (2014) 23:3245–3256.

[17] Feng An, Chunxiang Lu, Jinhai Guo, Huibin Lu. Preparation of CNT-hybridized carbon fiber by aerosol-assisted chemical vapor deposition. J Mater Sci (2012) 47:3327–3333.

List of Figures